

**The endophytic fungus *Stemphylium globuliferum* – secondary  
metabolites and biological activities**

**Dissertation**

zur

Erlangung des Doktorgrades (Dr. rer. nat.)

der

Mathematisch-Naturwissenschaftlichen Fakultät

der

Rheinischen Friedrich-Wilhelms-Universität Bonn

vorgelegt von

**Jan-Philipp Schrör**

aus

Moers

Bonn 2017

Angefertigt mit Genehmigung der Mathematisch-Naturwissenschaftlichen Fakultät  
der Rheinischen Friedrich-Wilhelms-Universität Bonn

1. Referentin : Prof. Dr. G. M. König

2. Referent : Prof. Dr. W. Knöss

Tag der Promotion : 02. November 2017



## Vorveröffentlichungen der Dissertation / In Advance Publications of the Dissertation

Teilergebnisse aus dieser Arbeit wurden mit Genehmigung der Mathematisch-Naturwissenschaftlichen Fakultät, vertreten durch die Mentorin/Betreuerin der Arbeit, in folgenden Beiträgen vorab veröffentlicht:

Parts of this study have been published in advance by permission of the Mathematisch-Naturwissenschaftlichen Fakultät, represented by the supervisor of this study:

### Publikationen / Research Papers

J. Schrör, S. Kehraus, N. Merten, G. M. König; “Stemphyloxin III and stemphylofuran, new insights into the mold fungus *Stemphylium globuliferum*”; **2017**, in preparation.

J. Seungwon, J. Lee, J. Schrör, C. Cerella, S. Chateauvieux, B. Orlikova, K. Kim, C. Christov, M. Dicato, B. Han, G. M. König, M. Diederich; “The dialkylresorcinol stemphol induces necroptosis by interference with endoplasmic reticulum/mitochondrial calcium homeostasis”; **2017**, in preparation.

H. Harms, A. Kloeckner, J. Schrör, S. Kehraus, M. Crüsemann, G.M. König, T.F.Schaeberle; “Antibiotic dialkylresorcins and derivatives from marine-derived organisms, insights in their mode of action and putative ecological role”, **2017**, in preparation.

### Tagungsbeiträge / Research presentations

J. Schrör, P. Hufendiek, S. Kehraus, M. Gütschow, G. M. König; “Secondary metabolites from the fungus *Stemphylium globuliferum* and their biological activities”, **2015**, Poster presented at the Marine Fungal Natural Product Consortium, Nantes, France

J. Schrör, P. Hufendiek, S. Kehraus, M. Gütschow, G. M. König; “The marine-derived fungus *Stemphylium globuliferum*: metabolites and biological activities”, **2015**, Poster presented at the European Conference of Natural Products, Frankfurt, Germany

## Acknowledgements

I wish to express my sincere gratitude to my supervisor, Prof. Dr. G. M. König, for her expert guidance, encouragement and outstanding support during the course of this project. I would like to thank her for providing excellent scientific working facilities, friendly atmosphere and trust in my work.

I would like to thank Prof. Dr. W. Knöss for officiating as second referee.

My appreciation goes to Prof. Dr. T. Schneider and Prof. Dr. H. Wägele for participating in the examination committee.

A part of this study involved cooperation with other research groups. For this work thanks go to:

Prof. Dr. H.-G. Sahl, Prof. Dr. T. Schneider, Dr. B. Henrichfreise, Dr. A. Klöckner and M. Josten, Institute for Medicinal Microbiology, University of Bonn, for providing antibacterial and chlamydial assays.

Dr. M. Kaiser, Swiss Tropical Institute, Basel, and his research team for evaluating antiprotozoal activities.

Prof. Dr. M. Diederich, S. Ji and the research team from Seoul National University, Seoul, for cytotoxic experiments with pure compounds.

Dr. C. Schoeder and Dr. D. Thimm, Institute for Medicinal Chemistry, University of Bonn, for conducting enzyme assays.

Many specific tasks involved in this study were performed in cooperation with other members of the Institute for Pharmaceutical Biology, University of Bonn. For this work cordial thanks go to:

E. Egereva for isolation of fungal strains, technical assistance and for friendly beginner-support as well as LC-MS measurements and E. Goralski for assistance in all administrative questions.

Dr. Max Crüsemann for performing LC-MS measurements.

Dr. S. Kehraus for performing special NMR experiments, for excellent discussions on analytical data, for proofreading manuscripts and for providing friendly laboratory support.

Dr. K. Fisch for their support during the writing of the thesis.

Raphael Reher, Peter Hufendiek and Antonio Davila for their support during this thesis as well as fruitful discussions of science and society.

Paul Barac for proofreading the thesis and support during the project.

I am grateful to all members of the Institute for Pharmaceutical Biology, University of Bonn, present or past for help and support in the laboratory.



---

<b>Table of contents</b>	<b>Page</b>
<b>1. Introduction</b> .....	<b>1</b>
1.1 Drug discovery from marine-derived fungi .....	1
1.2 Drugs of fungal origin .....	3
1.3 Marine-derived fungi and their associated metabolites .....	4
1.4 Phytopathogenic fungi with a focus of <i>Stemphylium</i> spp. ....	6
1.5 Resorcinol and its mono,- and dialkylated derivatives .....	9
<b>2. Scope of the present study</b> .....	<b>11</b>
<b>3. Materials and methods</b> .....	<b>12</b>
3.1 Origin, isolation and taxonomy of the fungus .....	12
3.2 Cultivation of the fungal strain .....	12
3.3 Extraction of the fungal material .....	13
3.4 Chromatography .....	13
3.4.1 Vacuum liquid chromatography (VLC) .....	13
3.4.2 High performance liquid chromatography (HPLC) .....	13
3.5 Structure elucidation .....	14
3.5.1 NMR spectroscopy .....	14
3.5.2 Mass spectrometry .....	15
3.5.3 UV measurement .....	15
3.5.4 IR spectroscopy .....	16
3.5.5 Optical rotation .....	16
3.5.6 CD spectroscopy .....	17
3.5.7 Molecular modeling .....	17
3.6 Evaluation of biological activity .....	17
3.6.1 Agar diffusion assay in the working group of Prof. König .....	17
3.6.2 Agar diffusion assay in the working group of Prof. Sahl .....	18
3.6.3 Antiprotozoal activity .....	19
3.6.4 Antichlamydial activity .....	20
3.6.4.1 Determination of minimal inhibitor concentration .....	20
3.6.4.2 Cell viability assay .....	20
3.6.5 Radioligand binding studies at CB <sub>1</sub> and CB <sub>2</sub> receptors .....	21
3.6.6 Free fatty acid receptor (FFAR) 1 assay .....	22
3.6.7 Cell viability test .....	22

---

3.6.8	Leukemic cell line assays .....	23
3.6.9	ROS measurements .....	23
3.7	Chemicals and solvents .....	24
<b>4.</b>	<b>Results .....</b>	<b>26</b>
4.1	Novel fungal metabolite stemphyloxin III (1).....	26
4.1.1	Cultivation and extraction of stemphyloxin III (1) .....	26
4.1.2	Isolation of stemphyloxin III (1) .....	27
4.1.3	Structure elucidation of stemphyloxin III (1).....	28
4.1.4	Antimicrobial activity of stemphyloxin III (1).....	32
4.2	Novel fungal metabolite stemphylofuran (2).....	35
4.2.1	Cultivation and extraction of stemphylofuran (2).....	35
4.2.2	Isolation of stemphylofuran (2).....	36
4.2.3	Results and discussion.....	37
4.2.4	Antimicrobial activity of stemphylofuran (2) .....	41
4.3	Fungal metabolite stemphol (3).....	42
4.3.1	Cultivation and extraction .....	42
4.3.2	Isolation of fungal metabolite stemphol (3).....	43
4.3.3	Results and discussion.....	44
4.3.4	Antimicrobial activity of stemphol (3).....	50
4.3.5	Antiparasitic activity .....	52
4.3.6	Radioligand binding studies at CB <sub>1</sub> / CB <sub>2</sub> receptors .....	53
4.3.7	Activity against free fatty acid receptor 1 (FFAR 1) .....	55
4.3.8	Antichlamydial activity .....	57
4.3.9	Cytotoxic activity .....	60
4.3.9.1	Activity towards four different leukemic cell lines.....	60
4.3.9.2	Activity towards reactive oxygen species .....	65
4.4	Further metabolites isolated from <i>Stemphylium globuliferum</i> .....	66
4.4.1	New natural product 4-butyl-3,5-dihydroxy benzoic acid (4).....	66
4.4.1.1	Cultivation and extraction of 4-butyl-3,5-dihydroxy benzoic acid (4) .....	66
4.4.1.2	Structure elucidation of 4-butyl-3,5-dihydroxy benzoic acid (4).....	67
4.4.1.3	Antibacterial activity of 4.....	68
4.4.2	Infectopyrone (5).....	68
4.4.3	Stemphyprone (6).....	69

---

<b>5. Discussion</b> .....	<b>71</b>
5.1 Discussion of the new metabolite stemphyloxin III (1).....	72
5.2 Discussion of the new metabolite stemphylofuran (2).....	72
5.3. Discussion of the metabolite stemphol (3).....	73
<b>6. Summary</b> .....	<b>77</b>
<b>7. References</b> .....	<b>80</b>
<b>8. Appendix</b> .....	<b>87</b>
8.1 NMR, UV and IR spectra of the isolated compounds.....	87

## Abbreviations

°C	degrees celsius
1D	one dimensional
2D	two dimensional
$[\alpha]_D^T$	specific rotatory power; Sodium D-line (589 nm); T: temperature
Å	Ångström
$\delta$	NMR chemical shift [ppm]
$\lambda$	wavelength [nm]
$\mu$	micro ( $10^{-6}$ )
$\nu$	wave number ( $\text{cm}^{-1}$ )
Ac	acetate
ACN	acetonitrile
ASW	artificial seawater
BMS	biomalt salt medium
br	broad
<i>c</i>	concentration
C <sub>18</sub>	C-18 modified silica gel
calcd	calculated
CB	cannabinoid
CB <sub>1</sub>	cannabinoid subtype 1
CB <sub>2</sub>	cannabinoid subtype 2
CD	circular dichroism
CDCl <sub>3</sub>	chloroform- <i>d</i>
CD <sub>3</sub> OD	methanol- <i>d</i> <sub>4</sub>
CH <sub>2</sub> CL <sub>2</sub>	dichloromethane (DCM)
CO <sub>2</sub>	carbon dioxide
CoA	coenzyme A
conc.	concentration
COSY	correlated spectroscopy
CYP	cytochrome P450
cm	$10^{-2}$ meter
d	doublet (in connection with NMR data)

---

Da	Dalton
DAD	diode array detector
DCM	dichloromethane
DEPT	distortionless enhancement by polarization transfer
dm	10 <sup>-1</sup> meter
dmol	10 <sup>-1</sup> mol
DNA	deoxyribonucleic acid
DPPH	2,2-diphenyl-1-picrylhydrazyl
DSM	Deutsche Sammlung von Mikroorganismen und Zellkulturen
EC <sub>50</sub>	half maximal effective concentration (drug concentration causing 50% of maximal effect)
<i>e.g.</i>	for example/ example given
EI	electron impact
ESI	electrospray ionization
<i>et</i>	et [Lat.]: and
<i>et al.</i>	et alii [Lat.]: and others
EtOAc	ethyl acetate
EtOH	ethanol
eV	electron Volt
g	gram
GI	growth inhibition
GI <sub>50</sub>	growth inhibition (drug concentration causing 50% growth inhibition)
GPCR	G protein-coupled receptor
G <sub>i</sub>	adenylate cyclase inhibitory G protein
HMBC	heteronuclear multiple-bond correlation
HPLC	high performance liquid chromatography
HR	high resolution
hrs	hours
HSQC	heteronuclear single quantum correlation
Hz	Hertz
H <sub>2</sub> O	water
IC <sub>50</sub>	Inhibition concentration (drug concentration causing 50% inhibition)
<i>i.e.</i>	id est [lat.] or that is
IFN	interferon

---

IR	infrared
<i>J</i>	spin-spin coupling constant [Hz]
K	Kelvin
kcal	kilocalories
L	liter
m	meter
m	multiplet (in connection with NMR data)
m/z	mass-to-charge ratio (in connection with mass spectrometry)
Me	methyl
MeOH	methanol
MeOD	methanol- <i>d</i> <sub>4</sub>
MeCN	acetonitrile
mg	10 <sup>-3</sup> gram
MHz	megahertz
min	minute
mL	10 <sup>-3</sup> liters
mm	10 <sup>-3</sup> meters
mM	10 <sup>-3</sup> molar
mol. wt.	molecular weight [g/mol]
MS	mass spectrometry
MTT	3-(4,5-dimethylthiazo-2-yl)-2,5-diphenyltetrazolium bromide
NAD(P)	nicotinamide adenine dinucleotide phosphate
n.d.	not determined
NF-κB	nuclear factor kappa B
ng	10 <sup>-9</sup> gram
nm	10 <sup>-9</sup> meter
NMR	nuclear magnetic resonance
no	number
NOE	nuclear Overhauser effect
NOESY	nuclear Overhauser effect spectroscopy
O <sub>2</sub>	oxygen
ORAC	oxygen radical absorbance capacity
p	pentet (in connection with NMR data)
PDA	photodiode-array

---

PE	petroleum ether
pH	potentia hydrogenii
PKS	polyketide synthase
ppm	parts per million
q	quartet (in connection with NMR data)
RP	reversed phase
RT	room temperature
s	singlet (in connection with NMR data)
SAR	structure activity relationship
sec	second
SEM	standard error of the mean
Si	silica gel
SoAc	Sodiumacetate
sp.	species
spp.	species (plural)
t	triplet (in connection with NMR data)
TI	total inhibition
TLC	thin layer chromatography
UV	ultraviolet
ver.	version
VLC	vacuum-liquid chromatography

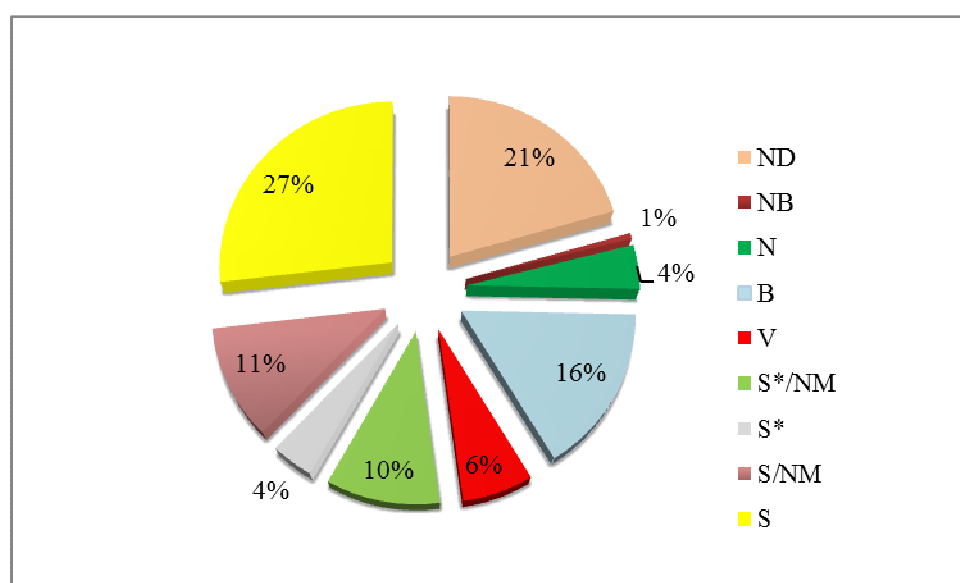


## 1. Introduction

### 1.1 Drug discovery from marine-derived fungi

Natural products are produced by all living organisms, and as primary metabolites serve the basic survival. In medicinal chemistry natural products are defined as secondary metabolites, that are biosynthesized for their biological function, *e.g.* to defend the producer against predators or competitors. They are known to be essential in pharmacology for the search and development of novel drugs. This is due to their bewildering diversity of carbon skeletons and scaffolds, resulting in a remarkable structural complexity. In the period of 1981 to 2014 over 50 % of 1562 new approved drugs were natural products, natural product derivatives or synthetic compounds with natural product derived origin (Newman und Cragg 2016) (Figure 1). This demonstrates the importance of natural product drugs for therapy, and also their usefulness as lead compounds that can be optimized to gain novel drugs.

**Figure 1: New approved drugs from 1981-2014 and their origin: n = 1562, adapted from Newmann and Cragg, 2016**

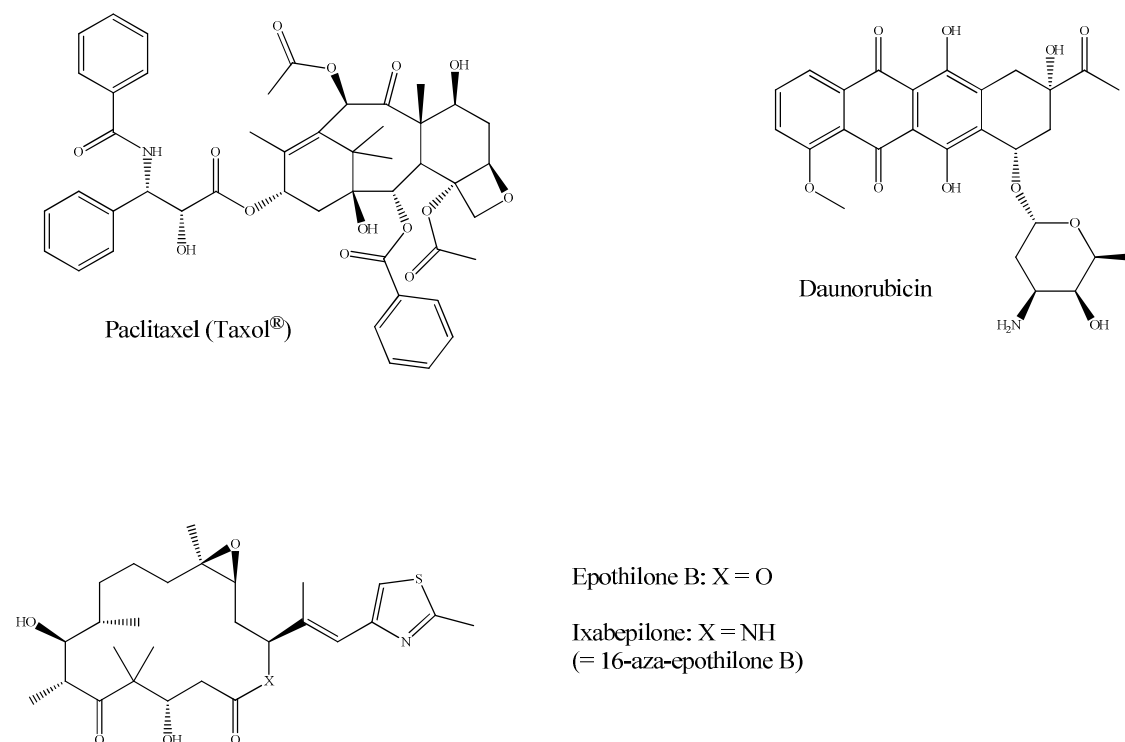


---

The most prominent producers of therapeutic natural products are three groups of organisms: plants, bacteria and fungi.

Plants were used for thousands of years for medicinal purposes, *e.g.* in the Traditional Chinese Medicine (TCM). The WHO estimated that approximately 65% of the population of the world predominantly relied on plant-derived traditional medicines for their primary health care (Fransworth et al. 1985). In 1971, Paclitaxel (Taxol<sup>®</sup>), as seen in Figure 2, was firstly isolated from the pacific yew tree (Wani et al. 1971). It is an inhibitor of the mitosis process in cells by interfering with the normal function of microtubule breakdown. It binds to  $\beta$ -tubulin thus arrests microtubule function. This way cells cannot use their cytoskeleton in a flexible manner (McGrogan et al. 2008). The semi-synthetic analog docetaxel (Taxotere<sup>®</sup>) and later the third generation taxane cabazitaxel (Jevtana<sup>®</sup>), which is approved for the treatment of hormone-refractory prostate cancer (Galsky et al. 2010), are successful examples of plant-based antitumor drugs.

Within the group of bacteria, actinomyces, myxobacteria and cyanobacteria are playing a major role as natural product producing organisms. Bacteria of the genus *Streptomyces*, produce, *e.g.* antitumor agents interacting with DNA like daunorubicin (Minotti et al. 2004). The myxobacterium *Sorangium cellulosum* produces epothilone B (Figure 2). A semi-synthetic derivative thereof is ixabepilone, which acts as microtubule-stabilizing agent like the taxanes described above and is used for the treatment of metastatic breast cancer since 2007 (WHO 2007) (Mani et al. 2007).

**Figure 2: Examples of antitumor lead structures and drugs from plants and bacteria**

## 1.2 Drugs of fungal origin

Fungi are a vast group of organisms, which produce a wide range of pharmaceutically significant compounds, belonging to all structural classes.

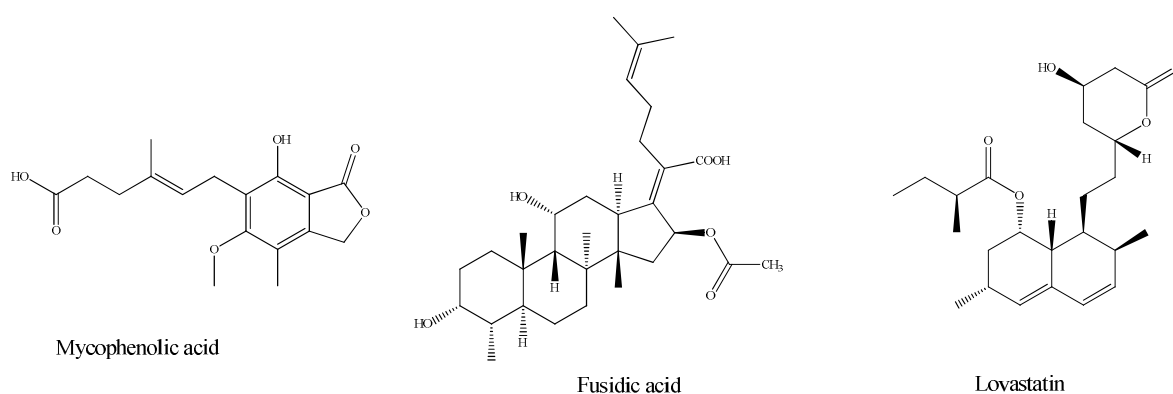
A most important fungal metabolite is the immunosuppressant drug mycophenolic acid (Figure 3). Already isolated in 1893, it was approved by the FDA in 1995 and is used for the prophylaxis of organ rejection in patients receiving an allogeneic renal transplant (FDA 2009). The dosage form is the prodrug mycophenolat-mofetil, which is metabolized in the body to the desired mycophenolic acid.

Fusidic acid (Figure 3) is a tetracyclic terpenoid compound from the fungus *Fusidium coccineum*, firstly investigated in the early 1960s as an antibacterial agent with strong *in vitro* activity against Gram-positive bacteria (Godtfredsen et al. 1962). The growing resistance posed by methicillin resistant *Staphylococcus aureus* (MRSA) and other staphylococcal infections has led to a revived interest in the use of fusidic acid in recent years. *In vitro* assays with fusidic acid showed efficacy against most staphylococcal infections, including those

caused by MRSA, vancomycin-intermediate *S. aureus* and most coagulase-negative staphylococci (Howden and Grayson 2006).

The statine lovastatin, isolated from *Aspergillus terreus*, is used as a cholesterol lowering agent and served also as a lead structure for *e.g.* pravastatin, a second generation drug thereof (Figure 3). Statins inhibit the activity of (3*S*)-hydroxy-3-methyl-glutaryl-coenzyme A (HMG-CoA) reductase by occupying a portion of the binding site of HMG-CoA, thus blocking access of this substrate to the active site. Near the carbonyl terminus of the reductase, several catalytically relevant residues are disordered in the enzyme-statin complex. HMG-CoA reductase catalyzes the formation of mevalonate, which is the limiting step in hepatic cholesterol synthesis.

**Figure 3: Examples of drug and drug lead structures from fungi**



### 1.3 Marine-derived fungi and their associated metabolites

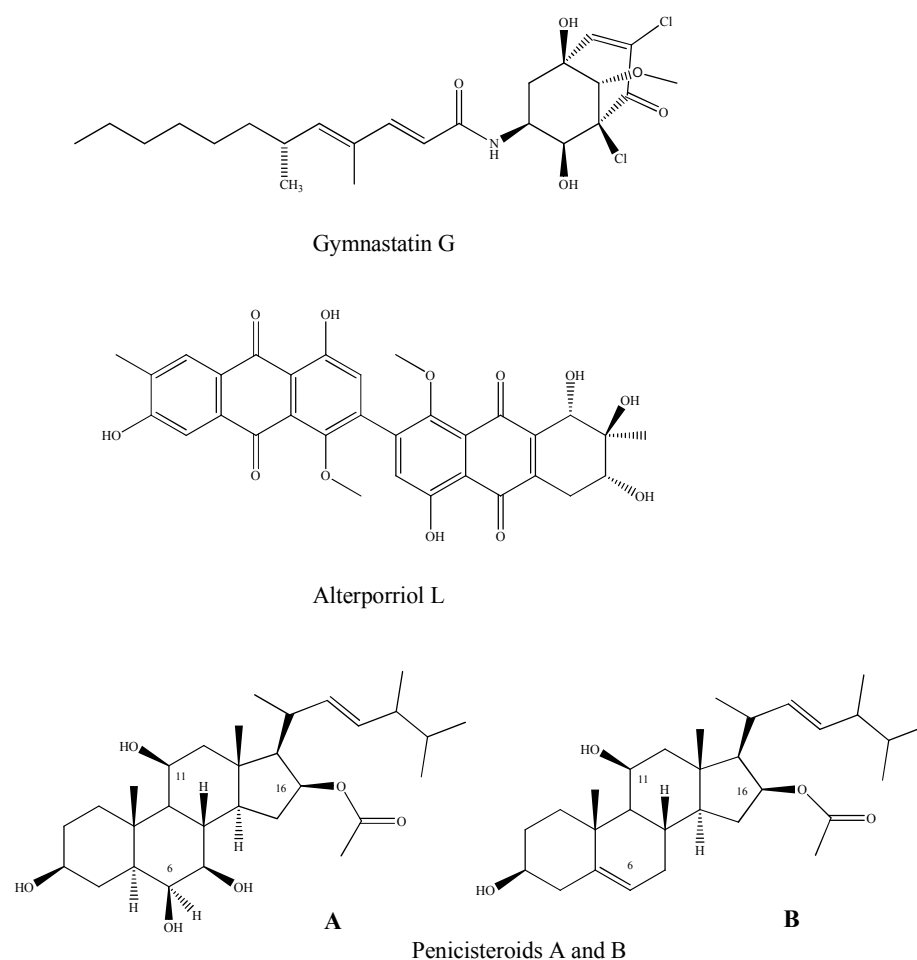
Besides the terrestrial fungi discussed above, fungal strains are also found in various, often underexplored habitats and their metabolomes are judged as valuable sources of bioactive compounds. The study of marine fungi has been mostly neglected for different reasons, *e.g.* the doubt of the existence of truly marine fungi or their low abundance in the environment. This attitude changed in recent years due to the fact that structurally diverse secondary metabolites were obtained from marine-derived fungi, and thus a considerable number of pharmaceutically relevant bioactivities and possible candidates for the development of new drugs were found (Imhoff 2016). Whereas in the whole year 1992 only 15 metabolites were reported from marine-derived fungi, the systematic chemical characterization of fungi from

the marine environment has now provided a large number of natural products from this source, some of them with clinically relevant pharmacological activity (Jin et al. 2016).

Most of the published data have a focus on just a few genera: *Aspergillus*, *Cladosporium*, *Fusarium* and *Penicillium* (Imhoff 2016). Many of these fungi are excellently adapted to the marine habitat, e.g. deep-sea hydrothermal ecosystems, algae or sponges. As obvious from the above mentioned genera many of the marine-derived fungal metabolites are similar to those of their terrestrial counterparts. However, examples like gymnastatin G with an unusual carbon skeleton indicate that marine fungal strains possess distinct biosynthetic capabilities (Bugni and Ireland 2004) (Figure 4). Gymnastatin G contains a unique bicyclo[3.3.1]nonane ring, and was found to exhibit potent growth inhibition against P388 leukemia cancer cell lines with an ED<sub>50</sub> of 0.03 µg/ml (Amagata et al. 2006) (Figure 4).

Alterporriol L, which was isolated from the marine-derived fungus *Alternaria* sp. showed modest cytotoxicity against two human breast cancer cell lines (MDA-MB-435 and MCF-7) with IC<sub>50</sub> values of 13.1 to 20.0 µM (Huang et al. 2011) (Figure 4). The cytotoxic effect was due to apoptosis and necrosis. The dose-dependent manner of cell death by the increased levels of cytosolic free calcium and the reactive oxygen species production as well as induced loss of mitochondrial membrane potential suggested that alterporriol L caused major stress in breast cancer cells by destroying mitochondria (Huang et al. 2012). Furthermore, a mixture of derivatives including alterporriol G and H showed considerable cytotoxicity against L5178Y mouse lymphoma cells with an EC<sub>50</sub> value of 2.7 µg/ml (Debbab et al. 2009).

Marine algicolous fungi produce unique and complex structural metabolites with a broad spectrum of biological activities, e.g. cytotoxic or antioxidant effects. Gao et al. investigated the new polyoxygenated steroids penicisteroids A and B, which were obtained from the extract of *Penicillium chrysogenum* QEN-24S, an endophytic fungus isolated from an unidentified marine red algal species of the genus *Laurencia* (Figure 4). Penicisteroid A, a structurally new steroid having four hydroxyl and a C-16-acetoxy group, displayed potent inhibitory activity against the pathogenic fungus *Aspergillus niger*, as well as selective cytotoxicity against cancer cell lines, e.g. an IC<sub>50</sub> of 15 µg/ml towards HeLa cells. Although steroids are one of the most abundant classes of natural products reported so far, only two structurally similar steroids containing a 11-OH and 16-OAc group have been reported (Mori et al. 2003a; Mori et al. 2003b; Igarashi et al. 2002). It is assumed, that the hydroxyl group at C-6 in the B ring is essential for the cytotoxicity, since the derivative without the hydroxyl group showed no activity (Gao et al. 2011).

**Figure 4: Examples of natural products from marine-derived fungi with cytotoxic activity**

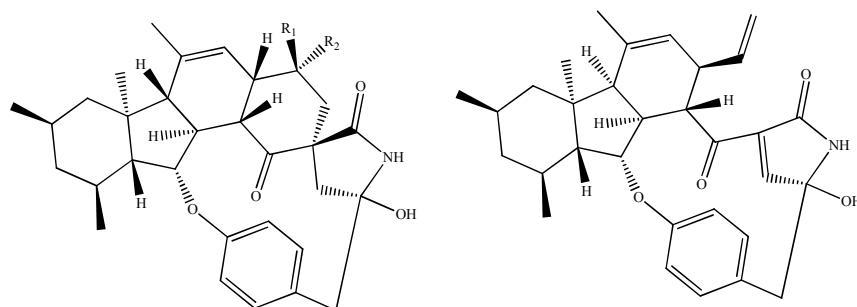
#### 1.4 Phytopathogenic fungi with a focus of *Stemphylium* spp.

In this study, the focus is on natural products produced by a fungus from the marine habitat, *i.e.* *Stemphylium globuliferum* isolated from the alga *Petalonia zosterifolia*. This alga-derived fungus is in the literature described for its phytotoxicity (Koike et al. 2013). Phytopathogenic fungi are rarely investigated for their bioactive compounds, but clearly have the potential to yield new lead structures.

Fungal damages to plants and especially agricultural plants is widely observed, *e.g.* *Neonectria ramulariae*, causes seed rot in japanese beech (Hirooka et al. 2012). Seeds of this plant (*Fagus crenata*) are eaten raw or cooked. *N. ramulariae* is producing pyrrospirones A

and B (Figure 5), which exhibit cytotoxicity and induced apoptosis of promyelocytic leukemia cells at a concentration of 30  $\mu\text{M}$  (Shiono et al. 2008). Pyrrocidine A and B, derivatives of pyrrospirones, showed potent antibiotic activity against MRSA at MIC values of 2 and 4  $\mu\text{g/ml}$ , respectively, as well as weaker activity towards *Candida albicans* and *Streptococcus pneumoniae* (He et al. 2002).

**Figure 5: Examples of bioactive compounds from phytopathogenic fungi**



$R_1 = \text{H}, R_2 = \text{OH}$  Pyrrospirone A

Pyrrocidine A

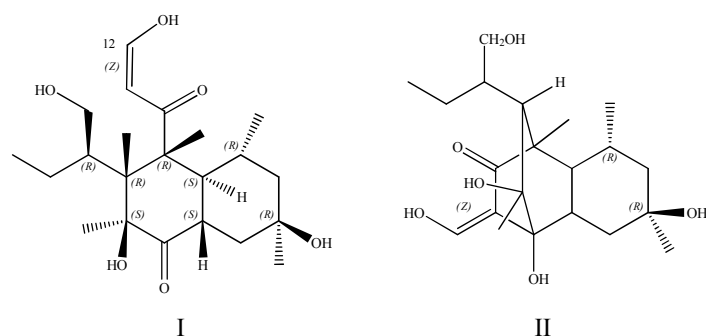
$R_1 = \text{OH}, R_2 = \text{H}$  Pyrrospirone B

The here investigated fungus *S. globuliferum* is a mold fungus and belongs to the Pleosporaceae, and was firstly described by Simmons in 1969 (Simmons 1969). Previously, the focus of research on *Stemphylium* spp. targeted the prevention of agricultural damages caused by these organisms. *Stemphylium* spp. are responsible for the leaf spot of lettuce, but also have been reported to infect different hosts worldwide to cause leaf spot symptoms (e.g. eggplant, pepper and tomato) (Nasehi et al. 2012, 2014) (Gannibal 2013) (Barash et al. 1975) (Andersen and Frisvad 2004). The *Stemphylium* leaf spot disease, caused by *S. vesicarium* and the closely related *S. botryosum* leads to the so called purple spot disease on *Asparagus officinalis*, which is the most important disease in German asparagus growing regions (Graf et al. 2016). Fungicides like epoxiconazol or prochloraz inhibit fungal ergosterol biosynthesis and can be used for prevention of the disease (Zapf et al. 2011).

Stemphyloxin I is a phytotoxin, which was firstly isolated from *S. botryosum*. This fungal metabolite is a natural compound possessing an enol group on C-12 (Figure 6), which may be in equilibrium with an aldehyde function via keto-enol-tautomerism. Injections of stemphyloxin I into tomato leaflets caused necrotic spots and wilted the whole leaf with visible symptoms beginning at 2.7  $\mu\text{M}$ . A derivative of stemphyloxin I, where the enol group is methylated, revealed a reduction of approximately 50 times in inhibitory activity as

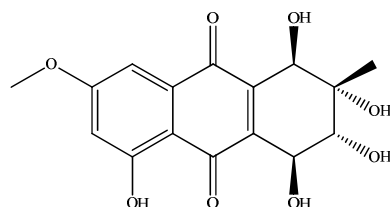
compared to the toxin (Barash et al. 1982). The tricyclic compound stemphyloxin II is approximately 100 times weaker compared to stemphyloxin I (Manulis et al. 1984).

**Figure 6: Stemphyloxin I and II**



Altersolanol A, which was found in *S. globuliferum* has an effect on K562 cells (Figure 7), with IC<sub>50</sub> values of 4 and 2.5 μM after 24 h and 48 h exposure, respectively. The anti-tumoral potential is linked to its pro-apoptotic and anti-invasive activity, which is caused by the inhibition of NF-κB transcriptional activity. This biological effect is related to the p-quinone moiety of the molecule (Teiten et al. 2013). The significance of a quinone moiety in potential anticancer molecules was also reported for the plant-derived anthraquinone parietin, which induces apoptosis in human cervical carcinoma HeLa cells by activating the caspase-3 pathway and forming reactive oxygen species (Wijesekara et al. 2014).

**Figure 7: Altersolanol A from *S. globuliferum***



*Stemphylium* spp., is also known for the production of the phytotoxin stemphol (Figure 8). It is a 2,5-dialkylated resorcinol with a butyl- and pentyl-chain attached to the aromatic ring in the C-2 and C-5 position, respectively. It has significant inhibitory activity towards the phylogenetically related fungus *Pleospora herbarum*. At 400 μg/ml stemphol tested, more

than 63% inhibition of self growth was observed for *P. herbarum* (Marumo et al. 1985). Furthermore, stemphol showed antibacterial activity against *B. subtilis* and *S. aureus*, as well as the yeast *Schizosaccharomyces pombe* and the plant pathogenic fungus *Mucor hiemalis* (Achenbach et al. 1979).

In bacteria, stemphol is biosynthetically produced by connecting a  $\beta$ -keto-acyl precursor with an  $\alpha,\beta$ -unsaturated acyl precursor followed by oxidation to form a dialkylresorcinol. Compared to the monoalkylresorcinols, which are synthesized by an iterative type III polyketide synthase (PKS III) that performs multiple catalytic reactions, PKSs responsible for dialkylresorcinol production only catalyze one reaction, *i.e.* the connection of the above mentioned precursors (Schöner et al. 2015).

However, a fungal gene cluster responsible for stemphol formation has not been found yet. This is in contrast to bacteria, for which such biosynthetic gene cluster are known (Schöner et al. 2015).

## 1.5 Resorcinol and its mono,- and dialkylated derivatives

The *S. globuliferum* derived stemphol (Figure 8) discussed in this thesis is part of a whole class of resorcinol derivatives.

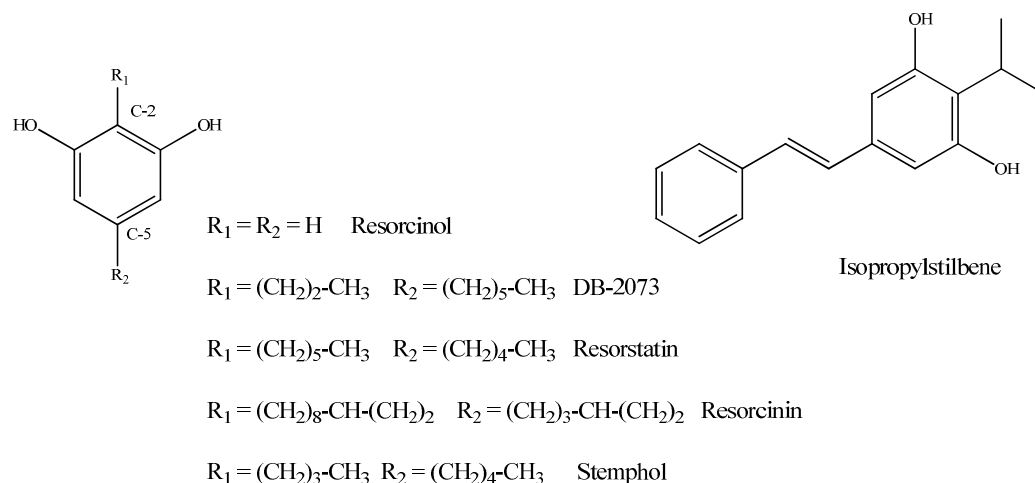
Resorcinol and its mono and dialkylated derivatives display a broad spectrum of biological activities (Figure 8). Resorcinol is an ingredient in skin protectant formulations like Resinol<sup>®</sup> or Clearasil<sup>®</sup>, and it is used for the treatment of psoriasis or seborrheic dermatitis. Due to high contents of resorcinol in argan oil this is utilized in the traditional Moroccan medicine against acne juvenile and flaking of the skin, but also against rheumatism and for the treatment of burns (Charrouf and Guillaume 2007) (El Babili et al. 2010).

Monoalkylated 4-hexylresorcinol inhibits NF- $\kappa$ B phosphorylation and has a synergistic effect with cisplatin, leading to a significantly decreased tumor growth rate in mice with cancer (Kim et al. 2011). In the past, it has been mainly used for antiparasitic purposes, until much more effective antiparasitic agents have been developed (Rabbani et al. 1985) (Pink et al. 2005). 5-Alkylated resorcinols showed moderate antibacterial and antifungal activity (Achenbach et al. 1979).

The 2,5-dialkylated derivatives like stemphol were shown to have an even broader antimicrobial spectrum. One example is DB-2073, where a propyl chain at the C-2 position and a hexyl chain at the C-5 position, are attached to the benzene ring. DB-2073 was firstly

isolated from *Pseudomonas* sp. B-9004 from a soil sample (Kanda et al. 1975) and its total synthesis is known (Covarrubias-Zúñiga et al. 2003). It is active against mycobacteria, yeasts, fungi and Gram-positive bacteria (e.g. MIC 25  $\mu\text{M}$  towards *St. aureus*) (Kanda et al. 1975). DB-2073 has free radical scavenging activity preventing lipid peroxidation. At an  $\text{IC}_{50}$  of 2.74  $\mu\text{M}$  concerning lipid peroxidation induced by free radicals, DB-2073 is much more active than flunarizine ( $\text{IC}_{50}$ : 55.0  $\mu\text{M}$ ). The latter is a migraine protective drug with free radical scavenging activity, and is less active than butylated hydroxytoluene (BHT,  $\text{IC}_{50}$ : 2.4  $\mu\text{M}$ ), a common antioxidant. Similar results were shown for resorstatin with an  $\text{IC}_{50}$  of 2.06  $\mu\text{M}$  (Kato et al. 1993). Besides the free radical scavenging activity of resorstatin (Figure 8), it has a weak antibacterial activity towards *B. subtilis* (Kato et al. 1993). Resorcinin, a derivative thereof, stimulates the proliferation of NIH 3T3 mouse fibroblasts cells at concentrations from 0.2  $\mu\text{g}/\text{ml}$  to 2  $\mu\text{g}/\text{ml}$ . The activity is slightly higher than that for a monoalkyl long chain reference. Isopropylstilbene (Figure 8), which has antiproliferative activity (Buscato et al. 2013) is another example for the structural and biological diversity of this class of molecules. Regarding resorcinol derivatives, a recent review by Schöner et al. summarizes occurrence, structural diversity, bioactivity and biosynthesis of these natural products (Schöner et al. 2015).

**Figure 8: Resorcinol and its mono,- and dialkylated derivatives**



---

## 2. Scope of the present study

The search for compounds possessing bioactivity and consequently pharmaceutical relevance is in high demand. Marine-derived fungi are a group of microorganism producing a wide range of pharmaceutically significant compounds belonging to different structural classes. This source of bioactive products is still very little investigated. This study focusses on the marine-derived fungus *Stemphylium globuliferum* strain No. 384, isolated from the alga *Petalonia zosterifolia*, and collected at the Baltic Sea, for the identification and aims of possible new lead structures for pharmaceutically purposes. The here investigated fungus is known for its phytopathogenity resulting massive agricultural damages.

In this study the main aspect lies on the investigation of this fungus from a different point of view. Is it possible to turn the known negative properties into positive pharmacological aspects? Furthermore the isolation from the unusual salt water habitat underlies the possibility to gain new bioactive natural products from this poorly investigated research area.

### **3. Materials and methods**

#### **3.1 Origin, isolation and taxonomy of the fungus**

The endophytic fungal strain, described in this study, was obtained from the fungal culture collection of Professor G. M. König (Institute for Pharmaceutical Biology, University of Bonn), and was isolated by Ekaterina Egereva using an indirect isolation method. The alga sample was rinsed three times with sterile H<sub>2</sub>O. After surface sterilization with 70% EtOH for 15 s, the alga was rinsed in sterile artificial seawater (ASW). Subsequently, the alga material was aseptically cut into small pieces and placed on agar plates containing isolation medium: agar 15 g/L, ASW 800 mL/L, glucose 1 g/L, peptone from soymeal 0.5 g/L, yeast extract 0.1 g/L, benzylpenicillin 250 mg/L, and streptomycin sulfate 250 mg/L. The fungus growing out of the alga material was separated on biomalt medium (biomalt 20 g/L, agar 10g/L, ASW 800 mL/L) until the culture was pure. The isolated fungus was identified by C. Decock and P. Massart, BCCM/MUCL, Catholic University of Louvain, Belgium. A specimen is deposited at the Institute for Pharmaceutical Biology, University of Bonn, strain number 384.

#### **3.2 Cultivation of the fungal strain**

For the screening examination, fungal strains were cultivated in petri dishes for fourty days on three different media: (a) biomalt salt agar medium, (b) potato dextrose agar medium, and (c) malt peptone yeast medium. For pre-cultivation, the fungal strains were inoculated on petri dishes with biomalt agar medium and incubated at 25 °C for 4 weeks. The large scale cultivation of the fungi was processed in 40 Fernbach flasks at room temperature and permanent light using three solid media (250 ml each), *e.g.* biomalt salt agar medium, potato dextrose agar medium, or potato dextrose with 0.1 % Sodiumacetate medium.

(a) Biomalt agar medium: 20 g/L biomalt, 15 g/L agar and 1 L ASW.

(b) Malt-yeast agar medium: 4 g/L yeast extract, 10 g/L malt extract, 4 g/L glucose, 15 g/L agar and 1 L ASW, pH 7.3.

(c) Potato dextrose agar medium: 15 g/L potato dextrose broth, 15 g/L agar and 1 L ASW.

---

Artificial seawater (ASW): [g/L] KBr (0.1), NaCl (23.48),  $\text{MgCl}_2 \times 6 \text{H}_2\text{O}$  (10.61),  $\text{CaCl}_2 \times 2 \text{H}_2\text{O}$  (1.47), KCl (0.66),  $\text{SrCl}_2 \times 6 \text{H}_2\text{O}$  (0.04),  $\text{Na}_2\text{SO}_4$  (3.92),  $\text{NaHCO}_3$  (0.19) and  $\text{H}_3\text{BO}_3$  (0.03).

### **3.3 Extraction of the fungal material**

Cultivation medium and mycelia were homogenized using an Ultra-Turrax T45 apparatus and extracted three times with ethyl acetate.

## **3.4 Chromatography**

### **3.4.1 Vacuum liquid chromatography (VLC)**

Sorbents for VLC were silica gel 60 (0.063-0.200 mm, Merck) or silica gel 60 (0.040-0.063 mm, Merck). Columns were wet-packed under vacuum, using PE or dichloromethane for normal-phase, and MeOH for reversed-phase conditions. Glass wool layer above the sorbent material was used to protect the sorbent material against disturbance. Before applying the sample solution, the columns were equilibrated with the first designated eluent.

### **3.4.2 High performance liquid chromatography (HPLC)**

Preparative HPLC was carried out using four different systems. A: Waters system, controlled by Waters Millennium software, consisting of a 600E pump, a 996 photodiode array detector, and a 717 plus autosampler; B: Merck-Hitachi HPLC system Model D-7000 Chromatography Data Station Software HPLC system Manager Version 4.0 software, consisting of L-6200A pump, D-6000A interface and L4500 photodiode array detector; C: HP ChemStation for LC.Rev.A.06.03[909] software, consisting of a L-7100 Merck Hitachi pump and a HP-series 1050 detector; D: Waters System 1525 $\mu$  equipped with Binary pump and 2998 photodiode array detector and Breeze 2 software, 2008; E: Reverleris Grace X2 flash-chromatography system equipped with pump, autosampler, UV- and RI-detector.

Columns used were either a: Knauer Si Eurospher-100 (5  $\mu\text{m}$ , 250 x 8 mm), b: Knauer C<sub>18</sub> Eurospher-100 (5  $\mu\text{m}$ , 250 x 8 mm), c: Macherey-Nagel Nucleodur 100-5 C<sub>18</sub> (5  $\mu\text{m}$ , 250 x 4.6 mm), d: Macherey-Nagel Nucleoshell C<sub>18</sub> (5  $\mu\text{m}$ , 250 x 4.6 mm), e: Phenomenex Kinetex C<sub>18</sub> (5  $\mu\text{m}$ , 250 x 4.6 mm) or Grace Reveleris SRC C<sub>18</sub> cartridge (12g).

### 3.5 Structure elucidation

Structures were elucidated mainly using one and two dimensional NMR techniques in combination with various MS methods. Optical rotation data as well as the UV and IR spectroscopic properties provided additional information. The relative and absolute stereochemistry of the new compounds was assigned using NOESY experiments. The identity of isolated compounds in comparison to previously published structures was judged on <sup>1</sup>H NMR and <sup>13</sup>C NMR data and other spectroscopic data, as well as specific optical rotation. In addition, calculated NMR shifts of the assumed structures with ACD (Labs-software, 2006) assisted in the elucidation of most structures. Based on literature searches, using MarinLit database<sup>®</sup>, Sci Finder database<sup>®</sup> and AntiBase database<sup>®</sup>, the structures were classified as new, if they could not be found in any of these databases.

#### 3.5.1 NMR spectroscopy

All NMR spectra were recorded using either a Bruker Avance 300 DPX operating at 300 MHz (<sup>1</sup>H) and 75 MHz (<sup>13</sup>C) or a Bruker Ascend 600 spectrometer operating at 600 MHz for (<sup>1</sup>H) and 150 MHz for (<sup>13</sup>C) respectively. NMR spectra were processed using Bruker 1D WIN-NMR, 2D WIN-NMR or XWIN-NMR Version 2.6, 3.1 and 3.5 software, or Bruker TopSpin software package Version 1.3. Spectra were recorded in CDCl<sub>3</sub>, acetone-*d*<sub>6</sub> or CD<sub>3</sub>OD and were referenced to residual solvent signals with resonances at  $\delta_{\text{H/C}}$  7.26/77.0 (CDCl<sub>3</sub>), 2.04/29.8 (acetone-*d*<sub>6</sub>) and 3.35/49.0 (CD<sub>3</sub>OD). Multiplicity of carbons was deduced by <sup>13</sup>C and DEPT experiments. Structural assignments were based on spectra resulting from one or more of the following NMR experiments: <sup>1</sup>H, <sup>13</sup>C, DEPT 135, <sup>1</sup>H-<sup>1</sup>H-COSY, <sup>1</sup>H-<sup>13</sup>C direct correlation (HSQC), <sup>1</sup>H-<sup>13</sup>C long range correlation (HMBC), <sup>1</sup>H-<sup>1</sup>H Overhauser Enhancement Spectroscopy (NOESY). Two dimensional NMR measurements were guided by

---

Dr. Stefan Kehraus (Institute for Pharmaceutical Biology, University of Bonn, Germany) or Dr. Sedana Nozinovic (Institute for Inorganic Chemistry, University of Bonn, Germany).

### 3.5.2 Mass spectrometry

HPLC-ESIMS (referred to as LC-MS or HPLC-MS) measurements were performed by Ekaterina Egereva (Institute for Pharmaceutical Biology, University of Bonn, Germany) employing an Agilent 1100 Series HPLC including DAD, with RP C<sub>18</sub> column (Macherey-Nagel Nucleodur 100, 125 mm x 2 mm, 5 μm) and gradient elution (0.25 mL/min, NH<sub>4</sub>Ac buffer 2 mmol, from MeOH 10: H<sub>2</sub>O 90 in 20 min to 100% MeOH, then isocratic for 10 min), coupled with an API 2000, Triple Quadrupole LC/MS/MS, Applied Biosystems/MDS Sciex and ESI source. The analyzed extracts, fractions and pure compounds were solved in MeOH (1 mg/ml) for injection into the HPLC-ESIMS system.

HPLC-MS/MS experiments were recorded on a micrOTOF-Q mass spectrometer (Bruker) with ESI-source coupled with a HPLC Dionex Ultimate 3000 (Thermo Scientific) using a EC10/2 Nucleoshell C<sub>18</sub> 2.7 μm column (Macherey-Nagel). The column temperature was 25°C. MS data were acquired over a range from 100-3000 m/z in positive mode. Auto MS/MS fragmentation was achieved with rising collision energy (35-50 keV over a gradient from 500-2000 m/z) with a frequency of 4 Hz for all ions over a threshold of 100. HPLC begins with 90 % H<sub>2</sub>O containing 0.1% acetic acid. The gradient starts after 1 min to 100%. Acetonitrile (0.1% acetic acid) in 20 min. 5 μl of a 1mg/ml sample solution was injected to a flow of 0.3 ml/min.

### 3.5.3 UV measurement

UV spectra were recorded on a Perkin-Elmer Lambda 40 with UV WinLab Version 2.80.03 software, using 1.0 cm quartz cells. Compounds were measured in methanol, chloroform or acetonitrile. The molar absorption coefficient was determined in accordance with the Beer-Lambert Law:

---

$$A = \varepsilon \cdot c \cdot d \Leftrightarrow \varepsilon \left[ \frac{\text{L}}{\text{mol} \cdot \text{cm}} \right] = \frac{A}{c \left[ \frac{\text{mol}}{\text{L}} \right] \cdot d [\text{cm}]}$$

A : absorption at peak maximum

c : concentration

$\varepsilon$  : molar extinction coefficient

d : layer thickness of solution

### 3.5.4 IR spectroscopy

IR spectra were recorded using a Perkin-Elmer FT-IR Spectrum BX spectrometer interfaced with a Specac Golden Gate Diamond ATR system. Analysis and reporting were performed with Spectrum v3.01 software.

### 3.5.5 Optical rotation

Optical rotation measurements were conducted on a Jasco model DIP-140 polarimeter (1 dm, 1 cm<sup>3</sup> cell) operating at  $\lambda = 589$  nm corresponding to the sodium D line at room temperature. Specific optical rotation  $[\alpha]_{\text{D}}^{\text{T}}$  was calculated pursuant to:

$$[\alpha]_{\text{D}}^{\text{T}} = \frac{100 \cdot \alpha}{c \cdot l}$$

$\alpha$  : rotation angle in degree

T : temperature [°C]

D : sodium D line at  $\lambda = 589$

c : concentration [g/100 mL]

l : cell length [dm]

The compounds were dissolved either in MeOH or chloroform. The rotation angles  $\alpha$  were determined as an average value based on at least 10 measurements.

### 3.5.6 CD spectroscopy

CD spectra were recorded in MeOH or CH<sub>3</sub>CN at room temperature using a JASCO J-810-150S spectropolarimeter with the kind help of Carsten Siering and Prof. Dr. S. Waldvogel, Kekulé-Institute for Organic Chemistry and Biochemistry, University of Bonn, Germany. The path length was  $l = 0.1$  cm. The CD (circular dichroism) was measured as ellipticity  $\Theta$  (in mdeg, millidegrees) and subsequently converted into the molar ellipticity  $[\Theta]_M$  and finally into  $\Delta\epsilon$  in accordance to the following equation, taken from Hesse, Meier and Zeeh, 1995:

$$[\Theta]_M = \frac{\Theta \times M}{100 \times c \times l} = 3.3 \times 10^3 \times \Delta\epsilon$$

$\Theta$  = ellipticity [degrees]

$[\Theta]_M$  = molar ellipticity [degrees  $\times$  cm<sup>2</sup>/dmol]

$c$  = concentration [mg/mL]

$l$  = path length [dm]

$M$  = molecular weight [g/mol]

### 3.5.7 Molecular modeling

All models were calculated employing conformation search (Boltzman jump) and a standard force field as implemented in the Cerius2 4.0 (MSI) molecular modeling software package. Models were further refined with 1500 iterations of minimization. Calculations were performed using a Silicon Graphics O2 workstation (Irix 6.5.6).

## 3.6 Evaluation of biological activity

### 3.6.1 Agar diffusion assay in the working group of Prof. König

Antimicrobial tests of extracts and isolated pure compounds were performed by Edith Neu (Institute for Pharmaceutical Biology, University of Bonn) following the method described by Schulz et al. (Schulz et al. 1995). The bacteria *Bacillus megaterium* de Bary (Gram-positive) and *Escherichia coli* (Migula) Castellani & Chambers (Gram-negative), the fungi *Microbotryum violaceum* (Pers.) Roussel (Ustomycetes), *Eurotium rubrum* (formerly *E. repens*) König, Spieckermann & Bremer (Ascomycetes) (all from DSMZ; Braunschweig, Germany) and *Mycotypha microspora* Fenner (Zygomycetes) (kindly provided by B. Schulz, Institute of Microbiology, University of Braunschweig, Germany) were used as test organisms. Sample solutions contained 1 mg/ml per test sample. 50  $\mu$ L (equivalent to 50  $\mu$ g) of each solution were pipetted onto a sterile antibiotic filter disk (Schleicher and Schell 2668), which was then placed onto the appropriate agar medium and sprayed with a suspension of the test organism. Growth media, preparation of spraying suspensions, and conditions of incubation were carried out according to Schulz et al. (Schulz et al., 1995). Growth inhibition was defined as follows: growth of the appropriate test organism was significantly inhibited compared to a negative control; total inhibition: no growth at all in the appropriate zone. Benzyl penicillin (1 mg/ml MeOH), streptomycin (1 mg/ml MeOH) and micronazole (0.5 mg/mL DCM) were used as positive controls.

### **3.6.2 Agar diffusion assay in the working group of Prof. Sahl**

Antimicrobial tests of extracts and isolated pure compounds were performed by Michaele Josten (Institute for Medicinal Microbiology, University of Bonn). Culture plates (5% sheep blood Columbia agar, BD) were overlaid with 3 ml Tryptic soy soft agar, inoculated with TSB (Tryptic soy broth, Oxoid) growth suspension of the bacteria to be tested. Compounds were diluted to a concentration of 1 mg/ml (Syringomycin 0.5 mg/ml) with DMSO and 3  $\mu$ L of this dilution were placed on the surface of the agar. Compounds diffuse into the agar and the size of the inhibition zone was measured after 24 hours incubation at 37 °C.

### **MIC determinations**

MIC determinations were carried out in microtiter plates. Strains were grown in half-concentrated Mueller-Hinton broth (Oxoid). MICs with serial twofold dilution steps were performed (1:2). Bacteria were added to give a final inoculum of 10<sup>5</sup> CFU/mL in a volume of

---

0.2 mL. After incubation for 24 hours at 37 °C the MIC was read as the lowest compound concentration causing inhibition of visible growth.

### 3.6.3 Antiprotozoal activity

The antiprotozoal tests were performed by Dr. M. Kaiser (Swiss Tropical Institute, Basel, Switzerland). Antiplasmodial activity was determined against the K1 strain of *Plasmodium falciparum*, using a modified [<sup>3</sup>H] hypoxanthine incorporation assay. Briefly, infected human erythrocytes were exposed to serial drug dilutions in microtiter plates for 48 h at 37° C in a gas mixture with reduced oxygen and elevated CO<sub>2</sub>. [<sup>3</sup>H] hypoxanthine was added to each well and after further incubation for 24 h the wells were harvested on glass fiber filters and counted in a liquid scintillation counter. From the sigmoidal inhibition curve the IC<sub>50</sub> value was calculated. Chloroquine was used as positive control in each test series.

Activity against *Trypanosoma brucei rhodesiense* (strain STIB 900), the causative agent of African sleeping sickness, was evaluated according to Ráz et al. (Ráz et al. 1997). Parasites were grown axenically in culture medium supplemented with horse serum. Following a 3-day exposure to test compounds, the viability of tryptomastigote parasites was quantified using the dye Almar Blue<sup>®</sup> by monitoring the reductive environment of living cells.

Fluorescence development was expressed as percentage of the control, and IC<sub>50</sub> values were calculated. Melarsoprol was included as positive control.

Activity against *Trypanosoma cruzi*, the causative agent of Chagas disease, was determined according to Buckner and co-workers (Buckner et al .1996). Briefly, the strain Tulahuen C4 of *T. cruzi*, which had been transfected with the galactosidase *lac-Z* gene, was cultivated for 4 days on rat skeletal myoblasts (5 % CO<sub>2</sub>, 37° C) in the presence of drug. For measurement of the IC<sub>50</sub> the substrate chlorophenol red-β-D-galactopyranoside was added. The colour reaction that developed during the following 2-6 h was quantified photometrically employing an ELISA reader. Benznidazole was included in each test series as positive control.

Evaluation of antileishmanial activity was carried out in mouse peritoneal macrophages. The ratio of infection with *Leishmania donovani* (strain MHOM-ET-67/L82), the causative agent of Kala-Azar disease, was determined microscopically after exposure to test compounds,

incubation and staining with Giemsa. IC<sub>50</sub> values were calculated by linear regression. Miltefosine was used as positive control.

Cytotoxicity was evaluated in rat skeletal myoblasts (L6-cells), using podophyllotoxin as positive control.

### **3.6.4 Antichlamydial activity**

#### **3.6.4.1 Determination of minimal inhibitor concentration**

Determination of the minimal inhibitor concentration (MIC) of antibiotics for *C. trachomatis* was performed in cell culture using fluorescence-microscopy based assays. 200 µl of Hep2 host cells suspension were incubated for 48 h in 96 µ well plates (Ibidi, Germany) followed by the infection with *C. trachomatis* D/UW-3/CX supernatant. After 2 h of incubation at 37 °C, 5% CO<sub>2</sub> medium was removed and 100 µl fresh medium, supplemented with serially diluted concentrations of the compounds, were added. Cultures were incubated for 30 h at 37 °C, 5% CO<sub>2</sub> and afterwards fixed with ice cold methanol for 5 min. Subsequently, plates can be stored at -70 °C. Samples were stained using fluorescein-conjugated antibodies specific for chlamydial lipopolysaccharide. Therefore Pathfinder Chlamydia Conformation System (BioRad, Germany) was diluted 1:5 with PBS buffer and 100 µl were added to each well and incubated for 30 min at 37 °C. Afterwards, the plate was incubated for 1 min with additionally 3 mg/ml DAPI followed by 2 washing steps with PBS, 10 min each. Finally, samples were analyzed via fluorescence microscopy. It is important during staining and analyzing procedure to protect plates from sunlight in order to avoid bleaching.

#### **3.6.4.2 Cell viability assay**

Determination of the MIC using a fluorescence based assay is expensive and time consuming, that is why Osaka et al. recommend using a simple resazurin-based assay for measuring chlamydial infections (Osaka und Hefty 2013). The Alamar blue assay (Life Technologies, Germany) is a method utilizing the indicator dye resazurin for estimating the number of viable cells present in 96 well plates. The principle of the assay consists in the fact that viable cells

retain the ability to reduce the darkblue resazurin into the pink highly fluorescent resorufin, whereby either fluorescence or absorbance can be used to record results. In contrast, nonviable cells rapidly lose metabolic capacity and are unable to convert resazurin in resorufin.

The fact, that chlamydiae are released through cell lysis and thereby destroying the host cell makes it possible to use the alamar blue assay for measuring the level of infection and to figure out whether an antibiotic is active against these bacteria.

After incubation of non-infected or infected Hep2 cells medium was removed and the monolayer was washed twice with HBSS. Subsequently, 10 µl of the ready to use alamar blue solution was added to 100 µl HBSS. Samples were incubated for 1 h at 37 °C and 5% CO<sub>2</sub> followed by measuring the absorbance at 570 nm.

Moreover, this assay is suitable to determine cytotoxicity of the compound on non-infected host cells. Therefore, 50000 Hep2 cells were incubated for 48 h, subsequently the compound of interest was added and incubated for additional 30 h. The following washing, incubation and measuring steps were performed as described above.

### 3.6.5 Radioligand binding studies at CB<sub>1</sub> and CB<sub>2</sub> receptors

Competition binding assays were performed using the CB agonist radioligand [<sup>3</sup>H](–)-cis-3-[2-hydroxy-4-(1,1-dimethylheptyl)phenyl]-trans-4-(3-hydroxypropyl)cyclohexanol (CP 55,940, final concentration 0.1 nM). As a source for human CB<sub>1</sub> and CB<sub>2</sub> receptors membrane preparations of Chinese hamster ovary (CHO) cells stably expressing the respective receptor subtype were used (30 µg of protein/well for CB<sub>1</sub> and 8 µg of protein/well for CB<sub>2</sub>-receptor preparations). Stock solutions of the test compound were prepared in DMSO. The final DMSO concentration in the assay was 2.5%. After addition of 15 µL of the test compound in DMSO, 60 µL of [<sup>3</sup>H]CP 55,940 solution in assay buffer, and 60 µL of membrane preparation to 465 µL of assay buffer (50 mM TRIS, 3 mM MgCl<sub>2</sub>, 0.1% Bovine Serum Albumine (BSA), pH 7.4), the suspension was incubated for 2 h at room temperature. Total binding was determined by adding DMSO without test compound. Nonspecific binding was determined in the presence of 10 µM of unlabeled CP 55,940. Incubation was terminated by rapid filtration through GF/C glass fibre filters presoaked for 0.5 h with 0.3% aq. polyethyleneimine solution, using a Brandel 96-channel cell harvester (Brandel, Gaithersburg, MD). Filters were washed

three times with ice-cold washing buffer (50 mM TRIS, 0.1% BSA, pH 7.4) and then dried for 1.5 h at 50 °C. Radioactivity on the filters was determined in a liquid scintillation counter (Topcount NXT, Packard/Perkin-Elmer) after 10 h of preincubation with 50 µl of scintillation cocktail (Multiscint 25, Perkin-Elmer). Data were obtained in three independent experiments, performed in duplicates. Data were analyzed using GraphPad Prism Version 4.02 (San Diego, CA, USA). For the calculation of  $K_i$  values the Cheng-Prusoff equation and a  $K_D$  value of 2.4 nM ( $[^3\text{H}]\text{CP 55,940}$  at  $\text{CB}_1$ ) and 0.7 nM ( $[^3\text{H}]\text{CP 55,940}$  at  $\text{CB}_2$ ) were used.

### 3.6.6 Free fatty acid receptor (FFAR) 1 assay

Free fatty acid receptor assay was done via measuring the concentration of calcium mobilization. To generate a cell line for calcium mobilization assays the cDNA sequence of GPR40 was inserted into the retroviral plasmid pLXSN. The retroviral transfection of 1321N1 astrocytoma cells was performed as previously described. On the day before the assay the cells recombinantly expressing GPR40 were seeded into 96 well plates (black, clear bottom) at a density of 50000 cells per well. On the day of the assay the medium was exchanged for 40 µl of a HBSS buffer solution containing 3 µM of the calcium dye Fluo-4-AM (Life Technology, Darmstadt, Germany) and 0.06% Pluronic F-127. After 60 min of incubation at rt in the dark the dye solution was exchanged for 190 µl of HBSS buffer in agonist assays. Using a FlexStation® 3 plate reader (Molecular Devices, Sunnyvale, CA) 10 µl of test compound (=agonist) solution were added to each well. The final DMSO concentration did not exceed 1%. Fluorescence was measured at 520 nm (excitation 485 nm) for 90 intervals of 1.2 s each. All compounds were tested at a final concentration of 10 µM. Signals induced by the test compounds were normalized to the signals induced by 10 µM of TUG-424 in agonist assays. Three to four independent experiments were performed in duplicates.

### 3.6.7 Cell viability test

Cell viability was assessed using a fluorimetric detection of resorufin (CellTiter-Blue Cell Viability Assay, Promega). HEK293 cells were seeded at a density of 27,000 cells per well into black 96-well poly-D-lysine-coated plates with clear bottom. Three hours after seeding, cells were treated with 0.3% DMSO or compound dissolved in medium for 24 h. To detect

cell viability, CellTiter-Blue reagent was added and cells were incubated for 1 h at 37°C according to the manufacturer's instructions. Fluorescence (excitation 560 nm, emission 590 nm) was measured using a FlexStation 3 Benchtop Multimode Plate Reader and data were expressed as percentage of cell viability relative to DMSO control. (The cytotoxic anticancer drug etoposide was used as a positive control). Tests were performed from Nicole Merten, University of Bonn.

### **3.6.8 Leukemic cell line assays**

Cell viability assessment was done with K562, Jurkat, Raji and U937 cells. Cells were incubated with different concentrations of stemphol during 8, 24, 48 and 72 h.

Trypan blue exclusion assay (Biowhittaker, South Korea) was applied for cell viability. Mode of cell death was determined and quantified based on nuclear morphology and staining status after staining with Hoechst 33342 (Sigma-Aldrich, South Korea) and propidium iodide (Sigma-Aldrich, South Korea). To check the caspase-dependency, 50µM zVAD-FMK (Calbiochem, South Korea) was pretreated to stemphol and cells were observed by fluorescence microscopy (Nikon eclipse Ti-U, Nikon Instruments Korea, South Korea).

Data were normalized to the control and reported as percentage of viable active cells.

### **3.6.9 ROS measurements**

After treating stemphol for indicated time period, stained the cells with 10µM of 2',7'-dichlorodihydrofluorescein diacetate (H2DCFDA) (LifeTechnologies) for 20min, 37°C in the dark. The fluorescence intensity was assessed using by FACSCalibur and H<sub>2</sub>O<sub>2</sub> was used as a control positive.

### 3.7 Chemicals and solvents

Acetic acid	Merck (Darmstadt, Germany)
Acetone-d <sub>6</sub> 99.8%	Deutero GmbH (Kastellaun, Germany)
Acetonitrile	KMF (Lohmar, Germany)
Acetonitrile Lichrosolv, LC-MS grade	Merck (Darmstadt, Germany)
Agar-Agar	Fluka (Buchs, Switzerland)
Ammonium acetate	Merck (Darmstadt, Germany)
Ammonium hydroxide	Merck (Darmstadt, Germany)
Benzyl penicillin	Fluka (Buchs, Switzerland)
Biomalt extract	Villa Natura (Kirn, Germany)
CaCl <sub>2</sub> × 2 H <sub>2</sub> O	Merck (Darmstadt, Germany)
Chloroform	Merck (Darmstadt, Germany)
Chloroform-d <sub>1</sub> 99.8%	Deutero GmbH (Kastellaun, Germany)
Dichloromethane	Sigma-Aldrich (Steinheim, Germany)
Glucose	Merck (Darmstadt, Germany)
HCl, 37%	Merck (Darmstadt, Germany)
H <sub>2</sub> O Lichrosolv, LC-MS grade	Merck (Darmstadt, Germany)
H <sub>2</sub> SO <sub>4</sub>	Merck (Darmstadt, Germany)
Hexanes (mixture of isomers)	Sigma-Aldrich (Steinheim, Germany)
Malt-extract	Roth (Karlsruhe, Germany)
Methanol Lichrosolv, LC-MS grade	Merck (Darmstadt, Germany)
Methanol-d <sub>4</sub> 99.8 % D	Deutero GmbH (Kastellaun, Germany)
NaCl	Merck (Darmstadt, Germany)
NaHCO <sub>3</sub>	Merck (Darmstadt, Germany)
NaOH	Merck (Darmstadt, Germany)
Na <sub>2</sub> SO <sub>4</sub>	Merck(Darmstadt, Germany)
Penicillin/Streptomycin	Biomol GmbH (Hamburg, Germany)
Tetrahydrofuran-d <sub>8</sub>	Deutero GmbH (Kastellaun, Germany)
Triethylamine	Sigma-Aldrich (Steinheim, Germany)
Yeast extract	Roth (Karlsruhe, Germany)
Vanillin	Merck (Darmstadt, Germany)

---

All other chemicals were supplied by Merck (Germany), Fluka (Switzerland), Roth (Germany) and Sigma-Aldrich (Germany). All other solvents were research grade and supplied by Infracor or BASF. Acetone,  $\text{CHCl}_3$ ,  $\text{CH}_2\text{Cl}_2$ , EtOAc, MeOH and PE were distilled prior to use. Water for HPLC was de-ionized using a Millipore (milli-Q<sup>®</sup> academic) system.

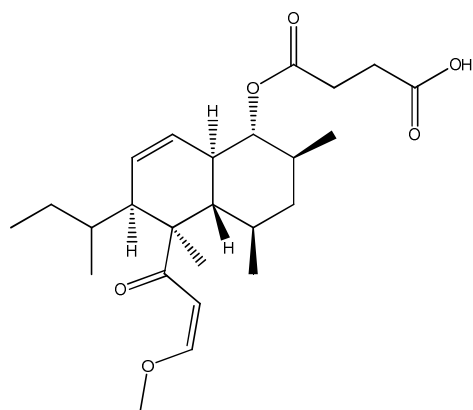
## 4. Results

### 4.1 Novel fungal metabolite stemphyloxin III (1)

#### 4.1.1 Cultivation and extraction of stemphyloxin III (1)

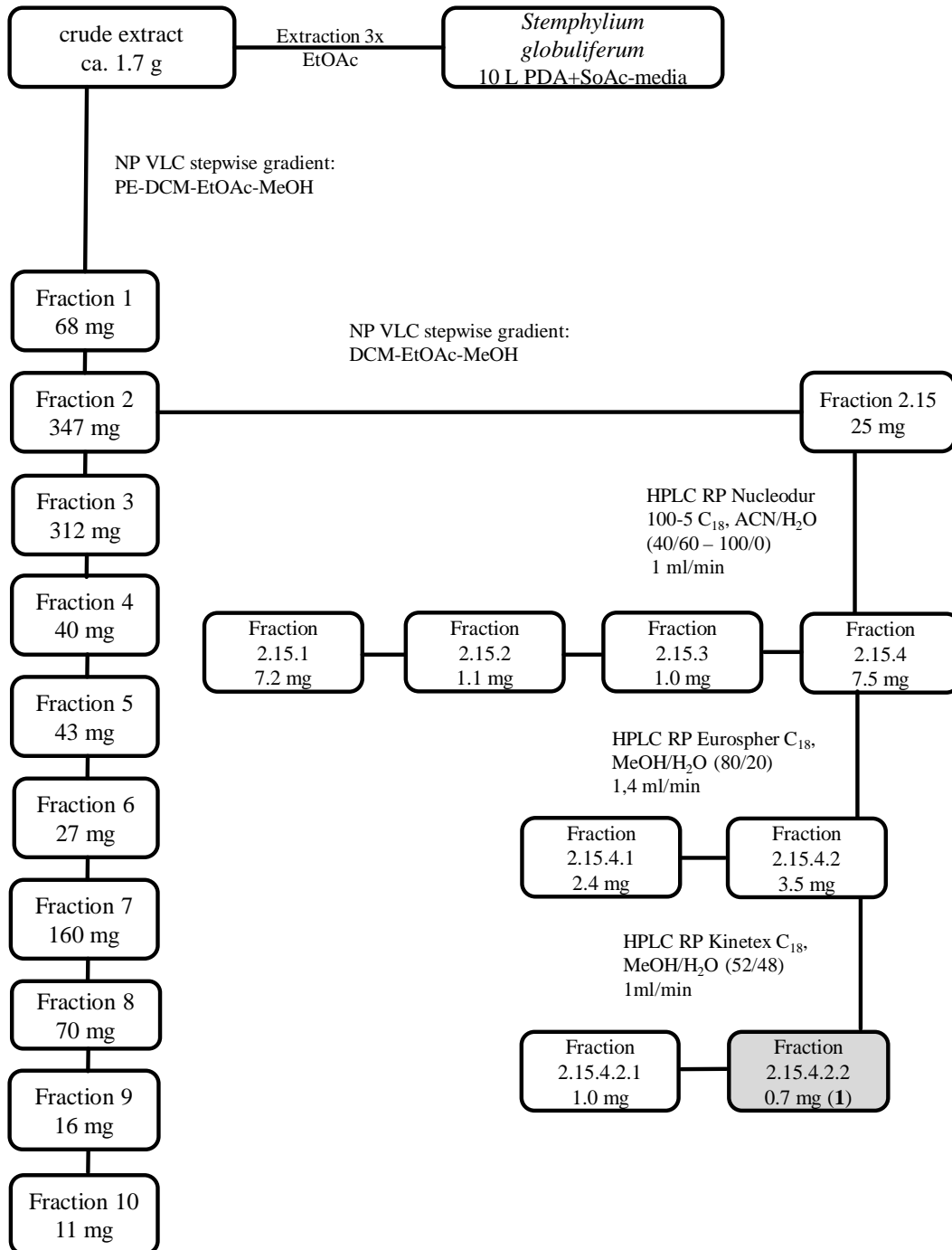
Fungal biomass and media were homogenized and extracted with EtOAc to yield 1.7 g of the extract. The material was fractionated employing NP-VLC (0.063-0.200 mm, Merck) using stepwise elution from petrolether to EtOAc to MeOH to afford 10 fractions. Of these, fraction 2 was further separated via another NP VLC (0.040-0.063 mm, Merck), whereas the subfraction 2.15 gained 25 mg (Figure 8). Further purification was achieved by RP-HPLC to afford 7.5 mg of Fraction 2.15.4. Stemphyloxin III (1) was finally isolated via two more HPLC fractionations to yield 0.7 mg (Figure 7).

**Figure 7: Structure of stemphyloxin III (1)**



## 4.1.2 Isolation of stemphyloxin III (1)

Figure 8: Isolation scheme of stemphyloxin III (1)



### 4.1.3 Structure elucidation of stemphyloxin III (1)

Compound **1** was isolated from the endophytic fungus *St. globuliferum* (OS1Test1-2) and its structure was elucidated via intensive analysis of spectroscopic data including one and two dimensional NMR data. The IR spectrum contained absorptions at  $1710\text{ cm}^{-1}$ ,  $1670\text{ cm}^{-1}$  and  $1580\text{ cm}^{-1}$  pointing towards carbonyl and carboxyl functions, respectively. The molecular formula was deduced from the results of a HR-ESI-MS measurement, whereby  $m/z = 435.2686$   $[\text{M} + \text{H}]^+$  corresponded to  $\text{C}_{25}\text{H}_{38}\text{O}_6$  (calcd:  $435.2702$   $[\text{M} + \text{H}]^+$ ). The  $^{13}\text{C}$ -NMR and DEPT-135 spectra showed 25 resonances for five methyl groups and a methoxy group, four methylene and eleven methine groups, as well as four quaternary carbon atoms (Table 1). Functional groups within **1** were deduced from  $^{13}\text{C}$ -NMR signals for a ketone at  $\delta$  205.5 (C-9), two carboxyl carbons resonating at  $\delta$  177.9 (C-23) and 174.5 (C-20), and additionally resonances for four olefinic carbons at  $\delta$  165.4 (C-11),  $\delta$  126.7 (C-4),  $\delta$  125.4 (C-3) and  $\delta$  103.1 (C-10).

Analysis of the  $^1\text{H}$ - $^1\text{H}$  COSY spectrum allowed to delineate partial structures A-D (Figure 9). Thus, COSY correlations of H-2 through to H-8a, including the methyl group resonances CH<sub>3</sub>-18 and CH<sub>3</sub>-19 gave the first partial structure A (Figure 9).

$^1\text{H}$ - $^1\text{H}$  COSY correlations of the  $^1\text{H}$ -NMR resonance signals for H-10 and H-11 and a coupling constant of  $J = 12.3$  Hz, as well as a NOESY correlation between H-10 and H-11 indicated a cis configured double bond (B in Figure 9). The third  $^1\text{H}$ - $^1\text{H}$  spin-system (C in Figure 9) is a four membered alkyl chain based on correlations between H-14, H<sub>3</sub>-17, H<sub>2</sub>-15 and H<sub>3</sub>-16 and represents a secondary-butyl-moiety. Moiety D (Figure 9) was elucidated via a COSY correlation between H<sub>2</sub>-21 and H<sub>2</sub>-22.

**Table 1: NMR spectroscopic data (600 MHz) of compound 1 in MeOH-d<sub>4</sub>**

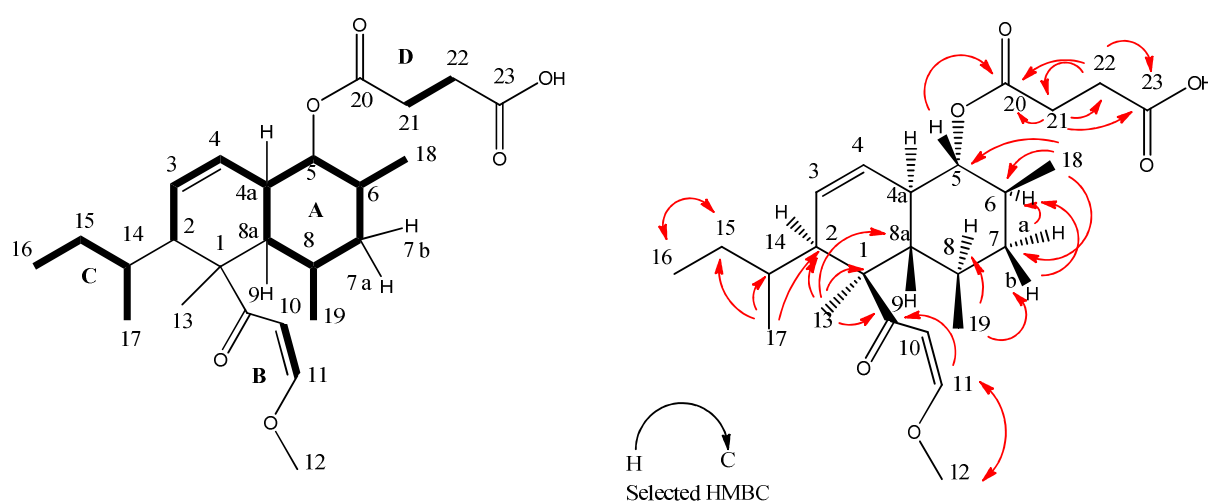
Pos.	$\delta_H$ in ppm, mult., $J$ (Hz)	$\delta_C$ in ppm	$^1H$ - $^1H$ COSY-Correlations	HMBC-Correlations	NOE-Correlations
1		53.7, C			
2	1.94, m	53.5, CH	H-3		H-3, H <sub>3</sub> -13, H-14, H <sub>3</sub> -17
3	5.72, m	125.4, CH	H-2, H-4		H-2, H <sub>3</sub> -17
4	5.69, m	126.7, CH	H-3, H-4a		H-4a, H-5
4a	1.99, br t (10.0)	45.0, CH	H-4, H-5, H-8a		H-4, H-6, H-8, H <sub>3</sub> -13, H <sub>2</sub> -21, H <sub>2</sub> -22
5	4.53, t (10.0)	82.2, CH	H-4a, H-6	C-20	H-4, H-7b, H-8a, H <sub>3</sub> -18
6	1.76, m	39.8, CH	H-5, H <sub>3</sub> -18		H-4a, H-8, H <sub>3</sub> -18
7a	a: 1.75, m	44.7, CH <sub>2</sub>	H-7b	C-6	H-7b, H-8, H <sub>3</sub> -18, H <sub>3</sub> -19
	b: 1.13, q (12.5)		H-6, H-7a, H-8	C-6	H-5, H-7a, H-8a, H <sub>3</sub> -19
8	1.49, m	38.0, CH	H-7b, H-8a, H <sub>3</sub> -19		H-4a, H-6, H <sub>3</sub> -19
8a	2.07, m	45.0, CH	H-4a, H-8		H-5, H-7b, H <sub>3</sub> -19
9		205.5, C			
10	6.18, d (12.3)	103.1, CH	H-11		H-11, H <sub>3</sub> -13
11	7.61, d (12.3)	165.4, CH	H-10	C-9, C-12	H-10, H <sub>3</sub> -12
12	3.80, s	58.6, CH <sub>3</sub>		C-11	
13	1.29, s	20.0, CH <sub>3</sub>		C-1, C-2, C-8a, C-9	H-2, H-4a, H-10, H-8
14	1.38, m	37.9, CH	H-15b, H <sub>3</sub> -17		H-2
15	a: 1.58, m	26.2, CH <sub>2</sub>	H-15b, H <sub>3</sub> -16	C-16	H-15b, H <sub>3</sub> -16
	b: 0.82, m		H-15a, H <sub>3</sub> -16	C-17	H-15a, H <sub>3</sub> -17
16	0.81, t (5.0)	12.9, CH <sub>3</sub>	H-15a	C-14, C-15	H-15a
17	0.94, d (7.0)	19.7, CH <sub>3</sub>	H-14	C-2, C-14, C-15	H-2, H-14
18	0.93, d (6.2)	18.9, CH <sub>3</sub>	H-6	C-5, C-6, C-7	H-5, H-6
19	0.73, d (7.0)	22.5, CH <sub>3</sub>	H-8	C-7, C-8, C-8a	H-7b, H-8, H-8a
20		174.5, C			
21	2.60, m	31.7, CH <sub>2</sub>	H <sub>2</sub> -22	C-20, C-22, C-23	
22	2.71, m	31.2, CH <sub>2</sub>	H <sub>2</sub> -21	C-20, C-21, C-23	
23		177.9, C			

The analysis of the HMBC spectrum led to the conclusion that the carboxyl function C-20 is attached to C-21 and the carboxylic carbon C-23 to C-22, as crosspeaks between H<sub>2</sub>-21 to C-20, C-22 and C-23, as well as H<sub>2</sub>-22 to C-20, C-21 and C-23 were detected (see Figure 10). Altogether this resulted in a succinyl-moiety. Further analysis of the HMBC spectra led to an extension of partial structure A, since crosspeaks between the resonances for the methyl group H<sub>3</sub>-13 and C-2, as well as C-1, C-8a and C-9 were observed. The latter carbon is part of residue B (Figure 9), due to a HMBC correlation from H-11 to C-9. Thus led to the conclusion that compound **1** has a decaline core structure, where C-1 connects the above

mentioned substructures A and B. The HMBC correlations between H<sub>3</sub>-17 to C-14, C-15 and C-2 showed the connection of the butyl residue (C in figure 9) to the decaline structure.

A HMBC correlation arising from the resonance of H-11 to CH<sub>3</sub>-12 clarified the position of the methoxy group and identified the side chain at C-1 as a methoxylated β-hydroxyenone. Finally, the succinyl moiety had to be connected via an ester bond to C-5 due to an HMBC correlation of H-5 to C-20.

**Figure 9: Selected partial structures of stemphyloxin III (1) deduced from <sup>1</sup>H-<sup>1</sup>H COSY correlations marked as bold lines** **Figure 10: Selected HMBC correlations of stemphyloxin III (1) marked as red arrows**



The relative configuration was deduced from data in a NOESY spectrum. Correlations between H-2 and H<sub>3</sub>-13, H<sub>3</sub>-13 to H-2 and H-4a and furthermore H-4a to H-6 and H-8 showed that all these protons are on the same side of the molecule, i.e.  $\alpha$ . In addition, NOE correlations of H-8a to H-5 and H-7b indicated these protons to be  $\beta$  positioned. The position of H-4a is approved by <sup>1</sup>H coupling constant of  $J_{4a-5} = 10$  Hz, which showed that the dihedral angle between these protons is 180° (Figure 11). Therefore, the connection of the decaline ring is *trans* (H-4a to H-8a, Figure 12), which corresponds with literature data of coincenal D (Wang et al., 2013). The coupling constant of  $J_{7a-7b} = 12.5$  Hz pointed towards a geminal coupling towards H-7a and H-7b. Additionally, the vicinal coupling constants of  $J_{7b-6} = 12.5$  Hz and  $J_{7b-8} = 12.5$  Hz showed that H-7b is axial to H-6 and H-8.

The NOE coupling of H-2 and H<sub>3</sub>-13 pointed towards an equatorial position of the secondary butyl group, which is connected to C-2, and the β-hydroxyenone moiety which is connected to C-1, respectively. Furthermore the coupling of H-6 and H-8 led to the conclusion, that H<sub>3</sub>-18 and H<sub>3</sub>-19 are in equatorial position connected to C-6 and C-8, respectively (Figure 12).

Finally the relative configuration of stemphyloxin III is shown in Figure 7.

**Figure 11: 3D model of stemphyloxin III (1) determined by conformation search (Boltzmann jump) using CVFF1.01 (see 3.5.7)**

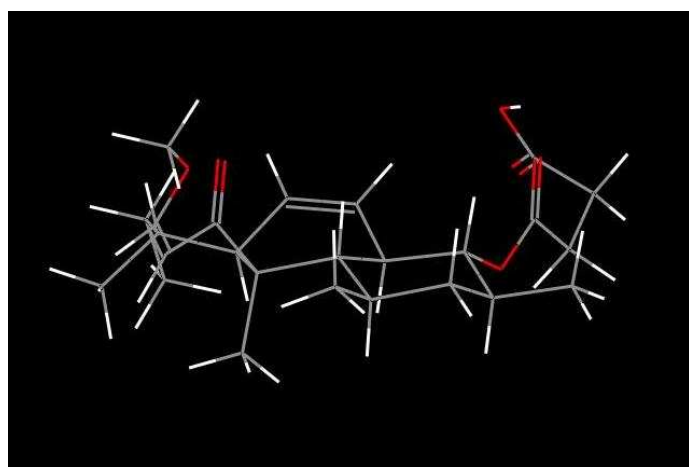
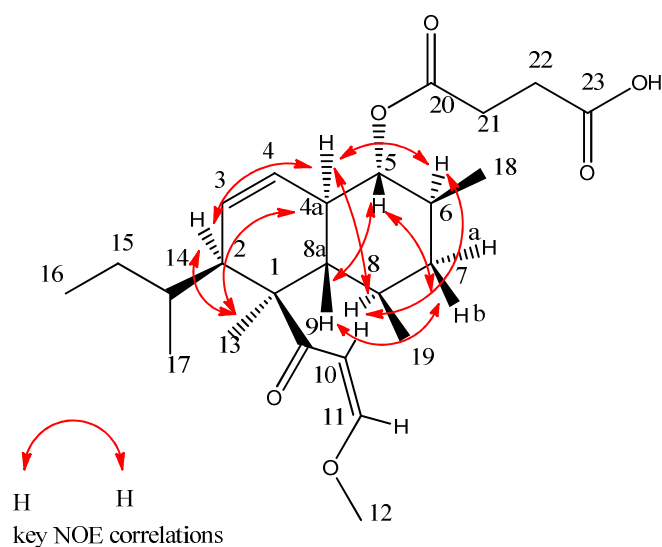


**Figure 12: Key NOE correlations of compound 1 marked as red arrows**



The structure of compound **1** has similarities to three known natural products, *i.e.* stemphyloxin I (Figure 14), probetaenone I (Figure 16) and coicenol D derivative (Figure 15) (Sakamura et al., 1988; Liu et al., 2013; Barash et al., 1984). The  $^{13}\text{C}$ -NMR resonances of the decaline core structure and the secondary butyl moiety of **1** are mostly alike to those of probetaenone I (Table 2) except for C-5, where compound **1** has the linkage to the succinyl unit (Sakamura et al., 1988). In turn, the  $^{13}\text{C}$ -NMR resonances of the succinyl residue had similarities to a coicenol D derivative, where also the succinyl unit is linked to the decaline core structure (Liu et al., 2013). Furthermore, the  $^{13}\text{C}$ -NMR signals at  $\delta$  205.5 (C-9),  $\delta$  165.4 (C-11) and  $\delta$  103.1 (C-10) are similar to those reported for stemphyloxin I, which also has an enone group attached to the decaline core structure (Barash et al., 1984).

Based on the intensive study of the above mentioned spectroscopic data the unambiguous configuration of compound **1** is shown in Figure 7, and the compound is named stemphyloxin III.

#### 4.1.4 Antimicrobial activity of stemphyloxin III (**1**)

Stemphyloxin III (**1**) was tested against a broad spectrum of microorganisms, that is, the Gram-positive bacteria *Staphylococcus aureus* 133, *Bacillus subtilis* 168, *Micrococcus luteus* 4698, *Arthrobacter crystallopoites* DSM 20117, the Gram-negative bacteria *Escherichia coli* I-11276b, *Klebsiella pneumoniae* sp. *ozeanae* I-10910 and the fungus *Candida albicans* I-11301. The compound revealed a moderate antibiotic activity against *Arthrobacter crystallopoietes* with an inhibition of 7 mm and against *Micrococcus luteus* with an inhibition of 5 mm (3 $\mu\text{g}$ /assay). The test was performed by Michaele Josten from the group of Prof. Tanja Schneider, Institute of Pharmaceutical Microbiology, University of Bonn.

Figure 13: Stemphyloxin III (1)

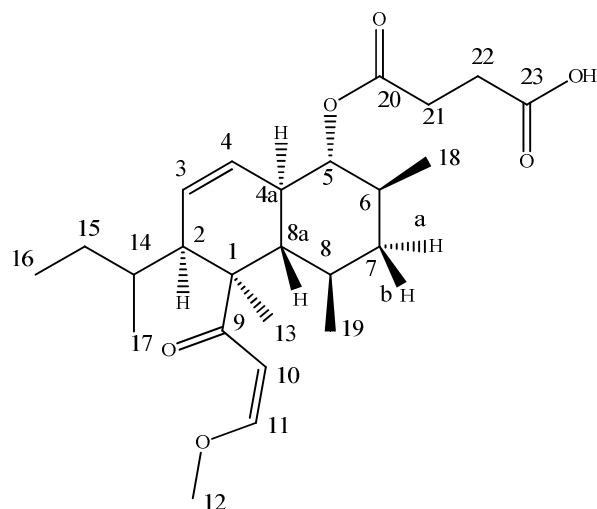


Figure 14: Stemphyloxin I (Barash et al., 1984)

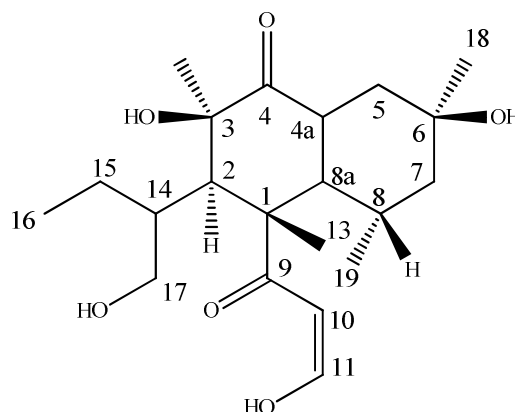


Figure 15: Coicenol D derivative (Liu et al., 2013)

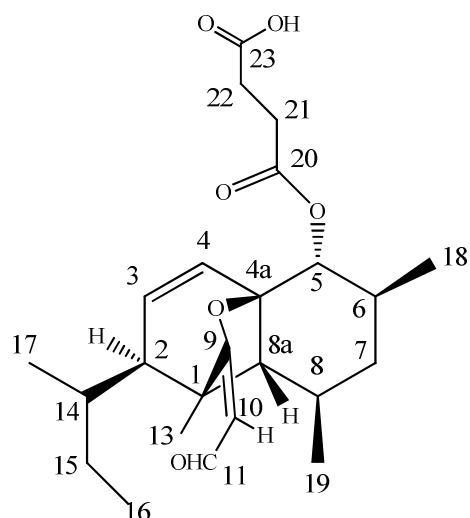
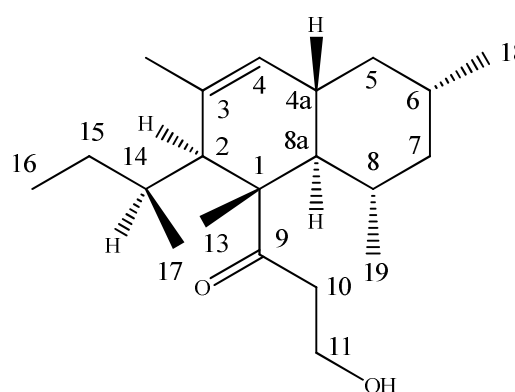


Figure 16: Probetaenone I (Sakamura et al., 1988)



Stemphyloxin III (**1**) was obtained as white powder (0.07 mg/L).  $[\alpha]_D^{20} = -15.71$  ( $c = 0.07$ , EtOH); UV (EtOH)  $\lambda_{\max}$  (log  $\epsilon$ ): 258 nm (3.96); IR  $\nu_{\max}$  2860, 1710, 1650, 1580, 1250, 1180  $\text{cm}^{-1}$  (see Appendix);  $^1\text{H}$ - and  $^{13}\text{C}$  data see Table 1; HR-ESI-MS 435.2686  $[\text{M} + \text{H}]^+$  for  $\text{C}_{25}\text{H}_{38}\text{O}_6$  (calcd: 435.2702  $[\text{M} + \text{H}]^+$ ).

**Table 2: Compared  $^{13}\text{C}$  NMR Spectroscopic Data of compound 1, probetaenone I, stemphyloxin I and coicenol D derivative**

Pos.	$\delta_{\text{C}}$ in ppm compound 1 <sup>a</sup>	$\delta_{\text{C}}$ in ppm probetaenone I <sup>1, b</sup>	$\delta_{\text{C}}$ in ppm stemphyloxin I <sup>2, c</sup>	$\delta_{\text{C}}$ in ppm coicenol D derivative <sup>3, c</sup>
1	53.7	53.9	49.9	50.4
2	53.5, CH	57.1	45.0	50.0
3	125.4, CH	130.8	75.9	132.4
4	126.7, CH	127.2	216.5	125.5
4a	45.0, CH	42.6	55.0	84.9
5	82.2, CH	42.4	41.6	78.5
6	39.8, CH	34.0	68.7	34.2
7	44.7, CH <sub>2</sub>	46.6	47.6	43.3
8	38.0, CH	38.0	31.1	29.7
8a	45.0, CH	44.4	40.5	59.9
9	205.5, C	215.0	207.2	182.5
10	103.1, CH	41.4	101.7	102.8
11	165.4, CH	58.0	172.2	190.2
12	58.6, CH <sub>3</sub>			
13	20.0, CH <sub>3</sub>	17.8		21.6
14	37.9, CH	34.8	43.0	33.2
15	26.2, CH <sub>2</sub>	27.0	19.7	26.5
16	12.9, CH <sub>3</sub>	13.3		12.5
17	19.7, CH <sub>3</sub>	21.7	66.1	21.0
18	18.9, CH <sub>3</sub>	22.3		17.4
19	22.5, CH <sub>3</sub>	23.6		19.5
20	174.5, C			171.8
21	31.7, CH <sub>2</sub>			29.2
22	31.2, CH <sub>2</sub>			28.7
23	177.9, C			174.9

<sup>a</sup> in MeOD, <sup>b</sup> in C<sub>6</sub>D<sub>6</sub>, <sup>c</sup> in CDCl<sub>3</sub>; <sup>1</sup> Sakamura et al; J.Chem.Soc., Chem. Commun., 1988; 600-602

<sup>2</sup> Barash et al.; Phytochemistry, 1984, Vol.23, No. 10, 2193-2198

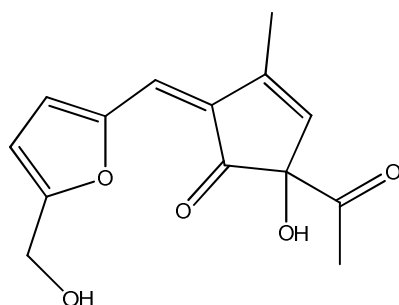
<sup>3</sup> Liu et al.; Organic Letters, 2013, Vol. 15, 3982-3985

## 4.2 Novel fungal metabolite stemphylofuran (2)

### 4.2.1 Cultivation and extraction of stemphylofuran (2)

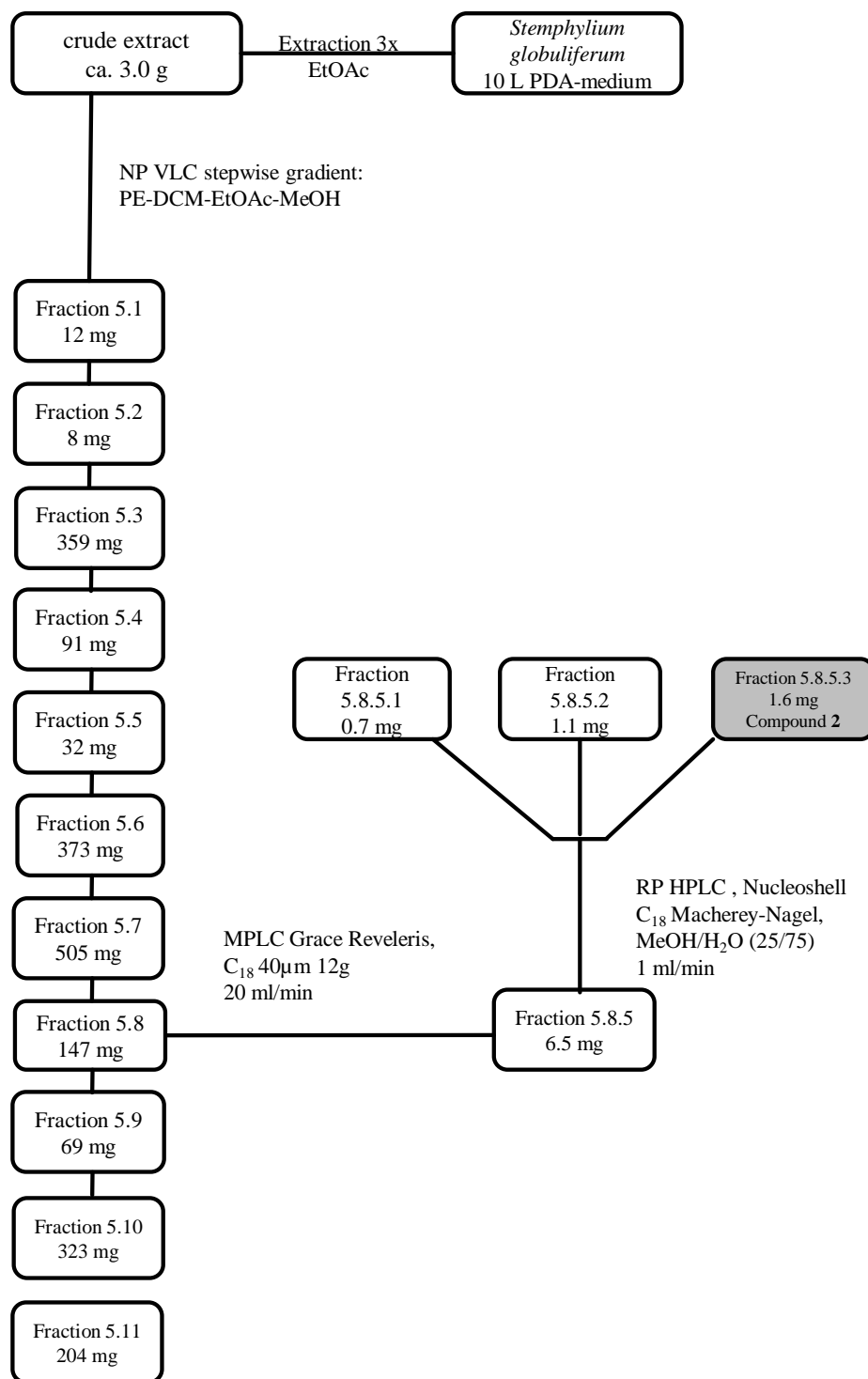
Stemphylofuran (2) was isolated from the endophytic fungus *St. globuliferum*. After homogenization and extraction of the fungal biomass and media with EtOAc 3.0 g of crude extract were obtained (Fig. 18). The material was fractionated employing NP-VLC (0.063-0.200 mm, Merck) using stepwise elution from petrolether to EtOAc to MeOH to afford 11 fractions. Of these, fraction 5.8 was further separated via a medium pressure liquid chromatography of which the subfraction 5.8.5 gained 6.5 mg. Stemphylofuran (2) was finally isolated via an RP-HPLC fractionation to yield 1.2 mg (Figure 17).

**Figure 17: Structure of stemphylofuran (2)**



## 4.2.2 Isolation of stemphylofuran (2)

Figure 18: Isolation scheme of stemphylofuran (2)



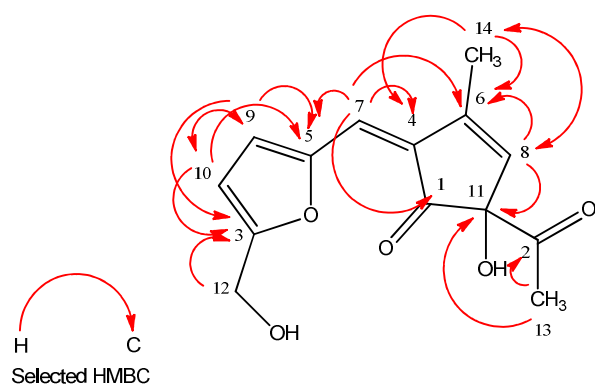
### 4.2.3 Results and discussion

The molecular formula was deduced from the results of a HRESIMS measurement, *i.e.*  $m/z = 263.0886 [M + H]^+$  corresponded to a molecular formula of  $C_{14}H_{14}O_5$  (calcd:  $263.0875 [M + H]^+$ ). The calculated number of double bond equivalents was 8. The UV spectrum showed a maximum at 350 nm, clearly evidencing an extended chromophore. The IR spectrum of **2** contained absorptions at  $1650\text{ cm}^{-1}$  and  $3300\text{ cm}^{-1}$  pointing towards carbonyl and hydroxyl functional groups, respectively. The structure of stemphylofuran (**2**) was elucidated via intensive analysis of one and two dimensional NMR data. The  $^{13}\text{C}$ -NMR and DEPT-135 spectra showed 14 resonances for two methyl groups, one methylene and four methine groups, as well as seven quaternary carbon atoms. Functional groups within the molecule could be deduced from  $^{13}\text{C}$ -NMR signal, for two ketones at  $\delta$  199.5 (C-1) and  $\delta$  199.3 (C-2), respectively (Table 3).

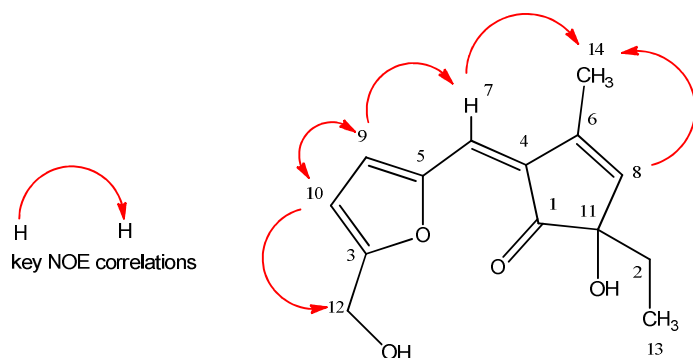
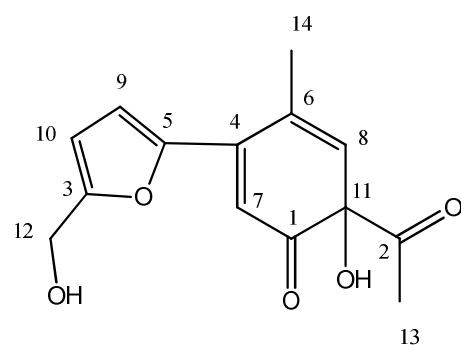
**Table 3: NMR spectroscopic data (600 MHz) of compound 2 in MeOH- $d_4$**

Pos.	$\delta_{\text{H}}$ , in ppm, mult., $J$ (Hz)	$\delta_{\text{C}}$ in ppm	$^1\text{H}$ - $^1\text{H}$ COSY- Correlations	HMBC-Correlations	NOE-Correlations
1		199.5, C			
2		199.3, C			
3		161.1, C			
4		156.7, C			
5		151.4, C			
6		129.3, C			
7	7.27, brs	128.5, CH	H <sub>3</sub> -8, H-9, H-10	C-1, C-4, C-5, C-6, C-9, C-11	H <sub>3</sub> -14
8	6.13, s	124.5, CH	H-14, H-7	C-6, C-11, C-14	H <sub>3</sub> -14
9	7.57, d (3.5)	122.1, CH	H-10, H <sub>2</sub> -12, H-7	C-3, C-5, C-7, C-10	H-10
10	6.56, d (3.5)	111.9, CH	H-9, H <sub>2</sub> -12	C-9, C-5, C-3	H-9, H <sub>2</sub> -12
11		85.7, C			
12	4.61, s	57.6, CH <sub>2</sub>	H-10	C-10, C-3	H-10
13	1.55, s	26.6, CH <sub>3</sub>		C-11, C-2	
14	2.34, s	20.3, CH <sub>3</sub>	H-8	C-8, C-6, C-4,	H-7, H-8



**Figure 20: Selected HMBC correlations of stemphylofuran (2) marked as red arrows**

The final structure of stemphylofuran was established by analyzing a NOE spectrum. Correlations of both H-7 and H-8 to H<sub>3</sub>-14 led to the conclusion that all protons are on the same side (Figure 21) and thus established the configuration of the double bond  $\Delta^{4,7}$  to be Z. The configuration at C-11 could not be resolved. The CD experiment lead to a positive, but very weak cotton effect at 382 nm.

**Figure 21: Key NOE correlations of compound 2****Figure 22: Alternative structure of (2)**

In part our spectroscopic data would also support the structure for **2**, as shown in Figure 22. Thus was rejected, since H-9 has a HMBC correlation to C-7, but not to C-4, which indicated a five membered ring structure. The other fact is that there is a NOE correlation of H-7 to H<sub>3</sub>-14, which is only possible if **2** is as described in Figure 21. With the six membered ring a NOE correlation between these protons H<sub>3</sub>-14 and H-7 is not possible because of sterical reasons. This led to the conclusion, that the metabolite has a five membered cyclopentenone ring.

Based on the intensive study of the above mentioned spectroscopic data of compound **2**, its structure is as shown as in Figure 7 and it is named stemphylofuran.

Stemphylofuran (**2**) has similarities to phellinusfuran A (Figure 23), a furan derivative from *Phellinus linteus* (Min et al. 2006). The <sup>13</sup>C-NMR resonances of the furan moiety as well as that of C-7, the linkages of both molecules are mostly alike (Table 2). Furthermore, NMR shifts of hydroxymethyl C-12 with is connected to the furan moiety are similar to the literature. C-4 of stemphylofuran resonating at  $\delta_C$  156.7 is downfield shifted compared to phenillusfuran A ( $\delta_C$  126.7). The structure of the investigated metabolite is a rare carbon skeleton, only found in the fungus *Phellinus linteus* so far.

**Figure 23: Phellinusfuran A (Min et al., 2006)**

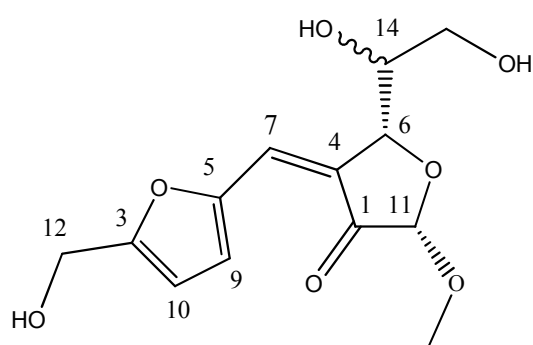


**Table 4: Comparison of  $^{13}\text{C}$  NMR spectroscopic data of compound 2 and Phellinusfuran A**

Pos.	$\delta_{\text{C}}$ , Compound 2 <sup>a</sup>	$\delta_{\text{C}}$ , phellinusfuran A <sup>b</sup>
1	199.5, C	196.8, C
2	199.3, C	
3	161.1, C	160.6, C
4	156.7, C	126.7, C
5	151.4, C	149.3, C
6	129.3, C	80.8, CH
7	128.5, CH	121.4, CH
8	124.5, CH	
9	122.1, CH	121.7, CH
10	111.9, CH	110.3, CH
11	85.7, C	99.1, CH
12	57.6, CH <sub>2</sub>	56.0, CH <sub>2</sub>
13	26.6, CH <sub>3</sub>	
14	20.3, CH <sub>3</sub>	74.4, CH

<sup>a</sup> in MeOD; <sup>b</sup> in DMSO-d<sub>6</sub>, Min et al., Bioorg. & Med. Chem. Letters 16 (2006) 3255-3257

Stemphylofuran (**2**) was obtained as yellow powder (0.12 mg/L).  $[\alpha]_{\text{D}}^{20} = 0.04$  ( $c = 0.1$ , EtOH); UV (EtOH)  $\lambda_{\text{max}}$  (log  $\epsilon$ ): 350 nm (3.45); CD (MeOH):  $\Delta\epsilon_{382} = +0.45$ ; IR  $\nu_{\text{max}} = 3300, 2850, 2380, 1650, 1410, 1190, 1110 \text{ cm}^{-1}$  (see Appendix);  $^1\text{H}$ - and  $^{13}\text{C}$ -data see Table 3; HR-ESI-MS 263.0886  $[\text{M} + \text{H}]^+$  for  $\text{C}_{14}\text{H}_{14}\text{O}_5$  (calcd: 263.0875  $[\text{M} + \text{H}]^+$ ).

#### 4.2.4 Antimicrobial activity of stemphylofuran (**2**)

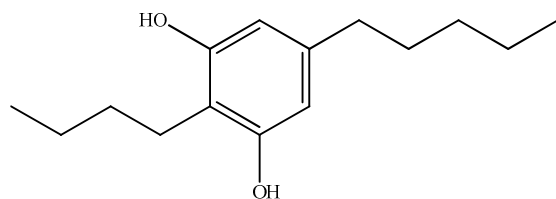
Stemphylofuran (**2**) was tested against a broad spectrum of microorganisms, that is, the Gram-positive bacteria *Staphylococcus aureus* 133, *Bacillus subtilis* 168, *Micrococcus luteus* 4698, *Arthrobacter crystallopoietes* DSM 20117, the Gram-negative bacteria *Escherichia coli* I-11276b, *Klebsiella pneumoniae* subsp. *ozeanae* I-10910 and the fungus *Candida albicans* I-11301. The compound revealed a moderate antibiotic activity towards *Arthrobacter crystallopoietes* with an inhibition of 5 mm, and against *Micrococcus luteus* with an inhibition of 3 mm (3  $\mu\text{g}$ /assay). The test was performed by Michaele Josten from the group of Prof. Tanja Schneider, Institute of Pharmaceutical Microbiology, University of Bonn.

## 4.3 Fungal metabolite stemphol (3)

### 4.3.1 Cultivation and extraction

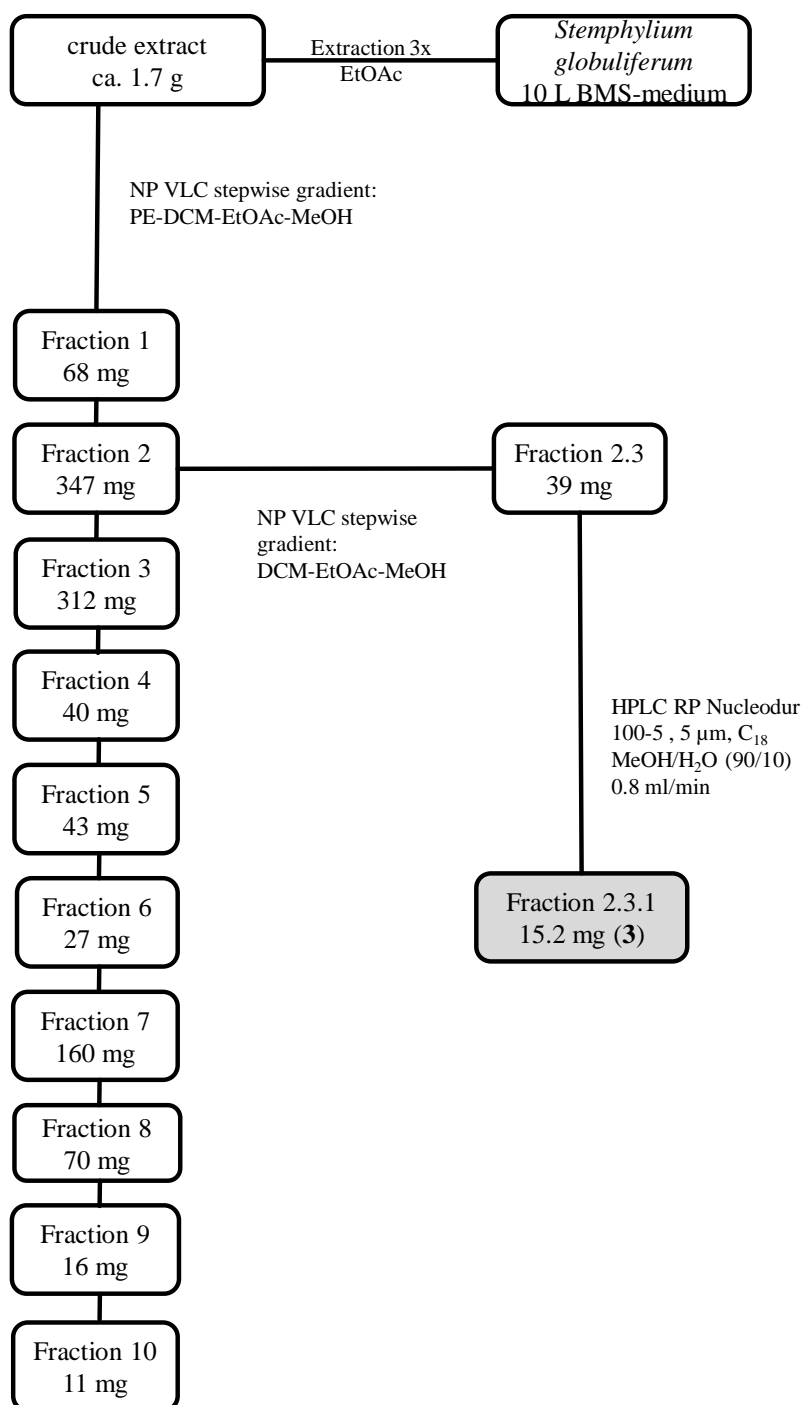
The fungus *Stemphylium globuliferum* was grown on Biomalt salt agar + 1% SoAcetate for 40 days (room temperature and permanent light). Fungal biomass and media were homogenized and extracted three times with EtOAc to yield 1.7 g of the extract. The material was fractionated employing NP-VLC (0.063-0.200 mm, Merck) using stepwise elution from petroleum ether to EtOAc to MeOH to afford 10 fractions. Of these, fraction 2 was further separated via another NP VLC (0.040-0.063 mm, Merck), to gain 39 mg of subfraction 2.3 (Table 6). Further purification was achieved by RP-HPLC to afford 15.2 mg of fraction 2.3.1, *i.e.* stemphol (3) (Figure 24).

**Figure 24: Isolation scheme of stemphol (3)**



### 4.3.2 Isolation of fungal metabolite stemphol (3)

Table 5: Isolation scheme of stemphol (3)



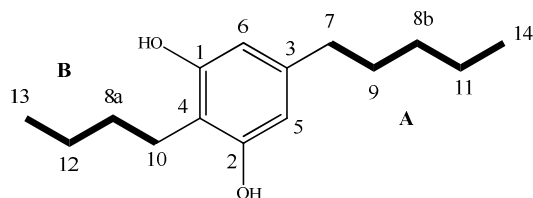
### 4.3.3 Results and discussion

Structure elucidation of **3** was done via intensive analysis of one and two dimensional NMR spectra, as well as by mass spectrometric measurements. The molecular formula was deduced from a HR-ESI-MS measurement *i.e.*  $m/z = 237.1836$   $[M + H]^+$  corresponded to the molecular formula of  $C_{15}H_{24}O_2$ , (calcd:  $237.1854$   $[M + H]^+$ ).

The  $^{13}C$ -NMR and DEPT-135 spectra revealed 14 resonances for two methyl, seven methylene and two methine groups, as well as four quaternary carbons (Table 6). The  $^1H$ -NMR showed two prominent resonances at  $\delta$  6.89 (H-5) and  $\delta$  6.46 (H-6), that pointed to two aromatic protons.

Analysis of the  $^1H$ - $^1H$  COSY spectrum allowed to delineate partial structures A and B. Thus, COSY correlations of H<sub>2</sub>-7 through to H<sub>3</sub>-14 gave evidence for partial structure A, correlations between H<sub>2</sub>-10, H-8a, H-12 and H<sub>3</sub>-13 for partial structure B (Figure 25).

**Figure 25:** Selected partial structures of compound **3** deduced from  $^1H$ - $^1H$  COSY correlations marked as bold lines



In this thesis, HMBC spectroscopic data were analyzed to identify the length of the alkyl chains on the resorcinol core structure. The analysis of the HMBC spectrum revealed that H-5 has correlations to carbons C-2, C-4, C-6 and C-7 (Figure 26) and furthermore correlations of H-6 to carbons C-1, C-4, C-5 and C-7. Together with HMBC correlations of H<sub>2</sub>-7 to C-3, C-5 and C-6 this led to the conclusion that carbons C-1 – C-6 form a phenyl ring with moiety A connected to carbon C-3. Furthermore, NOE correlations of H<sub>2</sub>-7 to H-5 and H-6 underline the assumption (Figure 27). A COSY correlation between H-5 and H-6 together with a coupling constant of 1.3 Hz indicated these two protons to be in meta position to each other. Fragment B had to be connected to C-4 due to HMBC correlations of H<sub>2</sub>-10 to C-1, C-2 and

C-4 (Figure 26). Based on the NMR data and the mass spectra the two remaining hydroxyl groups had to be attached to C-1 and C-2 respectively, which is confirmed by the downfield shift of these carbons in the  $^{13}\text{C}$ -NMR spectrum (Table 6).

**Figure 26: Selected HMBC correlations of compound 3 marked as arrows**

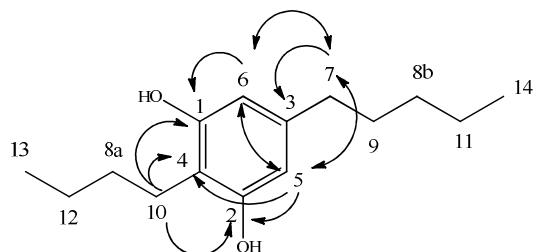


**Figure 27: Key NOE correlations of compound 3 marked as arrows**

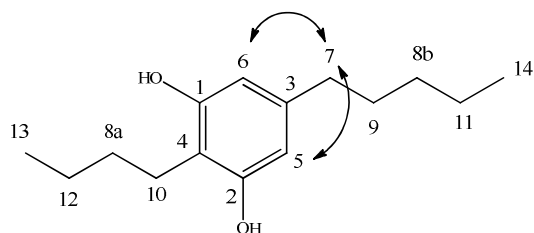


**Table 6: NMR spectroscopic data (300 MHz) of compound 3 in MeOH-d<sub>4</sub>**

Pos.	$\delta_{\text{H}}$ in ppm, mult., <i>J</i> (Hz)	$\delta_{\text{C}}$ in ppm	<sup>1</sup> H- <sup>1</sup> H COSY- Correlations	HMBC- Correlations	NOE-Correlations
1		156.9, C			
2		152.7, C			
3		142.0, C			
4		120.9, C			
5	6.89, d (1.3)	113.7, CH	H-6, H <sub>2</sub> -7	C-2, C-4, C-6, C-7	H <sub>2</sub> -7, H <sub>2</sub> -9
6	6.46, d (1.3)	112.5, CH	H-5, H <sub>2</sub> -7, H <sub>2</sub> -9	C-1, C-4, C-5, C-7	H <sub>2</sub> -7, H <sub>2</sub> -9
7	2.50, t (7.5)	36.7, CH <sub>2</sub>	H <sub>2</sub> -9, H <sub>2</sub> -5, H-6	C-3, C-5, C-6, C-8b, C-9, C-11	H-5, H-6, H <sub>2</sub> -9, H <sub>2</sub> -8b
8a	1.55, m	32.7, CH <sub>2</sub>	H <sub>2</sub> -10	C-10, C-13	H <sub>2</sub> -10, H <sub>2</sub> -12, H <sub>3</sub> -13
8b	1.36, m	32.7, CH <sub>2</sub>	H <sub>2</sub> -9	C-7, C-9, C-11, C-14	H <sub>2</sub> -7, H <sub>3</sub> -14
9	1.62, m	32.2, CH <sub>2</sub>	H <sub>2</sub> -7, H <sub>2</sub> -8b	C-7, C-8b, C-11	H-5, H-6, H <sub>2</sub> -7, H <sub>2</sub> -8b
10	2.70 t (7.5)	24.6, CH <sub>2</sub>	H <sub>2</sub> -8a, H <sub>2</sub> -5, H <sub>2</sub> -6	C-1, C-2, C-4, C-8a, C-12	H <sub>2</sub> -12, H <sub>2</sub> -8a
11	1.37, m	23.6, CH <sub>2</sub>	H <sub>3</sub> -14, H <sub>2</sub> -7	C-8b, C-14	H <sub>2</sub> -9
12	1.38, m	24.0, CH <sub>2</sub>	H <sub>2</sub> -8a, H <sub>3</sub> -13	C-8a, C-13	H <sub>3</sub> -13
13	0.96, t (7.0)	14.5, CH <sub>3</sub>	H <sub>2</sub> -12, H <sub>2</sub> -8a	C-12, C-8a	H <sub>2</sub> -8a
14	0.93, t (6.8)	14.4, CH <sub>3</sub>	H <sub>2</sub> -11	C-11, C-8b	H <sub>2</sub> -8b

**Table 7:  $^{13}\text{C}$ -NMR spectroscopic data of compound **3** compared to stemphol<sup>b</sup>**

Pos.	$\delta_{\text{C}}$ , in ppm compound <b>3</b> <sup>a</sup>	$\delta_{\text{C}}$ , in ppm compound <b>3</b> + TFA <sup>a</sup>	$\delta_{\text{C}}$ , in ppm stemphol <sup>b</sup>
1	156.9, C	156.9, C	154.2
2	152.8, C	152.7, C	154.2
3	142.0, C	142.1, C	142.1
4	120.9, C	114.5, C	112.4
5	113.7, CH	107.7, CH	108.0
6	112.6, CH	107.7, CH	108.0
7	36.7, CH <sub>2</sub>	36.7, CH <sub>2</sub>	35.1
8a	32.7, CH <sub>2</sub>	32.7, CH <sub>2</sub>	31.4
8b	32.7, CH <sub>2</sub>	32.7, CH <sub>2</sub>	31.4
9	32.1, CH <sub>2</sub>	32.2, CH <sub>2</sub>	30.7
10	24.6, CH <sub>2</sub>	23.9, CH <sub>2</sub>	22.8
11	24.0, CH <sub>2</sub>	23.7, CH <sub>2</sub>	22.8
12	23.6, CH <sub>3</sub>	23.6, CH <sub>3</sub>	22.5
13	14.5, CH <sub>3</sub>	14.5, CH <sub>3</sub>	14.0
14	14.4, CH <sub>3</sub>	14.4, CH <sub>3</sub>	14.0

a in MeOD (300MHz); b in CDCl<sub>3</sub>, Marumo, S., *Argic. Biol. Chem.*, 49 (5), 1985, 1521-1522, assignment of the respective carbons to their  $^{13}\text{C}$ -NMR resonances was done according to the best Literature for compound **3**

According to literature, compound **3** had similarities to those of the known metabolite stemphol (Marumo et al. 1985) except for two proton signals at 6.46 ppm and 6.89 ppm for H-5 and H-6, respectively of compound **3** instead of a  $^1\text{H}$ -NMR signal at 6.2 ppm for H-2 of stemphol (Figure 29 and App. F1). This phenomenon can be explained by the phenol phenolate reaction. Phenol has higher acidities, e.g. compared to alcohols, due to the aromatic ring coupling and the possibility of a hydrogen ion loss. This proton loss correlates with the building and mesomeric stabilization of the gained phenolat-ion. The negative charge on oxygen is delocalized on to the ortho and para carbon atoms (Figure 28). After addition of TFA to compound **3** the protonated phenolicform was gained which is underlined by the fact that the  $^1\text{H}$ -NMR spectra showed a signal at 6.2 ppm for the magnetically equivalent protons H-5 and H-6 (Figure 29), similar as reported in the literature for stemphol (Marumo et al. 1985).

**Figure 28: Phenol phenolate reaction based on mesomeric stabilization of the negative charge of the phenolate ion**

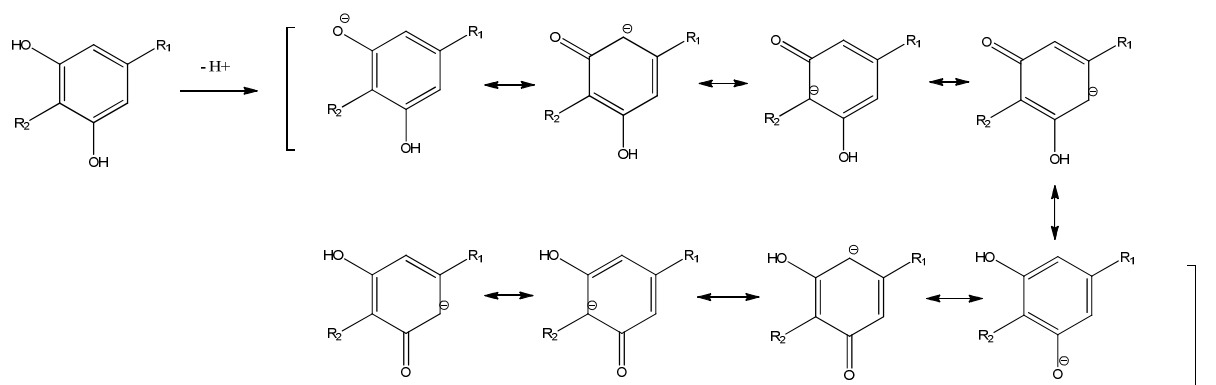
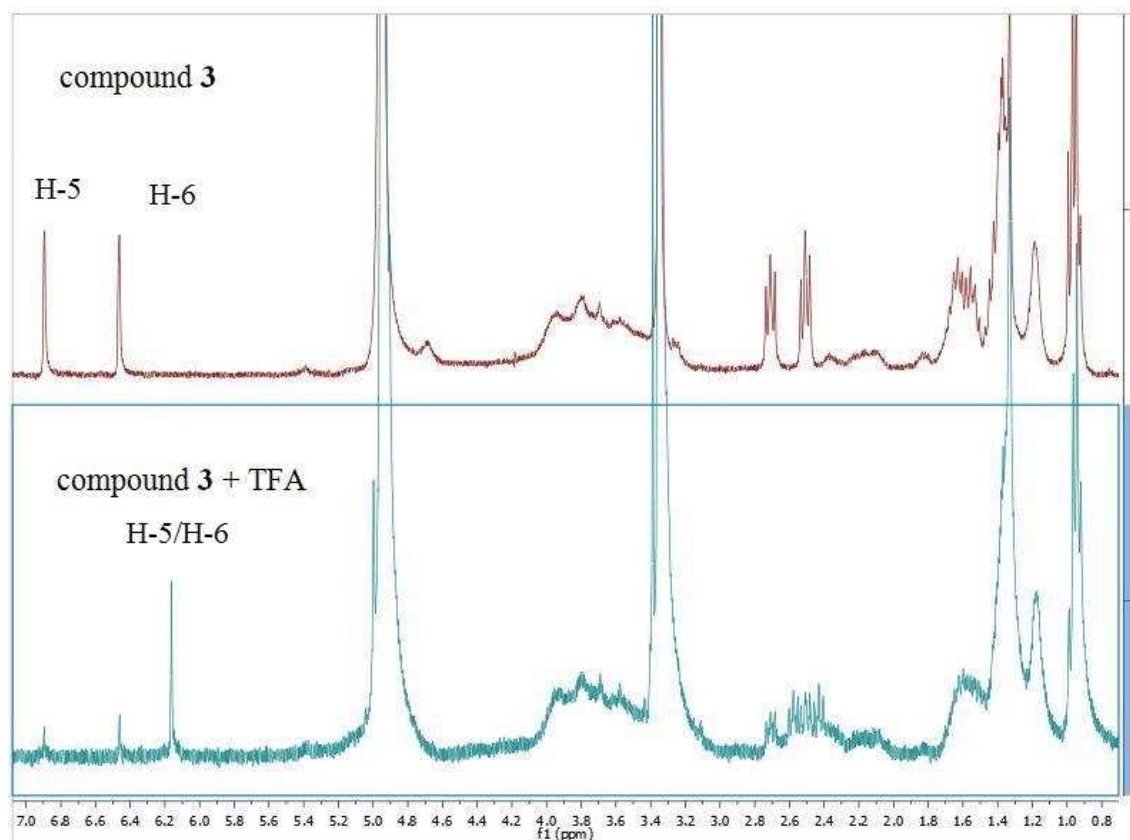


**Figure 29: Phenolate (marked in red) compared to phenolate with added TFA (blue) of (3) and their  $^1H$ -NMR (300 MHz) shifts between 6.13 ppm, 6.46 ppm and 6.89 ppm, respectively**

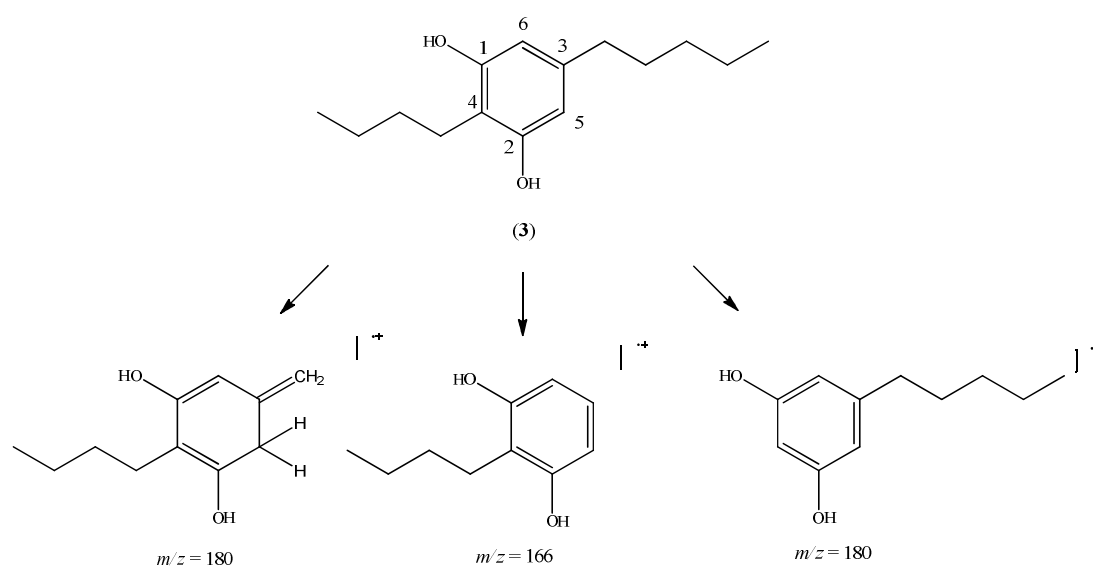


MS fragmentation also supported the structure of **3**. Thus, fragments at  $m/z = 166$  and  $m/z = 180$  in the LC-MS (see 3.5.2) spectrum can be explained by the cleavage of the two alkyl groups from the phenol core structure, as well as  $\beta$ -cleavage and mesomeric stabilization at the C-3 position (Figure 30) according to literature (Oocolowitz 1964).

Taking together the above mentioned results of spectroscopic measurements, LC-MS measurements and MS fragmentation of the literature reports (Table 7) it was shown that **3** is the deprotonated form of 2-butenyl-,5-pentenyl-resorcin and thus, stemphol (**3**) as seen in Figure 24.

Stemphol:  $C_{15}H_{24}O_2$   $m/z = 237.1836$   $[M + H]^+$ ; white needles (1.52 mg/L); UV  $\lambda_{max}$ : 205nm (see Appendix);  $^1H$ -NMR (MeOD, 300 MHz)  $\delta$  6.13 (2H, s), 2.54 (2H, t,  $J = 8.0$  Hz), 2.39 (2H, t,  $J = 8.0$ ), 1.28-1.61 (10H, m), 0.93 (3H, t,  $J = 7.2$ ), 0.91 (3H, t,  $J = 6.9$ );  $^{13}C$ -NMR (MeOD, 75 MHz)  $\delta$  157.0, 142.1, 114.5, 107.6, 36.7, 32.7, 32.6, 32.2, 23.9, 23.7, 23.6, 14.5, 14.4 (corresponding to Marumo et al. 1985).

**Figure 30: MS fragmentation, alkyl cleavage of compound 3, pos.Mode LC-MS measurement**



#### 4.3.4 Antimicrobial activity of stemphol (3)

Stemphol (3) was evaluated for its antimicrobial potential by two different agar diffusion assays and a microtiter plate assay for further determination of the MIC-value (see 3.6.1 and 3.6.2) as shown in Table 8 and 9.

**Table 8: Agar diffusion assay of stemphol (3) in the group of Prof. König (see 3.6.1)**

Inhibition zones against test organisms [mm]					
Compound	<i>Escherichia coli</i>	<i>Bacillus megaterium</i>	<i>Microbotryum violaceum</i>	<i>Eurotium rubrum</i>	<i>Mycothypha microspora</i>
stemphol (3)	-	4	3	-	-

sample concentration: 1mg/ml (at 50 µg/disk)

Stemphol (3) showed antimicrobial activity against a range of microorganisms (Table 8 and 9). The activity against *Bacillus megaterium* and *Staphylococcus aureus* was originally reported by Achenbach et al. 1979 and could be confirmed with an inhibition zone of 4 mm (Table 8). Furthermore, an inhibition of *Microbotryum violaceum* of 3 mm revealed the fungal inhibition according to literature (Achenbach et al. 1979). However, stemphol (3) was tested against other Gram-positive and Gram-negative bacteria as well as against *Candida albicans*, but showed no inhibition.

**Table 9: Agar diffusion assay in the group of Prof. Sahl (and microtiter plates assay for MIC) values of stemphol (3) against certain microorganisms, shown are the inhibition zones [mm] as well as the minimal inhibition concentration [ $\mu\text{g/ml}$ ]**

inhibition zones and MIC against test organisms			
Test organism		stemphol (3)	
Strain	No.	Inhibition zone [mm]	MIC [ $\mu\text{g/ml}$ ]
<i>Staphylococcus aureus</i> (MSSA)	I-11574	4	n.t.
<i>Staphylococcus aureus</i> (MRSA)	LT-1334	3	4
<i>Staphylococcus aureus</i> (MRSA)	LT-1338	3	n.t.
<i>Staphylococcus aureus</i>	133	4	4
<i>Staphylococcus simulans</i>	22	4	4
<i>Bacillus subtilis</i>	168	3	
<i>Listeria welshimeri</i>	DSM 20650	4	
<i>Mycobacterium smegmatis</i>	ATCC 70084	3	
<i>Candida albicans</i>	I-11301	4	4
<i>Candida albicans</i>	I-11134	3	n.t.
<i>Arthrobacter crystallopoietes</i>	DSM 20117	4	
<i>Enterococcus faecium</i>	I-10910	3	16
<i>Klebsiella pneumoniae</i> sp. <i>ozeanae</i>	I-11054	4	64
<i>Citrobacter freundii</i>	I-11090	2*	
<i>Escherichia coli</i>	I-11276b	2*	
<i>Escherichia coli</i>	O-19592	2*	
<i>Stenotropomonas maltophilia</i>	O-16451	2*	
<i>Stenotropomonas maltophilia</i>	I-10717	2*	
<i>Pseudomonas aeruginosa</i>	I-10968	2*	

\* Some colonies remaining, no clear inhibition, sample concentration: 1mg/ml (at 3  $\mu\text{g/disk}$ ), assay was done by Michael Josten in the group of Prof. Sahl, University of Bonn; n.t.: not determined

Stemphol (3) showed good activity against the Gram-positive bacteria *St. aureus*, methicillin-resistant *St.aureus* and *St. simulans* with an MIC value of 4  $\mu\text{g/ml}$  as well as against *C. albicans* with an MIC value of 4  $\mu\text{g/ml}$ , which makes stemphol (3) to a considerable drug candidate towards these pathogens (Table 9). Furthermore, stemphol (3) was sensitive

---

towards *E. faecium* and *K. pneumoniae* subsp. *ozeanae*, with MIC values of 16 µg/ml and 64 µg/ml, respectively (Table 9). There is also a weak activity towards certain Gram-negative bacteria, e.g. *Stenotropomonas maltophilia* or *E. coli* with an inhibition zone of 2 mm including some single remaining colonies. These pathogens play a leading role in nosocomial infections because of their resistance to the available antimicrobial options.

#### 4.3.5 Antiparasitic activity

Protozoan parasites that are infectious to humans represent a significant threat to health. Malaria, a vector-borne disease caused by protozoan parasites of the genus *Plasmodium* e.g. *P. falciparum*, resulted in 214 million infections and claims 438.000 deaths every year (World Malaria Report 2015).

Infections with Trypanosoma cause various diseases e.g. sleeping sickness caused by *T. brucei* and Chagas disease, caused by *T. cruzi*. Chagas disease mainly affects the poor in remote areas and is endemic in rural Latin America, where an estimated 18 million people are infected with the causative parasite that is transmitted by insects (Lancet 2009).

*Leishmania* spp. are parasites that cause leishmaniasis, a disease with 12 million infected people and one of the world's most neglected diseases until few years ago (Srivastava et al. 2016). Leishmaniasis is divided in three forms: cutaneous, mucocutaneous and visceral leishmaniasis. They are transmitted via sandflies and during their life cycle stage in mammalian hosts, *Leishmania* spp. are housed within phagolysosomes of macrophages (McGwire and Satoskar 2014).

**Table 10: In vitro antiparasitic activity of stemphol (3) against several parasites and cytotoxic activity towards myoblast cell line**

	IC <sub>50</sub> values test organism/cell line [µg/ml]				
pos. control	<i>T. b. rhod.</i>	<i>T. cruzi</i>	<i>L. donovani</i>	<i>P. falciparum</i>	L6-cells
Melarsoprol	0.002				
Benznidazole		0.465			
Miltefosine			0.074		
Chloroquine				0.004	
Podophyllotoxin					0.009
<b>Stemphol (3)</b>	0.18	2.45	0.30	3.33	4.45

*T. b. rhod.*: *Trypanosoma brucei rhodesiense*; *T. cruzi*: *Trypanosoma cruzi*; *L. donovani*: *Leishmania donovani*; *P. falciparum*: *Plasmodium falciparum*; L6-cells: rat skeletal myoblasts cells, assay was done in the workgroup of Dr. Kaiser, Swiss Tropical and Public Health Institute, Basel (see 3.6.3)

Stemphol (3) revealed an antiparasitic activity towards *Trypanosoma brucei* subsp. *rhodesiense* and *Leishmania donovani* with an IC<sub>50</sub> value of 0.18 µg/ml and IC<sub>50</sub> 0.30 µg/ml but also showed pronounced cytotoxicity towards the control cell line, regarding the limited selectivity index of 25 and 15, respectively, making them problematic for further pharmaceutical drug development (Table 10). *T. cruzi* with an IC<sub>50</sub> value of 2.45 µg/ml and *P. falciparum* with an IC<sub>50</sub> value of 3.33 µg/ml are not selective compared to L6-cells (control). Another approach would be the derivatization of stemphol to reduce the cytotoxicity. All assays were done in the group of Dr. Kaiser, Swiss Tropical and Public Health Institute, Basel, Switzerland (see 3.6.3).

#### 4.3.6 Radioligand binding studies at CB<sub>1</sub> / CB<sub>2</sub> receptors

Cannabinoid receptors (CB<sub>1</sub> and CB<sub>2</sub>) belong to the family of G-protein coupled receptors and are part of the endocannabinoid system, which are involved in the regulation of various processes in the human body. They are located in the cell membrane and regulate via G<sub>i</sub> coupling the inhibition of adenylate cyclase, which forms cyclic adenosine monophosphate

(cAMP), a second messenger involved in signal transduction. Their activation results in reduced intracellular cAMP levels (Matsuda et al. 1990).

CB<sub>1</sub> receptors are mainly present in the central nervous system and they affect a variety of physiological responses including analgesia, psychoactive effects, *e.g.* euphoria, and stimulation of appetite. CB<sub>2</sub> is expressed in cells and organs of the immune system and its activation results in anti-inflammatory and analgesic effects (Racz et al. 2008; Pacher et al. 2006). The most prominent target for the cannabinoid receptor is  $\Delta^9$ -tetrahydrocannabinol ( $\Delta^9$ -THC), a secondary metabolite produced by the plant *Cannabis sativa*.

In the here employed competition binding assay, the CB agonist radioligand [<sup>3</sup>H](–)-cis-3-[2-hydroxy-4-(1,1-dimethylheptyl)phenyl]-trans-4-(3-hydroxypropyl)cyclohexanol (CP 55,940) was used. Nonspecific binding was determined in the presence of 10  $\mu$ M of unlabeled CP 55,940 (see 3.6.5). Here, the K<sub>i</sub> values determined a dissociation constant, which measures the affinity between a ligand (*e.g.* stemphol) and a protein (*e.g.* the CB receptor). Such ligand-protein affinities are influenced by non-covalent intermolecular interactions between the two molecules such as electrostatic interactions, hydrogen bonding and van der Waals forces. Here, the K<sub>i</sub> value corresponds to the concentration of ligand (*e.g.* stemphol) at which the binding site on the protein (*e.g.* CB receptor) is half occupied (Table 11).

**Table 11: Radioligand binding assay with stemphol (3) and other metabolites at human CB<sub>1</sub> and CB<sub>2</sub> receptors heterologous expressed in CHO cells**

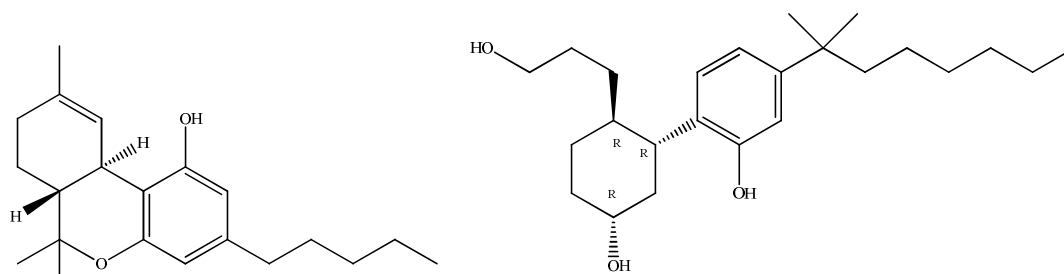
Compound	Radioligand binding	
	hCB <sub>1</sub> K <sub>i</sub> ( $\mu$ M) (%) inhibition of specific binding	hCB <sub>2</sub> K <sub>i</sub> ( $\mu$ M) (%) inhibition of specific binding
stemphol (3)	<b>6.65</b> $\pm$ 1.61	<b>2.92</b> $\pm$ 0.27
4-butyl-3,5-dihydroxy-benzoic acid (4)	>10 (11%)	>10 (9%)
infectopyrone (5)	>10 (7%)	>10 (8%)

assay performed by Dr. Clara Schoeder, group of Prof. Müller, University of Bonn

In the radioligand binding assay stemphol (3) showed an affinity towards CB<sub>1</sub> and CB<sub>2</sub> receptor at 6.65  $\mu$ M for CB<sub>1</sub> and 2.92  $\mu$ M for CB<sub>2</sub>, respectively. Further isolated metabolites

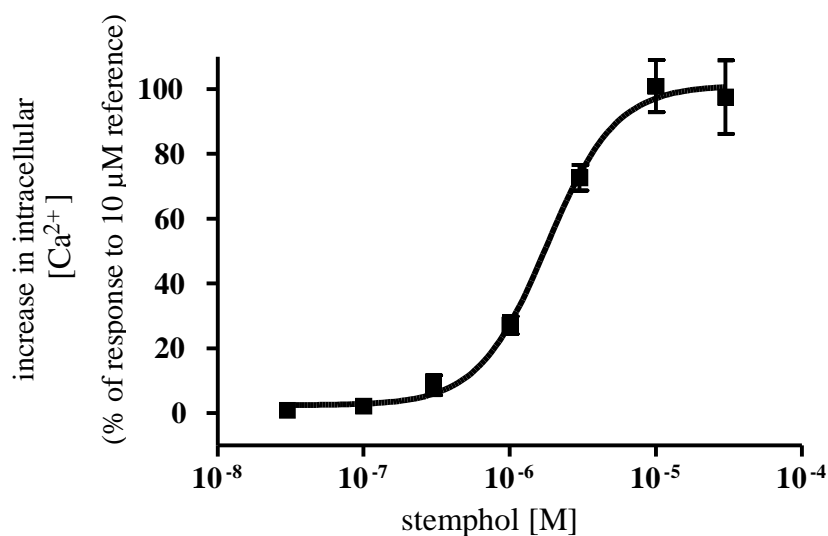
4-butyl-3,5-dihydroxy-benzoic acid (**4**) and Infectopyrone (**5**) had no effect. The results in the lower micromolar range for stemphol (**3**) showed that stemphol had weak affinity towards the CB<sub>1</sub> and CB<sub>2</sub> receptors compared to the lower nanomolar range of the positive control CP 55,940 of 2.4 nM at CB<sub>1</sub> and 0.7 nM at CB<sub>2</sub> receptor, respectively (see 3.6.5). This may be explained by the alkyl chains of stemphol, connected with the phenol core structure, which is similar to a partial structure of the naturally agonist  $\Delta^9$ -THC as well as the synthetic cannabinoid CP 55,940 (Figure 31).

**Figure 31: Structure of  $\Delta^9$ -THC (left) and CP 55,940 (right)**



#### 4.3.7 Activity against free fatty acid receptor 1 (FFAR 1)

Human free fatty acid receptor 1 (FFAR 1) is also known as GPR 40 and belongs to the family of G-protein coupled receptors. FFAR 1 is preferentially expressed in pancreatic  $\beta$ -cells and mediates the acute potentiating effect of fatty acids on glucose-stimulated insulin secretion, but not their chronic deleterious effects. As such, FFAR 1 is being considered as a new therapeutic target to enhance insulin secretion in type 2 diabetes mellitus. A number of preclinical studies and recent phase 2 clinical trials support the beneficial effects of a FFAR 1 agonist in type 2 diabetes (Ferdaoussi 2012). Furthermore, it is probably involved by stimulating new memory cells in the brain, therefore also interesting for treatment of Alzheimer and Parkinson's disease (Briscoe et al. 2003).

**Figure 32: FFAR 1 assay with stemphol (3), reference TUG-424**

assay performed by Dr. Dominik Thimm, group of Prof. Müller, University of Bonn

The assay was done by measuring the intracellular concentration of calcium mobilization. Stemphol (**3**) showed a half maximal effective concentration ( $EC_{50}$ ) of  $1.76 \pm 0.27 \mu\text{M}$  in the FFAR 1 receptor assay (reference TUG-424  $0.10 \mu\text{M}$ ) as seen in Figure 32. Based on the limited agonistic activity, the next step would be the modification of the natural product stemphol, *e.g.* different alkyl chain length or the use of derivatives of stemphol to gain activity in the nanomolar range towards the FFAR 1 receptor. Stemphol (**3**) had no effect towards the also tested GPR 17, GPR 55 and GPR 84 receptors, respectively (see 3.6.6).

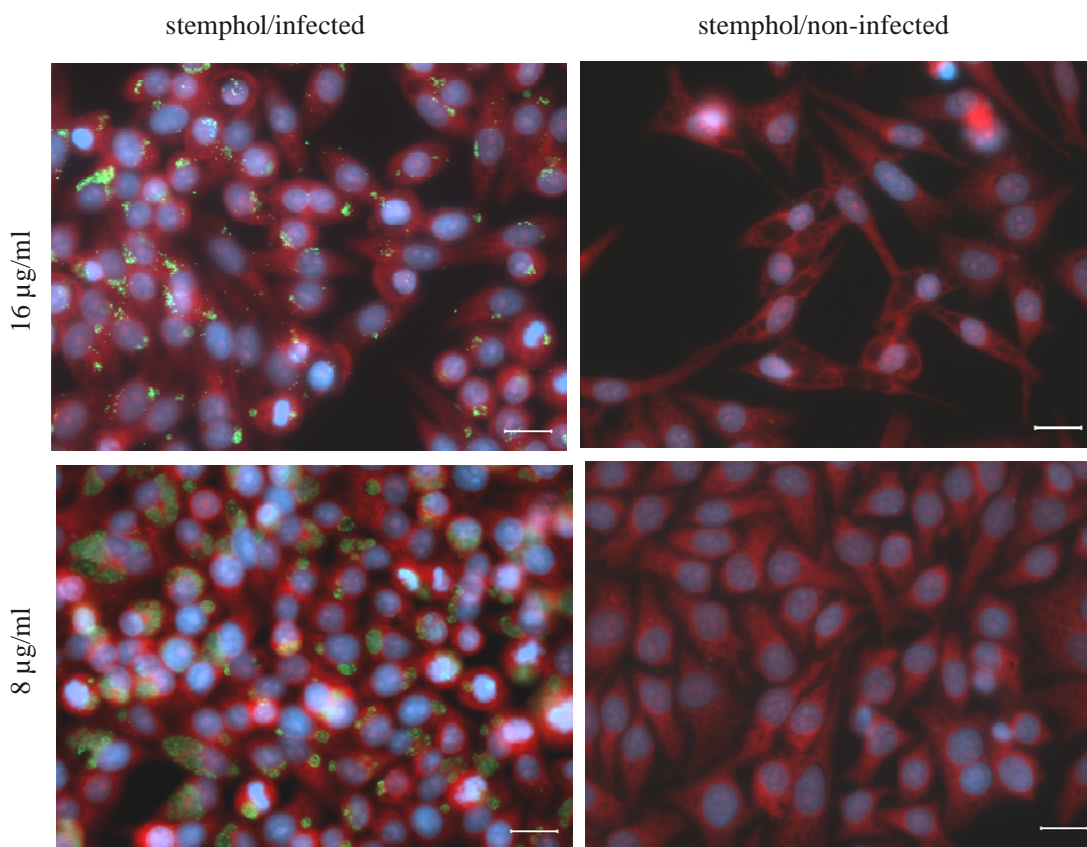
### 4.3.8 Antichlamydial activity

*Chlamydia trachomatis* is a Gram-negative, obligate intracellular bacterium that belongs to the phylum *Chlamydiae*. It is the most prevalent cause of sexually transmitted diseases and the leading cause of non-congenital blindness in developing nations. Furthermore it causes respiratory infections, and is linked to a number of chronic diseases, *e.g.* asthma and cardiovascular disease (Bachmann et al. 2014). Up to now, no effective vaccine exists (Elwell et al. 2016). The parasite has a remarkable biphasic development cycle involving infection of the host cells by extracellular elementary bodies (EBs), transformation of EBs within the host cells to reticulate bodies (RBs), which are the metabolic active form. Differentiation and replication of the reticulate bodies followed by a transformation of RBs back to EBs, and release of EBs following host cell lysis complete the life cycle (Storey and Chopra 2001) and opens the door for further infections.

Beside the main form of the development cycle there is another development cycle that includes formation of aberrant bodies (AB). Aberrant bodies can be built from reticulate bodies. ABs refers to an intracellular, persistent form which is built during non-ideal growth conditions in the host cell. It is the permanent form with reduced metabolism and can transform back to reticulate bodies. The aberrant bodies are in connection with reactive arthritis and thus of medicinal interest (Carter and Hudson 2010).

Conducting the activity of stemphol towards the main life cycle form we investigated the impact of stemphol (**3**) towards *C. trachomatis* D/UW-3/CX and the host cells, respectively. *C. trachomatis* D/UW-3/CX was grown in HEp-2 host cells. Cultures were incubated for 30 h in the presence of serially diluted concentrations of stemphol (**3**), fixed with methanol and stained for chlamydial inclusions using fluorescein-conjugated antibodies (see 3.6.4).

**Figure 33: Stemphol (3) and its inhibition of chlamydial growth in HEp-2 host cells at concentrations of 8  $\mu\text{g/ml}$  and 16  $\mu\text{g/ml}$ , respectively compared to non-infected cells**

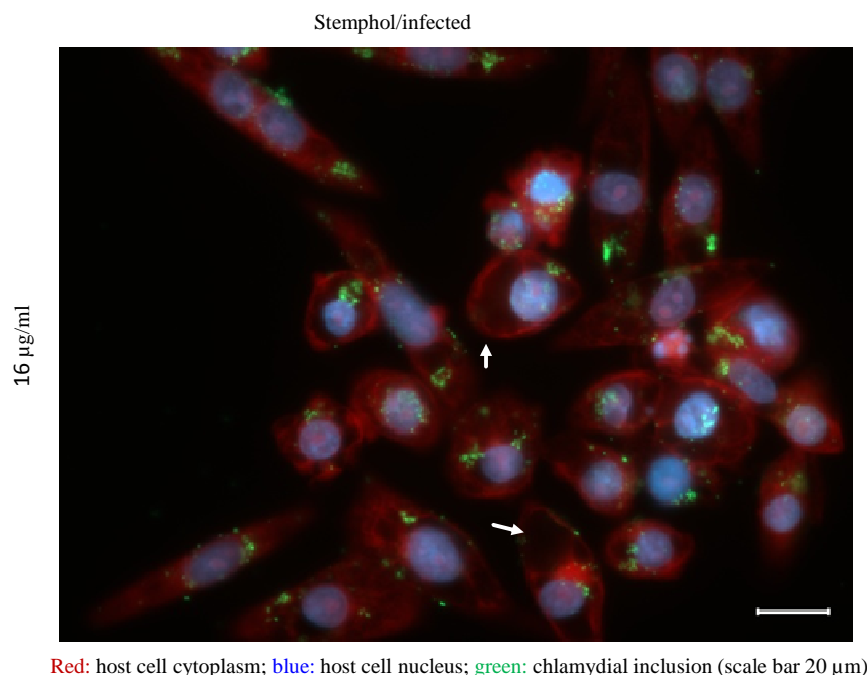


**Red:** host cell cytoplasm; **blue:** host cell nucleus; **green:** chlamydial inclusion (scale bar 20  $\mu\text{m}$ )

assay was performed by Anna Klöckner, work group of Prof. Sahl, University of Bonn

Stemphol (**3**) showed an inhibition of chlamydial growth in a range of 8-16  $\mu\text{g/ml}$  as seen in Figure 33. Green marked chlamydial inclusions at 16  $\mu\text{g/ml}$  stemphol addition were reduced in quantity and size (marked in green) compared to the 8  $\mu\text{g/ml}$  stemphol added cells, where the green color is dominant within the host cells. At 16  $\mu\text{g/ml}$  it is perceived that there is an obvious chlamydial inhibition growth as well as a partial transformation in the cytoplasm of the host cells. The morphology of the cell changes by increasing the cell volume. This phenomenon is showed as white arrows in Figure 34, an enlarged detail of Figure 33. These results led to the conclusion that stemphol (**3**) had an impact of the chlamydial growth and their host cells in a dose-dependent manner. Furthermore, the cytotoxic effect of stemphol (**3**) towards the host cells may also be responsible for the inhibition of chlamydial growth as seen in Figure 33 and Figure 34 (16  $\mu\text{g/ml}$  stemphol/infected), respectively.

**Figure 34: Enlarged detail of partial transformation by added 16 µg/ml stemphol (3) of the cytoplasm of the host cells (white arrows) as seen in Figure 33**



assay was performed by Anna Klöckner, work group of Prof. Sahl, University of Bonn

Besides activity of stemphol towards the main life cycle form of *C. trachomatis* another approach aimed to determine an effect of stemphol (3) towards persistent chlamydial aberrant bodies. Therefore, the latter assay was conducted with interferon- $\gamma$  (IFN- $\gamma$ ) treatment of host cells. IFN- $\gamma$  is a pro-inflammatory cytokine, which activates the expression of indoleamine 2,3-dioxygenase. This reaction catabolizes L-tryptophan to N-formylkynurenine. *Chlamydiae* are tryptophan auxotroph and usually acquire this essential amino acid from the host. IFN- $\gamma$ -mediated depletion of tryptophan inhibits chlamydial growth and continuous exposure results in eradication of infection (Belland et al. 2003). These conditions gain non-ideal growth conditions for *Chlamydiae* to build the investigated aberrant bodies.

In this assay, HEp-2 cells were cultured and then incubated with IFN- $\gamma$ . Afterwards cells were infected with *C. trachomatis* with a serially diluted concentration of stemphol (3) and incubated for 30 h.

The conducted assay additionally showed an inhibition of the chlamydial growth and the host cells, respectively in the same concentrations of 8-16 µg/ml as seen by the assay with the main form development cycle. This can be explained by a possible pronounced cytotoxicity of stemphol (3) towards the host cells as seen for the non-persistent chlamydial assay.

### 4.3.9 Cytotoxic activity

#### 4.3.9.1 Activity towards four different leukemic cell lines

Stemphol (**3**) was tested towards four different human leukemic cell lines: chronic myelogenous K562 cells, immobilized human T lymphocyte Jurkat cells, hematopoietic Raji cells and histiocytic lymphoma U937 cells (see 3.6.8). The impact of stemphol (**3**) on cancer cells viability and proliferation is shown in Figure 36. The effect of viability and proliferation respectively at the indicated concentrations on the four cell lines was analyzed after 8, 24, 48, 72 h compared to the control (Co).

The calculated  $IC_{50}$  values of stemphol (**3**) towards the four different human leukemia cell lines (A: K562, B: Jurkat, C: Raji, D: U937) are shown in Table 12.

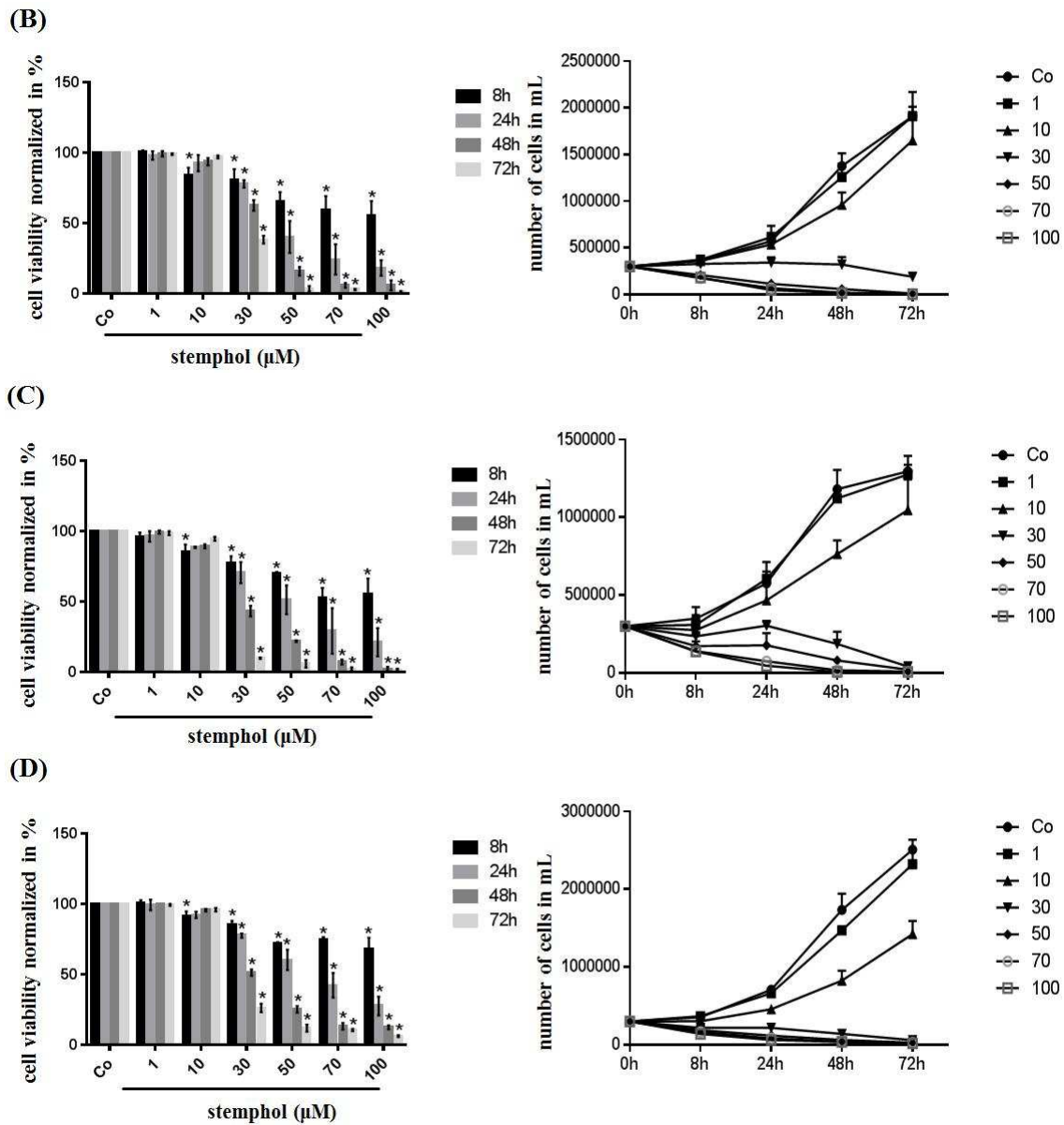
**Table 12: Calculated  $IC_{50}$  values of stemphol (**3**) towards four different human leukemia cell lines (A: K562, B: Jurkat, C: Raji, D: U937)**

$IC_{50}$ ( $\mu$ M)	8h	24h	48h	72h
A: K562	$240.2 \pm 59.9$	$54.9 \pm 2.8$	$31.5 \pm 0.8$	$29.1 \pm 0.7$
B: Jurkat	$123.1 \pm 24.1$	$45.6 \pm 2.2$	$33.9 \pm 1.0$	$27 \pm 0.5$
C: Raji	$118.1 \pm 20.4$	$47.4 \pm 3.3$	$26.7 \pm 0.9$	$18.7 \pm 0.8$
D: U937	$274.4 \pm 70.5$	$60.1 \pm 2.4$	$31.3 \pm 1.0$	$22.6 \pm 1.2$

Calculations were done by Seungwon Ji, work group of Prof. Diederich, Seoul National University

The strongest activity was found towards Raji cells at  $18.7 \mu$ M and against U937 cells at  $22.6 \mu$ M, respectively (Figure 35 and Table 12).

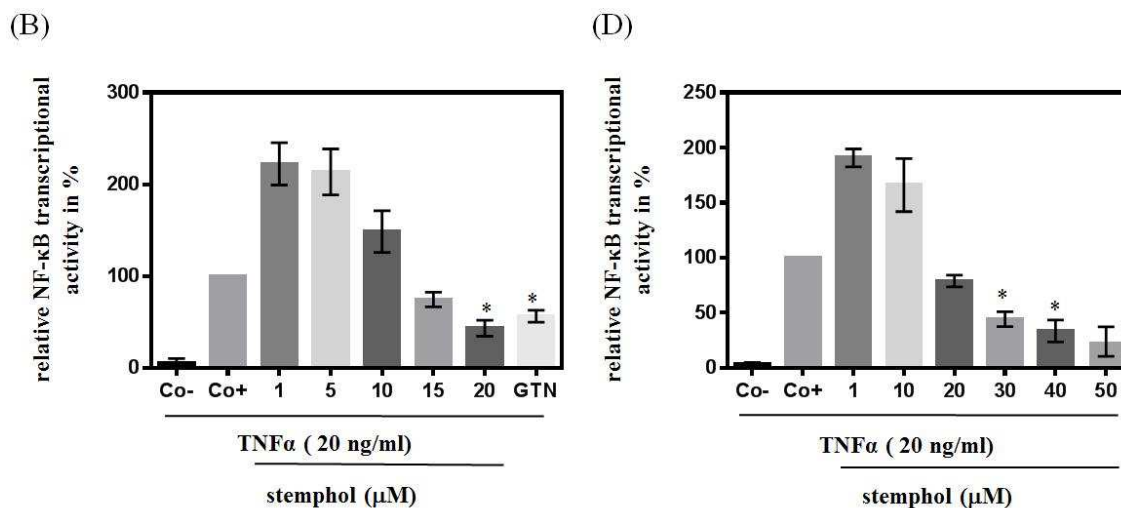
**Figure 35: Effect of stemphol (3) on proliferation and viability of human leukemic cells lines (B: Jurkat, C: Raji, D: U937, Co: control)**



Additionally the effect of stemphol (3) on NF- $\kappa$ B activity was investigated. NF- $\kappa$ B is a family of closely related protein dimers, a key transcription factor, which is involved in regulating, amongst other, proliferation of cancer cells and lead to expression of target genes involved in all steps of tumorigenesis. Therefore, it became a promising therapeutic target of hematological malignancies and solid tumors. In collaboration with the workgroup of Prof. Diederich, Seoul National University, we investigated the effect of stemphol (3) on TNF $\alpha$ , a tumor necrosis factor, a cytokine that is involved in inflammation and in regulation of immune cells and apoptotic cell death. Evidence further indicates strong association between

chronic inflammatory conditions and cancer (Coussens and Werb 2002). Stempfol (**3**) showed an inhibition of NF- $\kappa$ B activity in four different leukemia cell lines in a dose dependent manner. Thus, stemphol (**3**) inhibited TNF $\alpha$ -induced NF- $\kappa$ B activity with an IC<sub>50</sub> of 18  $\mu$ M in Jurkat and 30  $\mu$ M in U937, respectively (Figure 36).

**Figure 36: Inhibitious effect of stemphol (3) on TNF $\alpha$ -induced NF- $\kappa$ B activity in (B) Jurkat and (D) U937 cells in a dose-dependent manner; Co: control, GTN: goniothalamin (positive control)**



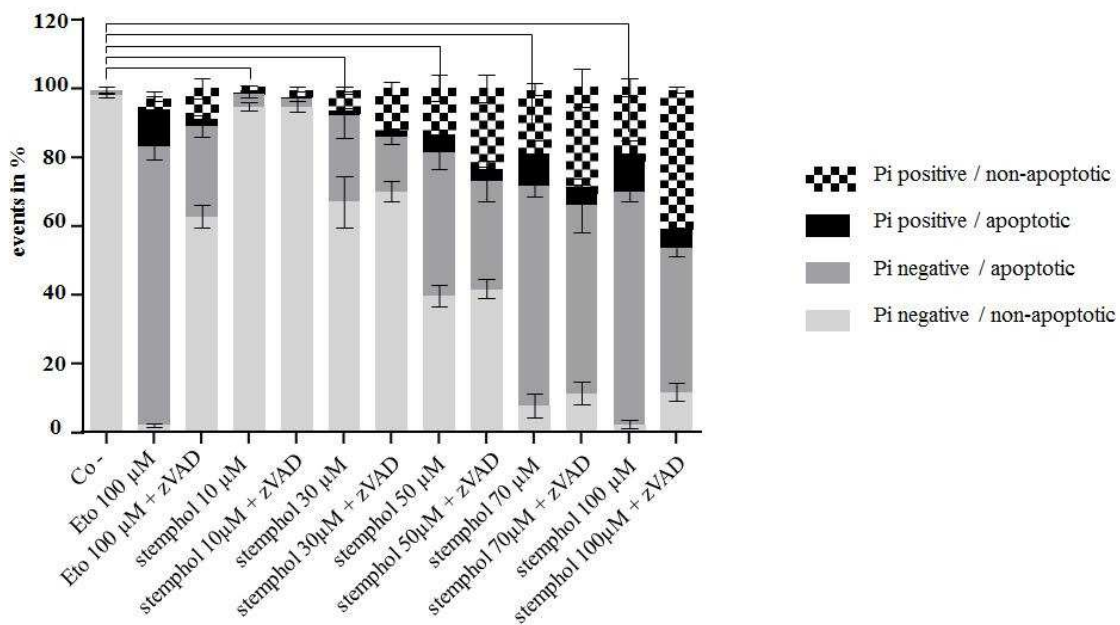
Each graph corresponds to the mean  $\pm$  SD of three independent experiments. \* indicate  $p < 0.05$  compared to control negative group, assay was done by Seungwon Ji, work group of Prof. Diederich, Seoul National University

NF- $\kappa$ B regulates at least 500 genes (Faustman and Davis 2010). Therefore, the focus on the further studies was to narrow down the signaling pathway, in which stemphol (**3**) is involved. The origin of cancer involves deregulated cellular proliferation and the suppression of apoptotic processes, ultimately leading to tumor establishment and growth. Caspases, which are an acronym for cysteine-aspartic proteases, cysteine aspartases and cysteine-dependent aspartate-directed proteases, respectively, are playing an essential role in programmed cell death.

Therefore, the next step was an assay with the caspase inhibitor zVAD. zVAD is a synthetic peptide-inhibitor, who contains the obligate amino acid aspartate at the C-terminal. Within the inhibitor is a benzyloxycarbonylgroup, whereby zVAD can bind nonspecific on the active center on every caspase. The consequence is direct and irreversible inhibition of the caspases (Bauhammer 2005). After addition of the caspase inhibitor zVAD and serially diluted amounts of stemphol (**3**), U937 cancer cells are stained with propidium Iodide (Pi). Pi is an intercalating agent and a fluorescent molecule which is used to stain membrane-disrupted cells for the assay analysis. At early stage of the apoptosis it is not possible to stain the cells.

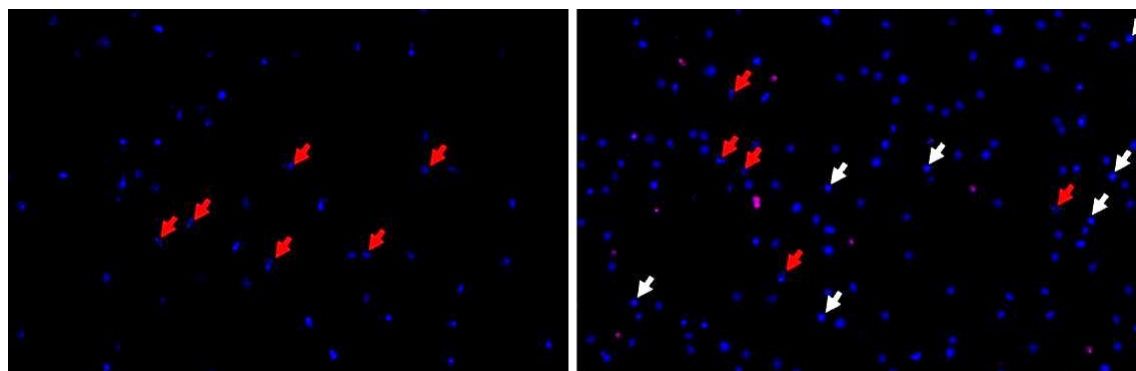
Therefore, for these cells the dark grey color was chosen including the term Pi negative / apoptotic (Figure 37). Healthy cells were also unable to stain and therefore marked as Pi negative / non-apoptotic in light grey color. Correspondingly, the term Pi positive / apoptotic colored in black was used for membrane-disrupted cells and the term Pi positive / non-apoptotic colored in white and black was used for dead cells built by other than the apoptotic pathway *e.g.* necrosis (Figure 37).

**Figure 37: Stemphol (3) induced caspase-independent U937 cell death at 24 h in a dose-dependent manner, Etoposide (Eto) - positive control, zVAD - caspase inhibitor, Pi -propidium iodide**



assay was done by Seungwon Ji, work group of Prof. Diederich, Seoul National University

**Figure 38: Enlarged picture of Etoposide (left) - positive control - and stemphol 30  $\mu$ M (right) treated U937 cells - nuclear fragmentation marked as red arrows, chromatin condensation marked as white arrows, respectively**



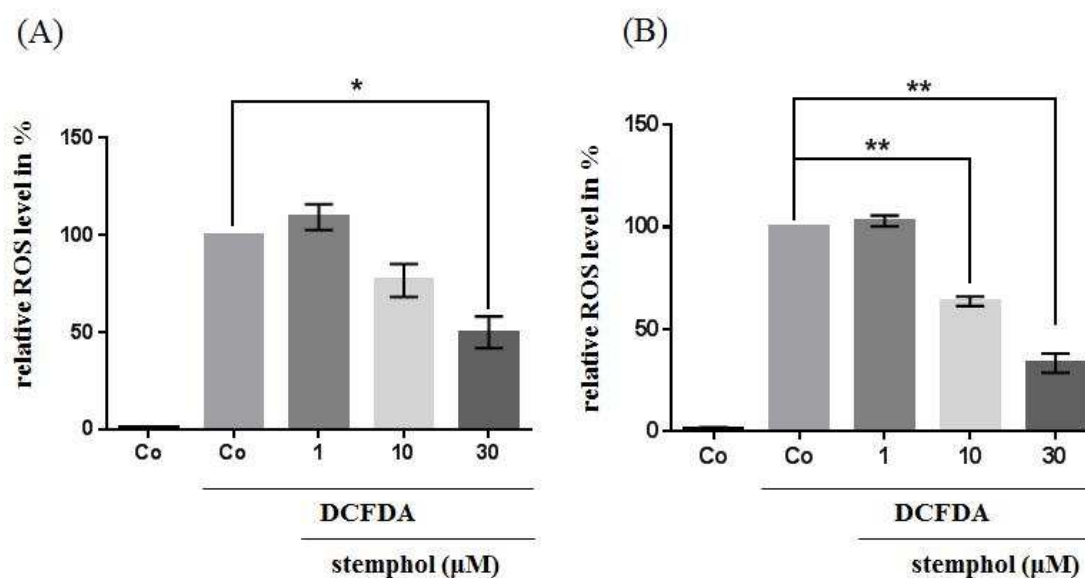
assay was done by Seungwon Ji, work group of Prof. Diederich, Seoul National University

The zVAD assay revealed that there is a stemphol-induced cell death even in the presence of caspase inhibitor zVAD in a dose-dependent manner. In figure 38 Etoposide, the positive control, leads to apoptosis of the cancer cells. After 24 h, more than 10% of the cells reached apoptosis whereas most of the rest is in an early stage of the apoptosis. At this stage Pi is not able to stain the cells, therefore the term Pi negative / apoptotic is used. By addition of the caspase inhibitor zVAD, 60 % of the cells are still alive after 24 h whereas 30% are on an early stage of apoptosis and 10 % are membrane-disrupted (Pi positive) non apoptotic cells, probably necrotic cells. Starting from 30  $\mu$ M stemphol (**3**) quantity of living cells (marked as Pi negative / non apoptotic in light grey color) decrease while the amount of apoptotic cells, induced by stemphol (**3**) and independent to zVAD significantly increase (marked as Pi negative / apoptotic in dark grey color). This effect is also seen by 50  $\mu$ M and 70  $\mu$ M addition of stemphol (**3**), independently of the addition of the caspase inhibitor zVAD (Figure 37). Typical for apoptosis are morphological changes such as nuclear fragmentation or chromatin condensation. These phenomenon is seen in Figure 39 for the positive control Etoposide (left) and the added 30  $\mu$ M stemphol (right), marked as red arrows and white arrows, respectively. The purple colored cells in Figure 38 (right) are membrane-disrupted and therefore Pi positive cells.

### 4.3.9.2 Activity towards reactive oxygen species

Reactive oxygen species (ROS) are constantly generated and eliminated in the biological system and are required to drive regulatory pathways *e.g.* they are one of the NF- $\kappa$ B inducing factors. By interferences of the usual equilibrium of intracellular mitochondrial produced ROS and eliminated reactive oxygen species through scavenging systems like antioxidants excessive ROS can damage lipids, proteins and DNA, which led to fatal lesions in cell and can implicate pathogenesis of cancer (Droege 2002). Therefore, the effect of stemphol (**3**) towards ROS provides a possibility for deeper investigations of the inhibition pathway through the isolated metabolite. During the cellular detection assay (DCFDA) stemphol (**3**) showed an antioxidant effect (Figure 39). 30  $\mu$ M of Stemphol (**3**) inhibited significantly intracellular ROS level of 50 % after 30 min and of 60 % after 4 hours respectively (see 3.6.9).

**Figure 39: Cellular reactive oxygen species detection assay (DCFDA) of stemphol (**3**) after 30 min (A) and 4 hours (B)**



Each graph corresponds to the mean  $\pm$  SD of three independent experiments. , \*, \*\* indicate  $p < 0.05$ ,  $p < 0.01$  compared to control negative group, respectively, assay was done by Seungwon Ji, work group of Prof. Diederich, Seoul National University

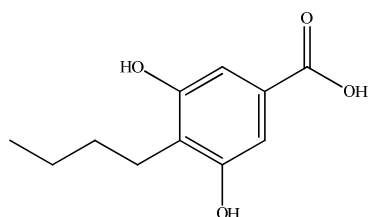
## 4.4 Further metabolites isolated from *Stemphylium globuliferum*

### 4.4.1 New natural product 4-butyl-3,5-dihydroxy benzoic acid (4)

#### 4.4.1.1 Cultivation and extraction of 4-butyl-3,5-dihydroxy benzoic acid (4)

4-butyl-3,5-dihydroxy benzoic acid (4) was isolated from the endophytic fungus *St. globuliferum*. After homogenization and extraction of the fungal biomass and BMS-media with EtOAc 1.7 g of crude extract were obtained. The material was fractionated employing NP-VLC (0.063-0.200 mm, Merck) using stepwise elution from petrolether to EtOAc to MeOH to afford 11 fractions. Of these, fraction 1.3 was further separated via another NP-VLC (0.040-0.063 mm, Merck) using stepwise elution from petrolether to EtOAc of which the subfractions 1.3.7 and 1.3.8 were collected and reunited. 4-butyl-3,5-dihydroxy benzoic acid (4) was finally isolated via an RP-HPLC fractionation to yield 1.2 mg (Figure 40).

**Figure 40: Structure of 4-butyl-3,5-dihydroxy benzoic acid (4)**



#### 4.4.1.2 Structure elucidation of 4-butyl-3,5-dihydroxy benzoic acid (4)

**Table 13: NMR spectroscopic data (300 MHz) of 4-butyl-3,5-dihydroxy benzoic acid (4) in MeOH-d<sub>4</sub>**

Pos.	$\delta_{\text{H}}$ , in ppm, mult., $J$ (Hz)	$\delta_{\text{C}}$ in ppm	$^1\text{H}$ - $^1\text{H}$ COSY- Correlations	HMBC-Correlations
1		170.5, C		
2a		157.3, C		
2b		157.3, C		
3		130.0, C		
4		122.9, C		
5a	7.00, brs	108.8, CH		C-2, C-3, C-4, C-5b
5b	7.00, brs	108.8, CH		C-2, C-3, C-4, C-5a
6	1.53, m	32.1, CH <sub>2</sub>	H <sub>2</sub> -7	C-4, C-8
7	2.67, tr (7.5)	24.1, CH <sub>2</sub>	H <sub>2</sub> -6	C-2, C-4, C-6, C-8
8	1.44, m	23.9, CH <sub>2</sub>	H <sub>3</sub> -9	C-6
9	0.94, tr (7.4)	14.4, CH <sub>3</sub>	H <sub>2</sub> -8	C-6, C-8

The  $^{13}\text{C}$ -NMR and DEPT-135 spectra showed 11 resonances for one methyl group, three methylene and two methine groups, as well as five quaternary carbon atoms. Functional groups within the molecule could be deduced from  $^{13}\text{C}$ -NMR signals, for one carboxylic acid at  $\delta$  170.5 (C-1) and two hydroxylated carbon atoms at  $\delta$  157.3 (C-2a and C-2b) (Table 13). Analysis of the  $^1\text{H}$ - $^1\text{H}$  COSY spectrum allowed to delineate a spin-system including H-6 to H-9 pointing towards a butyl chain. The analysis of the  $^1\text{H}$ - $^{13}\text{C}$ -HMBC spectrum showed the presence of a benzene ring. HMBC correlations of H<sub>2</sub>-7 to C-2, C-4, C-6 and C-8 indicated that the butyl chain must be connected via C-4 to the benzene ring. This assumption is supported by correlations of H<sub>2</sub>-6 to C-4 and C-8. Taking the molecular formula into account, two hydroxyl groups and a carboxylic acid still have to be connected. The hydroxyl groups are attached to C-2a and C-2b, respectively, the carboxylic acid is connected to C-3. This is supported by the  $^{13}\text{C}$ -NMR chemical shifts of these carbons.

#### 4.4.1.3 Antibacterial activity of 4

4-butyl-3,5-dihydroxy benzoic acid (4) was tested against a broad spectrum of microorganisms, that is, the Gram-positive bacteria *Staphylococcus aureus* 133, *Bacillus subtilis* 168, *Micrococcus luteus* 4698, *Arthrobacter crystallopoietes* DSM 20117, the Gram-negative bacteria *Escherichia coli* I-11276b, *Klebsiella pneumoniae* subsp. *ozeanae* I-10910 and the fungus *Candida albicans* I-11301. The compound revealed a moderate antibiotic activity against *E coli* with an inhibition of 3 mm (3 $\mu$ g/assay). The test was performed by Michael Josten from the group of Prof. Tanja Schneider, Institute of Pharmaceutical Microbiology, University of Bonn.

#### 4-butyl-3,5-dihydroxybenzoic acid (4)

C<sub>11</sub>H<sub>14</sub>O<sub>4</sub> (210.23)

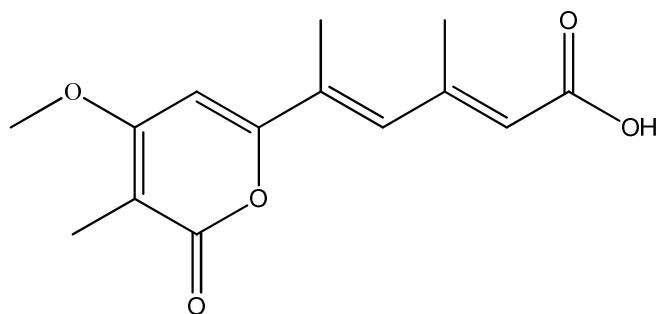
(3.6 mg)

0.36mg/L

#### 4.4.2 Infectopyrone (5)

Fungal biomass and Malt-yeast media were homogenized and extracted with EtOAc to yield 1.9 g of the extract. The material was fractionated employing NP-VLC (0.063-0.200 mm, Merck) using stepwise elution from petroleum ether to EtOAc to MeOH to afford 23 fractions. Of these, fraction 10 (250 mg) was achieved by RP-HPLC (Eurosphere C<sub>18</sub> MeOH/H<sub>2</sub>O = 80/20) to afford 17 mg of subfraction 2.10.5 (Figure 41).

Figure 41: Structure of infectopyrone (5)



Compound **5** was isolated and identified as the  $\alpha$ -pyrone derivative infectopyrone (Larsen et al. 2003).

$C_{14}H_{16}O_5$  (264.27)

1.5 mg/L

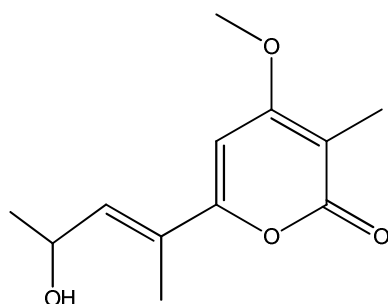
Pale yellow amorphous solid (15 mg)

- no antimicrobial activity
- no cytotoxicity
- no inhibition of Chlamydia
- no anti-parasitic activity
- no NF- $\kappa$ B inhibition

#### 4.4.3 Stemphyprone (**6**)

Stemphyprone (**6**) was isolated from the endophytic fungus *St. globuliferum*. After homogenization and extraction of the fungal biomass and media with EtOAc 1.7 g of crude extract were obtained. The material was fractionated employing NP-VLC (0.063-0.200 mm, Merck) using stepwise elution from petrolether to EtOAc to MeOH to afford 11 fractions. Of these, fraction 1.3 was further separated via another NP-VLC (0.040-0.063 mm, Merck) using stepwise elution from petrolether to EtOAc of which the subfractions 1.3.7 and 1.3.8 were collected and reunited. Stemphyprone (**6**) was finally isolated via an RP-HPLC (Knauer  $C_{18}$  Eurospher-100 MeOH/H<sub>2</sub>O = 55/45) fractionation to yield 2.8 mg (Figure 42).

**Figure 42: Structure of stemphyprone (**6**)**



Compound **6** was isolated as stemphypyrone according to Debbab et al. 2009

$C_{12}H_{16}O_4$  (224.25)

Red powder (2.8 mg)

0.28 mg/L

- no antimicrobial activity

## 5. Discussion

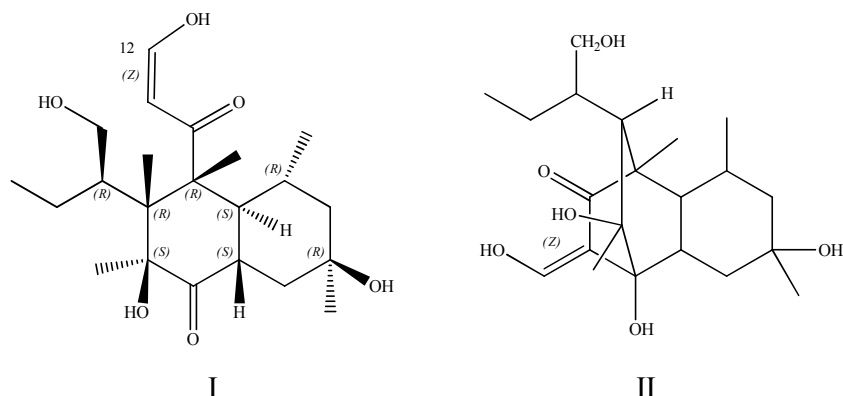
Fungi are a ubiquitously occurring group of organisms. They were shown to be a superior source for structurally new and biologically active compounds, which is reflected by the ever increasing number of published literature dealing with fungal secondary metabolites (Zheng et al. 2016; Newman und Cragg 2016).

The here investigated organism *Stemphylium globuliferum* is a mold fungus and belongs to the Pleosporaceae. *Stemphylium* spp. is known for their phytopathogenicity. Thus, the focus of former research targeted the prevention of agricultural damages, e.g. the Stemphylium leaf spot disease or the purple spot disease on *Asparagus officinalis* (Graf et al. 2016). Isolated metabolites, i.e. stemphyloxin I and II (Figure 43) as well as stemphol (Figure 24) confirmed this phytotoxicity in that they cause damage to leaves (Barash et al. 1982; Manulis et al. 1984). Beyond these compounds, the species is known for, e.g. the cytotoxic compound altersolanol A (Teiten et al. 2013) (Figure 7, introduction).

In the present study, *S. globuliferum* was isolated for the first time from the marine-derived alga *Petalonia zosterifolia*, and thus the fungus originated from the - in general - underexplored marine habitat. The secondary metabolites isolated from our marine fungal strain possess interesting pharmacological activities useful for further developments, and at the same time give insights into chemistry of fungi from a poorly investigated area.

Six metabolites were obtained from this fungus. Stemphol (**3**) and 4-butyl-3,5-dihydroxy benzoic acid (**4**) are known resorcinol-derivatives, whereas stemphylofuran (**2**) has a new unprecedented structure composed of a furan ring and a 3-pentenone moiety. Stemphypyrone (**6**) and infectopyrone (**5**) have a  $\alpha$ -pyrone core structure and are described in the literature (Debbab et al. 2009; Larsen et al. 2003), while the novel stemphyloxin III (**1**) is a decline-based metabolite with structural similarities to the known, polyketides stemphyloxin I and II (Barash et al. 1982; Larsen et al. 2003), respectively.

**Figure 43: The plant toxic compounds stemphyloxin I (left) and II (right) from *Stemphylium* spp.**

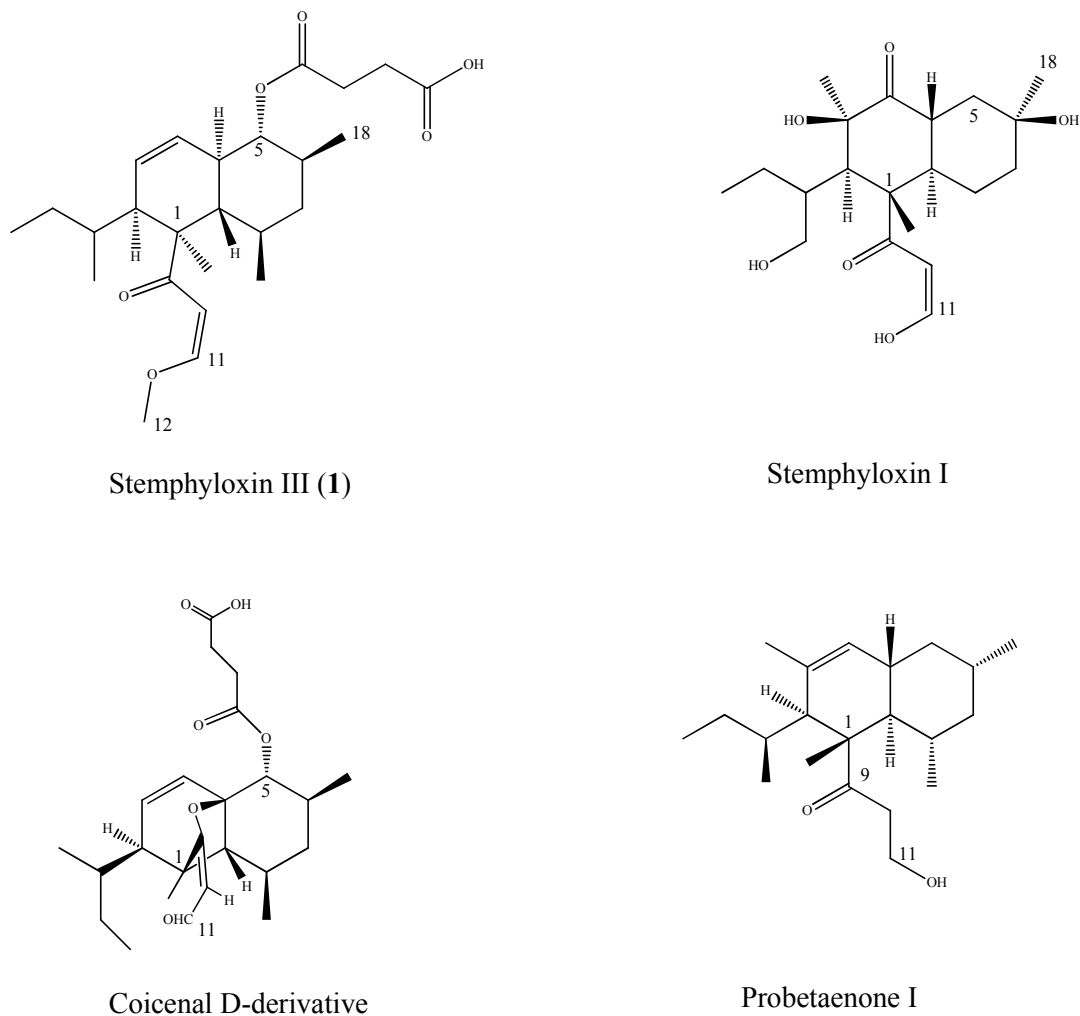


### 5.1 Discussion of the new metabolite stemphyloxin III (1)

The new metabolite stemphyloxin III (**1**) is closely related to the polyketides stemphyloxin I, probetaenone I and a coicenol D-derivative, which are all of fungal origin (Figure 44). All of these compounds are described as biologically active. Betaenone type compounds like probetaenone I are known as phytotoxins, but also inhibit protein kinase, *e.g.* CDK4-kinase and therefore of particular interest for the development of new anticancer drugs (Ichihara et al. 1983; Brauers et al. 2000). Stemphyloxin I is also toxic towards plants (Manulis et al. 1984). Coicenol D, firstly isolated from the plant pathogenic fungus *Bipolaris coicis*, has moderate nitric oxide (NO) inhibition potential, pointing to a possible therapeutic value in inflammatory diseases (Wang et al. 2013).

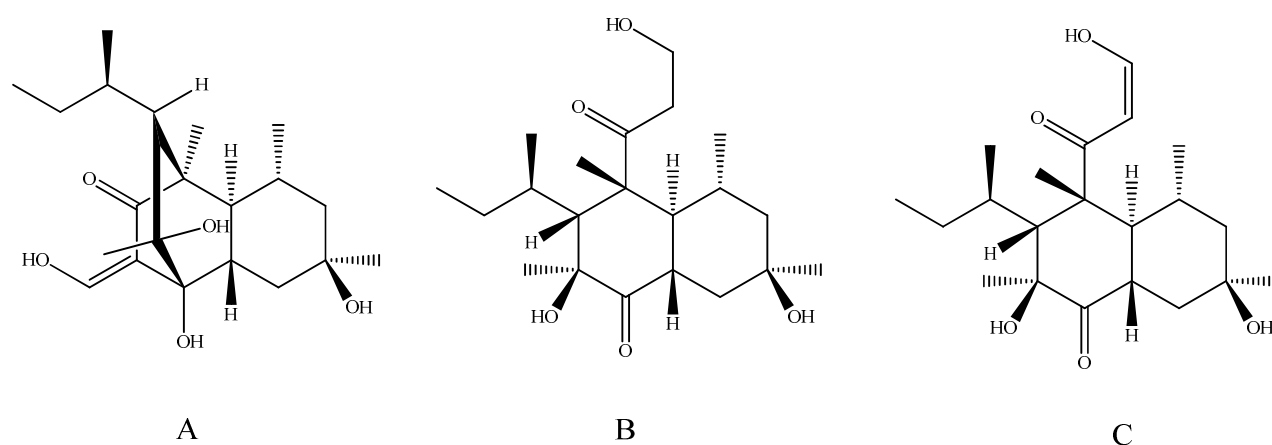
Agar diffusion assays revealed that **1**, isolated during the current study, leads to growth inhibition of *Micrococcus luteus* and *Arthrobacter crystallopoietes* with 5 mm and 7 mm inhibition zones (3  $\mu$ g), respectively, whereas no activity towards other groups of microorganisms could be detected (see 3.5.1). These results are similar to the ones obtained for coicenol D (Wang et al. 2013). Additionally, no cytotoxic effect up to 30  $\mu$ M for **1** could be observed.

**Figure 44: Structures of the decaline-derivatives stemphyloxin III (1), stemphyloxin I, a coincenal D-derivative and probetaenone I**

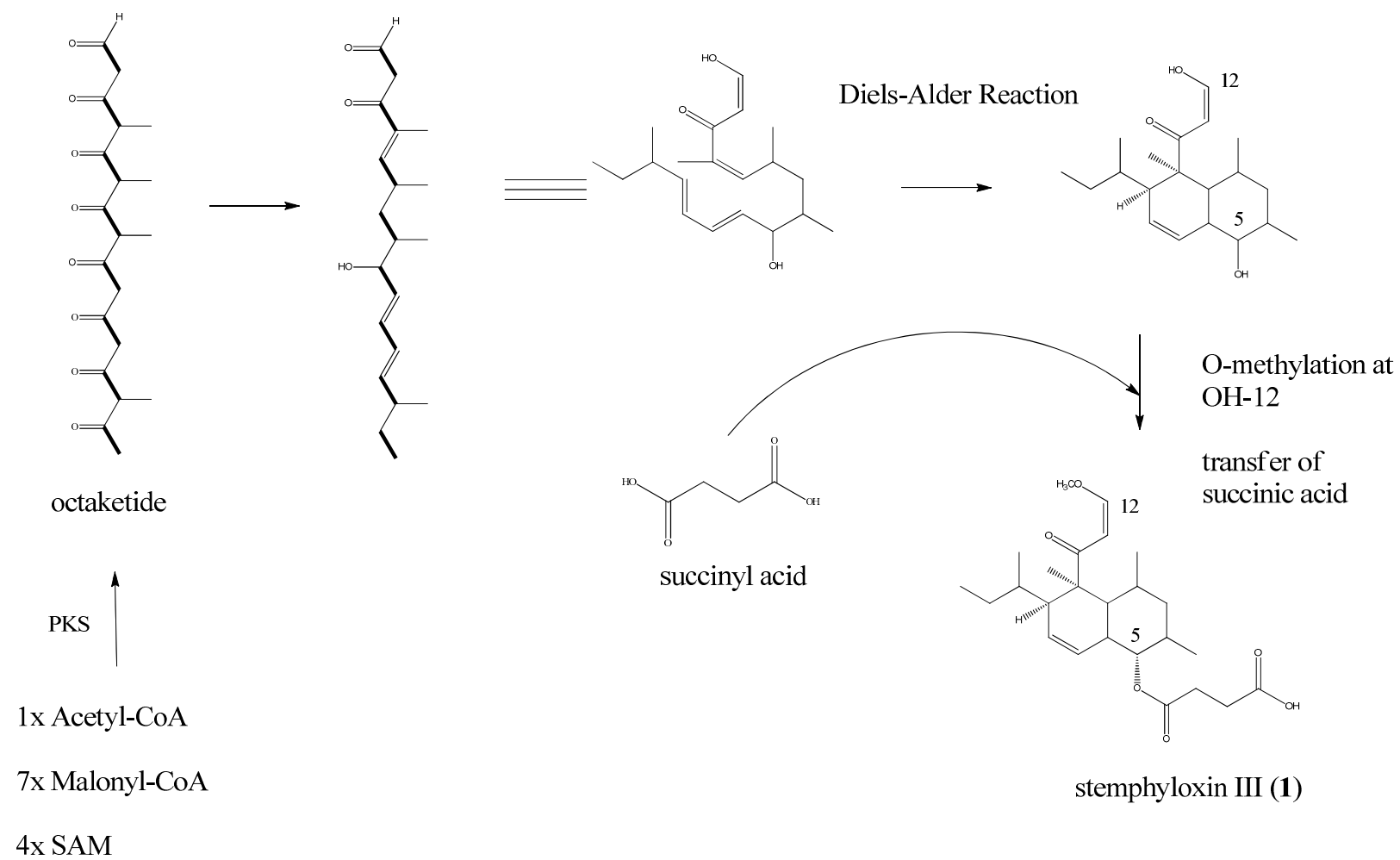


The decaline core structure of **1** and the secondary butyl moiety are alike to those of probetaenone I. At C-5 however, stemphyloxin III (**1**) is linked to a succinyl unit, which is missing in probetaenone I. In turn, the latter moiety is identical to that of a coincenal D-derivative described in the literature (Wang et al. 2013), where also a succinyl unit is attached to the decaline core structure. Furthermore, stemphyloxin III (**1**) has an enol functionality attached to C-1, which is alike that in stemphyloxin I, except the fact, that the here isolated natural product has merely a methoxy group at C-11, whereas the known toxin has a hydroxyl group (Figure 44). In the latter case the enol functionality can be regarded as a tautomeric form of an aldehyde group.

Future perspectives for the isolated new metabolite stemphyloxin III (**1**) can be the derivatization to enhance the bioactive potential of the new natural product.

**Figure 45: Betaenone A, B and C from the fungus *Phoma betae***

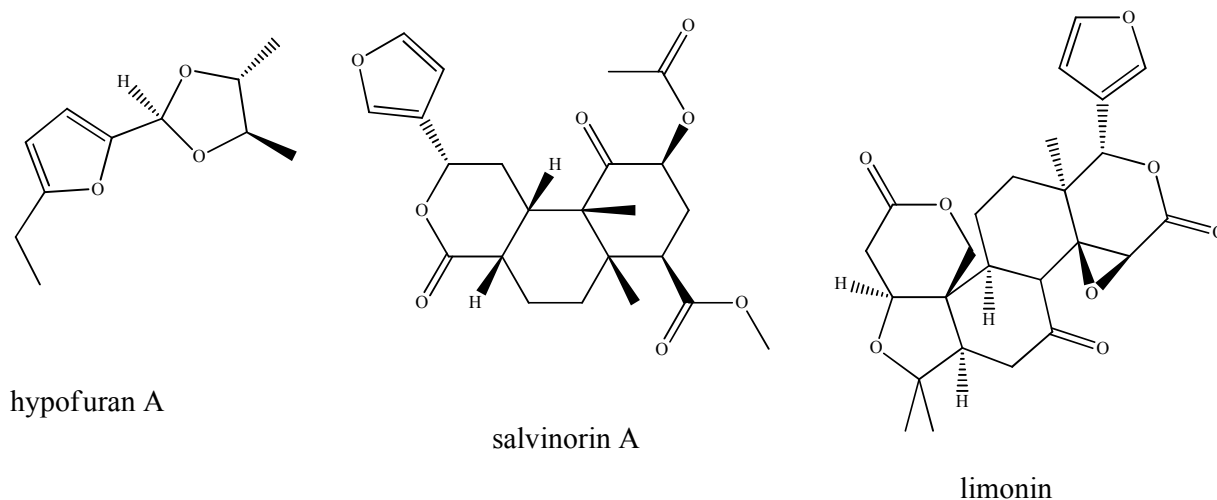
The biosynthesis of stemphyloxin III (**1**) may be related to the betaenone pathway from the fungus *Pleospora betae* (Ugai et al. 2015), a plant pathogen producing the known phytotoxins betaenone A, B and C (Figure 45). Based on the results for betaenones, a biosynthesis for stemphyloxin III (**1**) can be assumed as shown in Figure 46. Thus, the building blocks malonyl-CoA, acetyl-CoA and S-adenosyl-methionin (SAM), may form a linear polyketide chain in that the starter unit acetyl-CoA is connected with the malonyl-CoA units. Ketoreductases, dehydratases and enoylreductases modify the chain during chain elongation and a linear polyketide as shown in Figure 46 is generated. After the reductive chain-release to form the enol moiety on the C-terminal ending a [4+2] cycloaddition (Diels-Alder-reaction) of the alkyl chain leads to *trans*-decaline skeleton. The latter mechanism is similar to one observed for the well-studied fungal polyketide lovastatin, where also a [4+2] cycloaddition takes place (Ma and Tang 2007). After the cyclization follows a presumable methylation of OH-12 by an oxygen-methyltransferase, as well as the transfer of the succinic acid moiety to the hydroxyl group at C-5, to build the new natural product stemphyloxin III (**1**).

**Figure 46: Proposed biosynthetic pathway of stemphyloxin III (1)**

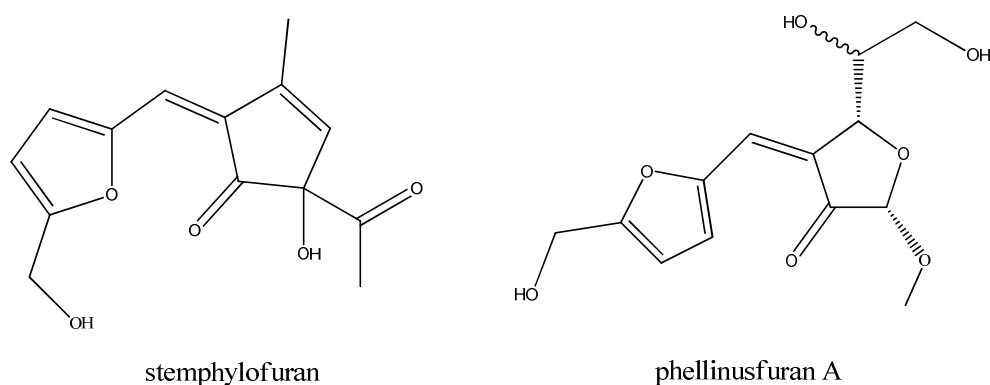
## 5.2 Discussion of the new metabolite stemphylofuran (2)

Furan rings often occur in natural products, and form a diverse group of biologically active compounds. Some of them shall be mentioned. The plant-derived salvinorin A from *Salvia divinorum* is a psychotropic molecule and has a long history of use as an entheogen by indigenous Mazatec shamans. Furthermore, limonin has a furan moiety and activity towards colon cancer cells, as well as being positive in a test against obesity in mice (Chidambara et al. 2011; Ono et al. 2011). The sponge-associated fungus *Hypocrea koningii* contains hypofuran A, which has radical scavenging properties (Ding et al. 2015) (Figure 47). Another example for furan-derivatives is the recently discovered murrano-furan A from the endophytic fungus *Culvularia sp.* isolated from the curry plant *Murraya koenigii* (Mondol et al. 2017).

**Figure 47: Furan-derivatives hypofuran A, left; salvinorin A, middle; limonin, right**



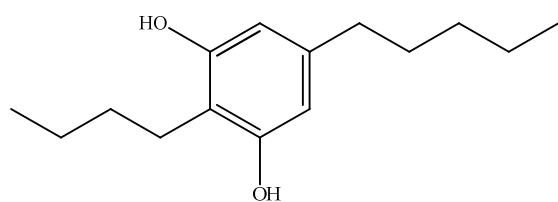
The here investigated stemphylofuran (2) is a furan-derivative with a 3-pentenone moiety, connected via a methine group to a furan ring (Figure 17). This carbon skeleton is a rare structural feature and only found in phellinusfuran A from the fungus *Phellinus linteus* (Figure 48). Beside data for the structure elucidation, no literature towards biological activity could be found for phellinusfurans. Stemphylofuran (2) is structurally similar phellinusfuran A (Min et al. 2006). It is remarkable that both metabolites were gained from alga-derived fungi, hinting towards some correlation to the unique saltwater habitat.

**Figure 48: Stemphylofuran (2) and phellinusfuran A**

The new isolated metabolite **2** was tested against a variety of microorganisms. Stemphylofuran (**2**) showed antimicrobial activity towards *Micrococcus luteus* and *Arthrobacter crystallopoietes* of 3 mm and 5 mm, respectively, whereas no activity towards other groups of microorganisms could be detected. Additionally, no cytotoxic effect up to 30  $\mu\text{M}$  of **2** could be observed.

### 5.3. Discussion of the metabolite stemphol (3)

Stemphol (**3**) is a 2,5-dialkylresorcinol, firstly isolated from *S. majusculum* in 1973 (Stodola et al. 1973) (Figure 49). Beside significant inhibitory activity towards the phylogenetically related fungus *Pleospora herbarum*, it showed antimicrobial effects against Gram-positive bacteria, a plant pathogenic fungus and a yeast (Achenbach et al. 1979). Resorcinol itself and its mono and dialkylated derivatives display a broad spectrum of biological activities, e.g. resorcinol is used for the treatment of psoriasis, the monoalkylated 4-hexylresorcinol significantly decreased the tumor growth rate in mice, and 2,5-dialkylated DB-2073 (Figure 8), was found active against mycobacteria, yeasts, fungi and Gram-positive bacteria (Kanda et al. 1975).

**Figure 49: Structure of stemphol (3) isolated from *S. globuliferum***

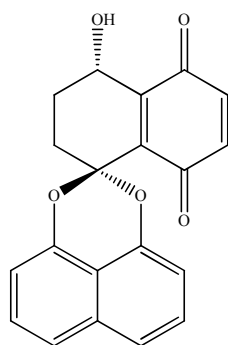
Our experiments addressing the antimicrobial activity of stemphol (**3**) confirmed the data in the literature, *i.e.* activity towards Gram-positive bacteria (Achenbach et al. 1979). Beyond that, we noticed that not only *S. aureus* but also methicillin-resistant *S. aureus* was inhibited with a MIC value of 4 µg/ml. Furthermore, inhibition of *E. faecium* and *K. pneumoniae* with MICs of 16 µg/ml and 64 µg/ml, respectively underlined the antibacterial potential of stemphol (**3**). These microorganisms are within the group of “ESKAPE” pathogens (*E. faecium*, *S. aureus*, *K. pneumoniae*, *Acinetobacter baumannii*, *Pseudomonas aeruginosa* and *Enterobacter* species) accentuating their capacity to “escape” from routine antimicrobial drugs (Khan and Khan 2016). Multidrug resistance is amongst the top three threats to global public health and can be caused by inappropriate use or excessive use of drugs (Santajit et al. 2016). The inhibition of three of these organisms through stemphol (**3**) is remarkable and may lead to further research in this discipline.

However, structure-activity relationships for the antimicrobial activity are not verified yet. Achenbach et al. only showed that a molecule with two pentyl chains, *i.e.* in C-2 and C-5 position of the benzene ring, have no activity towards *B. subtilis*, *S. aureus*, as well as *Schizosaccharomyces pombe* and *Mucor hiemalis*, whereas a molecule with a pentyl chain in C-2 position and a butyl chain in C-5 position was inhibitory against all four tested organisms (Achenbach et al. 1979, 1979).

Stemphol (**3**) was shown by us to lead to a diminished number of chlamydia in Hep-2 host cells (see. 4.3.8). During the assays it was noted, that the cell line in which the chlamydia grow was also affected by stemphol (**3**). Thus, the results of stemphol (**3**) towards the tested chlamydial organisms reveal that the potential of inhibition of these pathogens can be based on cytotoxic effects of **3** towards the host cells. This possible indirect inhibition can be an explanation for the partial transformation of the chlamydial host cells at 16 µg/ml (see 4.3.8). The morphological changes and thereby the increase of the cell volume revealing the stressful conditions for the host is due to the addition of the fungal metabolite (**3**).

The cytotoxicity can also be a reason for the weak selectivity of **3** towards the investigated protozoan parasites *Trypanosoma brucei rhodesiense*, *T. bruzi*, *Leishmania donovani* and *Plasmodium falciparum*. A good example for this are the results obtained for the inhibition of *L. donovani*, for which only a selectivity index of 15 was calculated, which is a weak value compared, e.g. palmarumycin CP18 from the endophytic fungus *Edenia sp.* with 245 times more antileishmanial activity than cytotoxicity (Figure 50) (Martinez-Luis et al. 2008). Derivatization of stemphol (**3**) can be an approach to gain a reduced cytotoxicity and an increase of selectivity, and may open the door for further drug development using the isolated fungal alkylresorcinol-derivative (**3**).

**Figure 50: Palmarumycin CP18 from the endophytic fungus *Edenia sp.***



Additionally, the free radical scavenging potential of stemphol (**3**) was tested using a reactive oxygen species assay (see 4.3.9.2), which showed that stemphol (**3**) has antioxidant potential as known of dialkylresorcinols, e.g. the derivatives DB-2073 and resorstatin (Figure 8, introduction) have free radical scavenging potential (Kato et al. 1993).

Furthermore, cytotoxicity assays against the four different cancer cell lines K562 cells, Jurkat cells, Raji cells and U937 cells, respectively, were done with the isolated metabolite (**3**). The assays revealed that stemphol (**3**) has a growth inhibitory activity towards these cell lines, even though the inhibition is weaker when compared to other natural products, e.g. 13 times weaker than for altersolanol A (Figure 7, introduction). Altersolanol A, which is also inhibiting the NF- $\kappa$ B transcriptional activity, as was shown for stemphol (**3**), possesses a p-quinone moiety possibly related to the bioactivity. Stemphol (**3**) however is merely a phenolic metabolite, of which a metabolic transformation to a quinone cannot be excluded. Stemphol (**3**) inhibited the TNF $\alpha$ -induced NF- $\kappa$ B pathway in a caspase-independent manner.

---

Furthermore, it shows specific morphological changes such as chromatin condensation in U937 cells hinting at a non-canonical pathway. The caspase independent inhibition of the NF- $\kappa$ B pathway through stemphol (**3**) making this isolated metabolite a valuable target for deeper investigations regarding anti-cancer drug development. Arisawa et al. showed that anticancer activity is based on hydroxylation of the benzene ring on C-1 and C-3, respectively, as well as C-5 medium length alkyl chain. The fact that methylated and acetylated derivatives of the hydroxylated benzene ring were inactive pointed to the importance of the hydroxyl groups (Arisawa et al. 1989).

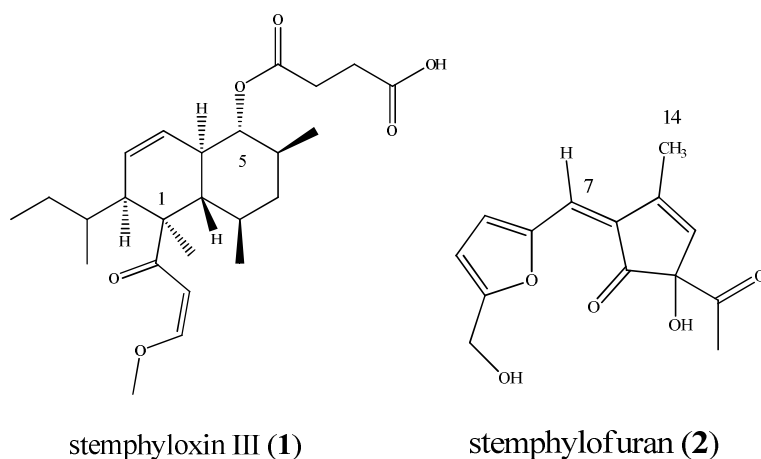
## 6. Summary

Fungi are a tremendous source of pharmaceutically significant compounds, *e.g.* the life saving immunosuppressant drug mycophenolic acid. The current project focused on the investigation of the mold fungus *Stemphylium globuliferum* obtained from the marine alga *Petalonia zosterifolia*, with the aim to find natural products with novel chemical structures and prominent pharmacological activities, particularly antibiotic and/or anticancer effects.

The fungus was cultivated on potato-dextrose-medium and found to produce strongly active antimicrobial metabolites. Subsequently, the extract was separated by vacuum liquid chromatography using a gradient elution system, as well as optimized HPLC separations. Six metabolites were obtained in pure form and characterized using spectroscopic methods. Stemphyloxin III (**1**) has structural similarities to the known stemphyloxins I and II, respectively, but differs concerning the moiety at C-5, where stemphyloxin III (**1**) has a linkage to a succinyl unit. Furthermore, the enol group at C-1 of stemphyloxin III (**1**) is methylated, whereas stemphyloxin I has no methylation on this functional group. Concerning the biosynthesis of **1**, a polyketide origin is most likely, as proven for the structurally closely related betaenones.

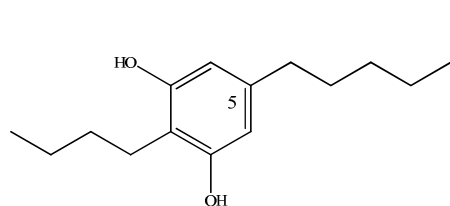
Compound **1** showed moderate antibacterial activities towards *Arthrobacter crystallopoietes* and *Micrococcus luteus* (agar diffusion assay, inhibition zone of 7 mm for *A. crystallopoietes*, 5 mm for *M. luteus* at 3µg, respectively).

The second new compound proved to be stemphylofuran (**2**), a structurally most unusual metabolite consisting of a cyclic pentenone moiety connected via a methine bridge to a furan ring. Due to the presence of four quaternary carbons in the cyclopentenone the structural assignment of this part of the molecule was a challenge that could finally be solved by NOE measurements. Correlations of H-7 to H<sub>3</sub>-14 in these measurements clearly pointed towards a cyclopentenone structure instead of an alternatively assumed six membered ring. This new metabolite showed limited antibacterial activities towards *A. crystallopoietes* and *M. luteus* (agar diffusion assay, inhibition zone of 5 mm for *A. crystallopoietes*, 3 mm for *M. luteus* at 3µg, respectively).

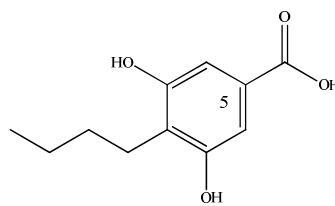


The prominent antimicrobial activity of the fungal extract could be traced back to the known metabolite stemphol (**3**), which showed antimicrobial effects towards methicillin-resistant *Staphylococcus aureus* and *S. simulans* with MIC values in both cases of 4  $\mu\text{g/ml}$ , as well as against *Candida albicans* with an MIC value of 4  $\mu\text{g/ml}$ . Stemphol (**3**) also had weak activities against the Gram-positive *Enterococcus faecium* and *Klebsiella pneumoniae* subsp. *ozeanae* with MIC values of 16  $\mu\text{g/ml}$  and 64  $\mu\text{g/ml}$ , respectively. Against Gram-negative bacteria only a weak activity was noted. From these results, stemphol (**3**) may be considered as an active agent against problematic Gram-positive pathogens.

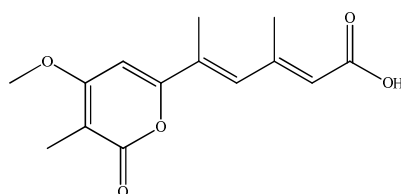
Furthermore, stemphol (**3**) was tested for its antichlamydial activity. Therefore, HEp-2 host cells were infected with *Chlamydia trachomatis* D/UW-3/CX. After gaining chlamydial inclusions in the host cells, the test system was incubated with serially diluted concentrations of stemphol (**3**). It inhibited chlamydial growth in the range of 8 to 16  $\mu\text{g/ml}$ , but also had a pronounced cytotoxicity towards the host cells at high stemphol concentrations. This cytotoxic activity was investigated further using four different human cancer cell lines (Jurkat, Raji, U937 and K562 cell lines), which yielded  $\text{IC}_{50}$  values for stemphol of  $18.7 \pm 0.8$   $\mu\text{M}$  towards Raji cells and  $22.6 \pm 1.2$   $\mu\text{M}$  towards U937 cells, respectively. Additionally the effect of stemphol (**3**) towards NF- $\kappa\text{B}$  was examined and revealed, that TNF $\alpha$ -induced NF- $\kappa\text{B}$  activity was inhibited with an  $\text{IC}_{50}$  of 18  $\mu\text{M}$  in Jurkat cells and 30  $\mu\text{M}$  in U937 cells, respectively. Overall, our results point towards a caspase-independent TNF $\alpha$ -induced NF- $\kappa\text{B}$  inhibition, making this metabolite interesting in the search for new cancer therapies.



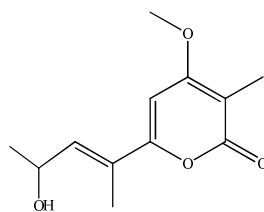
stemphol (3)



4-butyl-3,5-dihydroxy benzoic acid (4)



infectopyrone (5)



stemphyprone (6)

Stemphol (3) revealed limited activity against parasites, *e.g.* *Trypanosoma brucei* subsp. *rhodesiense* and *Leishmania donovani* with  $IC_{50}$  values of 0.18  $\mu\text{g/ml}$  and 0.30  $\mu\text{g/ml}$ , respectively, but again had pronounced cytotoxicity towards the control myoblast cells, showing the limited selectivity of the fungal metabolite. Radioligand binding studies revealed that 3 had weak affinity towards the cannabinoid receptors  $CB_1$  and  $CB_2$ . In contrast, the resorcinol-derivative 4-butyl-3,5-dihydroxy benzoic acid (4) was not active toward  $CB$  receptors, which may be explained by the alkyl chain of stemphol (3) at C-5 instead of a carboxylic acid group at C-5 in the case of 4-butyl-3,5-dihydroxy benzoic acid (4). Furthermore, stemphol (3) showed agonistic activity ( $EC_{50} = 1.76 \pm 0.27 \mu\text{M}$ ) at FFAR 1 receptor, but no effects towards GPR 17, GPR 55 and GPR 84 receptors, respectively.

In conclusion, this project led to the new natural products stemphyloxin III (1), stemphylofuran (2) and 4-butyl-3,5-dihydroxy benzoic acid (4) as well as the known compounds stemphol (3), infectopyrone (5) and stemphyprone (6). Their antibacterial, antifungal, antiplasmodial and cytotoxic activities, and furthermore their affinity toward  $CB_1$ ,  $CB_2$  and on FFAR1 receptors, respectively, showed the broad pharmacological potential of the gained metabolites.

The results of this study demonstrate that the mold fungus *Stemphylium globuliferum* is able to produce novel and promising lead structures for further pharmacological research and drug development based on natural products.

## 7. References

### Literaturverzeichnis

- Achenbach, H.; Kohl, W.; Kunze, B. (1979): Untersuchungen an Stoffwechselprodukten von Mikroorganismen, XIX. Über die Synthese einiger antibiotisch wirksamer 2,5-Dialkylresorcine — Synthese der Antibiotika DB 2073 und Stempchol. In: *Chem. Ber.* 112 (5), S. 1841–1848. DOI: 10.1002/cber.19791120534.
- Amagata, T.; Minoura, K.; Numata, A. (2006): Gymnastatins F-H, cytostatic metabolites from the sponge-derived fungus *Gymnascella dankaliensis*. In: *Journal of natural products* 69 (10), S. 1384–1388. DOI: 10.1021/np0600189.
- Andersen, B.; Frisvad, J. C. (2004): Natural occurrence of fungi and fungal metabolites in moldy tomatoes. In: *Journal of agricultural and food chemistry* 52 (25), S. 7507–7513. DOI: 10.1021/jf048727k.
- Arisawa, M.; Ohmura, K.; Kobayashi, A.; Morita, N. (1989): A cytotoxic constituent of *Lysimachia japonica* THUNB. (Primulaceae) and the structure-activity relationships of related compounds. In: *Chemical & pharmaceutical bulletin* 37 (9), S. 2431–2434.
- Bachmann, N. L.; Polkinghorne, A.; Timms, P. (2014): Chlamydia genomics: providing novel insights into chlamydial biology. In: *Trends in microbiology* 22 (8), S. 464–472. DOI: 10.1016/j.tim.2014.04.013.
- Barash, I.; Karr, A. L.; Strobel, G. A. (1975): Isolation and Characterization of Stemphylin, a Chromone Glucoside from *Stemphylium botryosum*. In: *Plant physiology* 55 (4), S. 646–651. DOI: 10.1104/pp.55.4.646.
- Barash, I.; Pupkin, G.; Netzer, D.; Kashman, Y. (1982): A Novel Enolic -Ketoaldehyde Phytotoxin Produced by *Stemphylium botryosum* f. sp. *lycopersici*. PARTIAL CHEMICAL AND BIOLOGICAL CHARACTERIZATION. In: *Plant physiology* 69 (1), S. 23–27. DOI: 10.1104/pp.69.1.23.
- Bauhammer, J. S. (2005): Wirkungen des Pancaspase-Inhibitors Wirkungen des Pancaspase-Inhibitors zVAD-FMK auf die Apoptose von Makrophagen und Lymphozyten Lymphozyten. Dissertation. Eberhard-Karls-Universität, Tübingen. Medizinische Fakultät. Online verfügbar unter <https://publikationen.uni-tuebingen.de/xmlui/handle/10900/44711>, zuletzt geprüft am 04.04.2017.
- Belland, R. J.; Nelson, D. E.; Virok, D.; Crane, D. D.; Hogan, D.; Sturdevant, D. et al. (2003): Transcriptome analysis of chlamydial growth during IFN-gamma-mediated persistence and reactivation. In: *Proceedings of the National Academy of Sciences of the United States of America* 100 (26), S. 15971–15976. DOI: 10.1073/pnas.2535394100.
- Brauers, G.; Edrada, R.; Ebel, R.; Proksch, P.; Wray, V.; Berg, A. et al. (2000): Anthraquinones and Betaenone Derivatives from the Sponge-Associated Fungus *Microsphaeropsis* Species. Novel Inhibitors of Protein Kinases. In: *J. Nat. Prod.* 63 (6), S. 739–745. DOI: 10.1021/np9905259.
- Briscoe, C.; Tadayyon, M.; Andrews, J.; Benson, W.; Chambers, J.; Eilert, M. et al. (2003): The orphan G protein-coupled receptor GPR40 is activated by medium and long chain fatty acids. In: *The Journal of biological chemistry* 278 (13), S. 11303–11311. DOI: 10.1074/jbc.M211495200.
- Buckner, F.S., Verlinde, C.L., La Flamme, A.C., Van Voorhis, W.C. (1996): Efficient technique for screening drugs for activity against *Trypanosoma cruzi* using parasites expressing beta-galactosidase. In: *Antimicrobial agents and chemotherapy* 40 (11), S. 2592–2597.

- Bugni, T.; Ireland, C. (2004): Marine-derived fungi: a chemically and biologically diverse group of microorganisms. In: *Natural product reports* 21 (1), S. 143–163. DOI: 10.1039/b301926h.
- Buscato, E.; Buttner, D.; Bruggerhoff, A.; Klingler, F.; Weber, J.; Scholz, B. et al. (2013): From a multipotent stilbene to soluble epoxide hydrolase inhibitors with antiproliferative properties. In: *ChemMedChem* 8 (6), S. 919–923. DOI: 10.1002/cmdc.201300057.
- Carter, J.; Hudson, A. (2010): The evolving story of Chlamydia-induced reactive arthritis. In: *Current opinion in rheumatology* 22 (4), S. 424–430. DOI: 10.1097/BOR.0b013e32833a43a2.
- Charrouf, Z.; Guillaume, D. (2007): Phenols and Polyphenols from *Argania spinosa*. In: *American J. of Food Technology* 2 (7), S. 679–683. DOI: 10.3923/ajft.2007.679.683.
- Chidambara, N.; Jayaprakasha, G. K.; Kumar, V.; Rathore, K.; Patil, B. (2011): Citrus limonin and its glucoside inhibit colon adenocarcinoma cell proliferation through apoptosis. In: *Journal of agricultural and food chemistry* 59 (6), S. 2314–2323. DOI: 10.1021/jf104498p.
- Coussens, L. M.; Werb, Z. (2002): Inflammation and cancer. In: *Nature* 420 (6917), S. 860–867. DOI: 10.1038/nature01322.
- Covarrubias-Zúñiga, A.; Avila-Zárraga, J.; Arias Salas, D. (2003): A Total Synthesis of the Antibiotic DB-2073. In: *Synthetic Communications* 33 (18), S. 3173–3181. DOI: 10.1081/SCC-120023438.
- Debbab, A.; Aly, A.; Edrada-Ebel, R.; Wray, V.; Muller, W.; Totzke, F. et al. (2009): Bioactive metabolites from the endophytic fungus *Stemphylium globuliferum* isolated from *Mentha pulegium*. In: *Journal of natural products* 72 (4), S. 626–631. DOI: 10.1021/np8004997.
- Ding, L.; Gu, B.; Jiao, W.; Yuan, W.; Li, Y.; Tang, W. et al. (2015): New Furan and Cyclopentenone Derivatives from the Sponge-Associated Fungus *Hypocrea Koningii* PF04. In: *Marine drugs* 13 (9), S. 5579–5592. DOI: 10.3390/md13095579.
- Droege, W. (2002): Free radicals in the physiological control of cell function. In: *Physiological reviews* 82 (1), S. 47–95. DOI: 10.1152/physrev.00018.2001.
- El Babili, F.; Bouajila, J.; Fouraste, I.; Valentin, A.; Mauret, S.; Moulis, C. (2010): Chemical study, antimalarial and antioxidant activities, and cytotoxicity to human breast cancer cells (MCF7) of *Argania spinosa*. In: *Phytomedicine : international journal of phytotherapy and phytopharmacology* 17 (2), S. 157–160. DOI: 10.1016/j.phymed.2009.05.014.
- Elwell, C.; Mirrashidi, K.; Engel, J. (2016): Chlamydia cell biology and pathogenesis. In: *Nature reviews. Microbiology* 14 (6), S. 385–400. DOI: 10.1038/nrmicro.2016.30.
- Faustman, D.; Davis, M. (2010): TNF receptor 2 pathway: drug target for autoimmune diseases. In: *Nature reviews. Drug discovery* 9 (6), S. 482–493. DOI: 10.1038/nrd3030.
- FDA (2009): Approval of mycophenolic acid. Online verfügbar unter <https://www.fda.gov/Drugs/DrugSafety/PostmarketDrugSafetyInformationforPatientsandProviders/ucm148735.htm>, zuletzt aktualisiert am 05.06.2009, zuletzt geprüft am 04.04.17.
- Ferdaoussi (2012): G protein-coupled receptor (GPR)40-dependent potentiation of insulin secretion in mouse islets is mediated by protein kinase D1. In: *diabetologia* 55 (10), S. 2682–2692.
- Fransworth, N. R.; Akerele, O.; Bingel, A. S.; Soejarto, D. D.; Guo, Z. (1985): medicinal plants in therapy. In: *Bulletin of the World Health Organization* 63 (6), S. 965–981.
- Galsky, M.; Dritselis, A.; Kirkpatrick, P.; Oh, W. (2010): Cabazitaxel. In: *Nature reviews. Drug discovery* 9 (9), S. 677–678. DOI: 10.1038/nrd3254.

- Gannibal, P. (2013): First report of *Stemphylium lycopersici* from Far East Russia. A new record and new host. In: *Mycotaxon* 121 (1), S. 371–374. DOI: 10.5248/121.371.
- Gao, S.; Li, X.; Li, C.; Proksch, P.; Wang, B. (2011): Penicisteroids A and B, antifungal and cytotoxic polyoxygenated steroids from the marine alga-derived endophytic fungus *Penicillium chrysogenum* QEN-24S. In: *Bioorganic & Medicinal Chemistry Letters* 21 (10), S. 2894–2897. DOI: 10.1016/j.bmcl.2011.03.076.
- Godtfredsen, W. O.; Jahnsen, S.; Lorck, H.; Roholt, K.; Tybring, L. (1962): Fusidic Acid. A New Antibiotic. In: *Nature* 193 (4819), S. 987. DOI: 10.1038/193987a0.
- Graf, S.; Bohlen-Janssen, H.; Miessner, S.; Wichura, A.; Stammler, G. (2016): Differentiation of *Stemphylium vesicarium* from *Stemphylium botryosum* as causal agent of the purple spot disease on asparagus in Germany. In: *Eur J Plant Pathol* 144 (2), S. 411–418. DOI: 10.1007/s10658-015-0777-6.
- He, H.; Yang, H.; Bigelis, R.; Solum, E.; Greenstein, M.; Carter, G. (2002): Pyrrocidines A and B, new antibiotics produced by a filamentous fungus. In: *Tetrahedron Letters* 43 (9), S. 1633–1636. DOI: 10.1016/S0040-4039(02)00099-0.
- Hirooka, Y.; Ichihara, Y.; Masuya, H.; Kubono, T. (2012): Seed Rot, a New Disease of Beech Tree Caused by *Neonectria ramulariae* (anamorph. *Cylindrocarpon obtusiusculum*). In: *Journal of Phytopathology* 160 (9), S. 504–506. DOI: 10.1111/j.1439-0434.2012.01934.x.
- Howden, B.; Grayson, M. (2006): Dumb and dumber--the potential waste of a useful antistaphylococcal agent: emerging fusidic acid resistance in *Staphylococcus aureus*. In: *Clinical infectious diseases : an official publication of the Infectious Diseases Society of America* 42 (3), S. 394–400. DOI: 10.1086/499365.
- Huang, C.; Jin, H.; Song, B.; Zhu, X.; Zhao, H.; Cai, J. et al. (2012): The cytotoxicity and anticancer mechanisms of alterporriol L, a marine bianthraquinone, against MCF-7 human breast cancer cells. In: *Applied microbiology and biotechnology* 93 (2), S. 777–785. DOI: 10.1007/s00253-011-3463-4.
- Huang, C.; Pan, J.; Chen, B.; Yu, M.; Huang, H.; Zhu, X. et al. (2011): Three bianthraquinone derivatives from the mangrove endophytic fungus *Alternaria* sp. ZJ9-6B from the South China Sea. In: *Marine drugs* 9 (5), S. 832–843. DOI: 10.3390/md9050832.
- Ichihara, A.; Oikawa, H.; Hayashi, K.; Sakamura, S.; Furusaki, A.; Matsumoto, T. (1983): Structures of betaenones A and B, novel phytotoxins from *Phoma betae* Fr. In: *J. Am. Chem. Soc.* 105 (9), S. 2907–2908. DOI: 10.1021/ja00347a070.
- Igarashi, Y.; Sekine, A.; Fukazawa, H.; Uehara, Y.; Yamaguchi, K.; Endo, Y. et al. (2002): Anicequol, a novel inhibitor for anchorage-independent growth of tumor cells from *Penicillium aurantiogriseum* Dierckx TP-F0213. In: *The Journal of antibiotics* 55 (4), S. 371–376.
- Imhoff, J. F. (2016): Natural Products from Marine Fungi--Still an Underrepresented Resource. In: *Marine drugs* 14 (1), S. 19. DOI: 10.3390/md14010019.
- Jin, L.; Quan, C.; Hou, X.; Fan, S. (2016): Potential Pharmacological Resources: Natural Bioactive Compounds from Marine-Derived Fungi. In: *Marine drugs* 14 (4). DOI: 10.3390/md14040076.
- Kanda, N.; Ishizaki, N.; Inoue, N.; Oshima, M.; Handa, A. (1975): DB-2073, a new alkylresorcinol antibiotic. I. Taxonomy, isolation and characterization. In: *The Journal of antibiotics* 28 (12), S. 935–942.
- Kato, S.; Shindo, K.; Mochizuki, J. (1993): Studies on free radical scavenging substances from microorganisms. Isolation and structural elucidation of a novel free radical scavenger, resorstatin. In: *The Journal of antibiotics* 46 (6), S. 1024–1026.

- Khan, S. N.; Khan, A. U. (2016): Breaking the Spell: Combating Multidrug Resistant 'Superbugs'. In: *Frontiers in microbiology* 7, S. 174. DOI: 10.3389/fmicb.2016.00174.
- Kim, S.; Lee, S.; Park, Y.; Jeong, J.; Choi, J. (2011): 4-hexylresorcinol inhibits NF-kappaB phosphorylation and has a synergistic effect with cisplatin in KB cells. In: *Oncology reports* 26 (6), S. 1527–1532. DOI: 10.3892/or.2011.1436.
- Koike, S.; O'Neill, N.; Wolf, J.; van Berkum, P.; Daugovish, O. (2013): Stemphylium Leaf Spot of Parsley in California Caused by Stemphylium vesicarium. In: *Plant Disease* 97 (3), S. 315–322. DOI: 10.1094/PDIS-06-12-0611-RE.
- Lancet, The (2009): Chagas disease. A neglected emergency. In: *The Lancet* 373 (9678), S. 1820. DOI: 10.1016/S0140-6736(09)61002-3.
- Larsen, T. O.; Perry, N. B.; Andersen, B. (2003): Infectopyrone, a potential mycotoxin from *Alternaria infectoria*. In: *Tetrahedron Letters* 44 (24), S. 4511–4513. DOI: 10.1016/S0040-4039(03)01018-9.
- Ma, S. M.; Tang, Y. (2007): Biochemical characterization of the minimal polyketide synthase domains in the lovastatin nonaketide synthase LovB. In: *The FEBS journal* 274 (11), S. 2854–2864. DOI: 10.1111/j.1742-4658.2007.05818.x.
- Mani, S.; Ghalib, M.; Goel, S.; Serradell, N.; Bolós, J.; Rosa, E. (2007): Ixabepilone. In: *Drugs Fut* 32 (12), S. 1033. DOI: 10.1358/dof.2007.032.12.1157611.
- Manulis, S.; Kashman, Y.; Nertz, D.; Barash, I. (1984): Phytotoxins from stemphylium botryosum. Structural determination of stemphyloxin II, production in culture and interaction with iron. In: *Phytochemistry* 23 (10), S. 2193–2198. DOI: 10.1016/S0031-9422(00)80518-X.
- Martinez-Luis, S.; Della-Togna, G.; Coley, P. D.; Kursar, T. A.; Gerwick, W. H.; Cubilla-Rios, L. (2008): Antileishmanial constituents of the Panamanian endophytic fungus *Edenia* sp. In: *Journal of natural products* 71 (12), S. 2011–2014. DOI: 10.1021/np800472q.
- Marumo, S.; Hattori, H.; Katayama, M. (1985): Stemphol from *Pleospora herbarum* as a Self-Inhibitor. In: *Agric. Biol. Chem* 49 (5), S. 1521–1522.
- Matsuda, L. A.; Lolait, S. J.; Brownstein, M. J.; Young, A. C.; Bonner, T. I. (1990): Structure of a cannabinoid receptor and functional expression of the cloned cDNA. In: *Nature* 346 (6284), S. 561–564. DOI: 10.1038/346561a0.
- McGrogan, B.; Gilmartin, B.; Carney, D.; McCann, A. (2008): Taxanes, microtubules and chemoresistant breast cancer. In: *Biochimica et biophysica acta* 1785 (2), S. 96–132. DOI: 10.1016/j.bbcan.2007.10.004.
- McGwire, B. S.; Satoskar, A. R. (2014): Leishmaniasis: clinical syndromes and treatment. In: *QJM : monthly journal of the Association of Physicians* 107 (1), S. 7–14. DOI: 10.1093/qjmed/hct116.
- Min, B.; Yun, B.; Lee, H.; Jung, H. J.; Jung, H. A.; Choi, J. (2006): Two novel furan derivatives from *Phellinus linteus* with anti-complement activity. In: *Bioorganic & Medicinal Chemistry Letters* 16 (12), S. 3255–3257. DOI: 10.1016/j.bmcl.2006.03.027.
- Minotti, G.; Menna, P.; Salvatorelli, E.; Cairo, G.; Gianni, L. (2004): Anthracyclines: molecular advances and pharmacologic developments in antitumor activity and cardiotoxicity. In: *Pharmacological reviews* 56 (2), S. 185–229. DOI: 10.1124/pr.56.2.6.
- Mondol, M.; Farhouse, J.; Islam, M.; Schuffler, A.; Laatsch, H. (2017): Metabolites from the Endophytic Fungus *Curvularia* sp. M12 Act as Motility Inhibitors against *Phytophthora capsici* Zoospores. In: *Journal of natural products* 80 (2), S. 347–355. DOI: 10.1021/acs.jnatprod.6b00785.

- Mori, T.; Shin-ya, K.; Aihara, M.; Takatori, K.; Hayakawa, Y. (2003a): Byssochlamysol, a new antitumor steroid against IGF-1-dependent cells from *Byssochlamys nivea*. I. Taxonomy, fermentation, isolation and biological activity. In: *The Journal of antibiotics* 56 (1), S. 1–5.
- Mori, T.; Shin-ya, K.; Takatori, K.; Aihara, M.; Hayakawa, Y. (2003b): Byssochlamysol, a new antitumor steroid against IGF-1-dependent cells from *Byssochlamys nivea*. II. Physico-chemical properties and structure elucidation. In: *The Journal of antibiotics* 56 (1), S. 6–8.
- Nasehi, A.; Kadir, J.; Nasr-Esfahani, M.; Abed-Ashtiani, F.; Wong, M.; Rambe, S.; Golkhandan, E. (2014): Analysis of genetic and virulence variability of *Stemphylium lycopersici* associated with leaf spot of vegetable crops. In: *Eur J Plant Pathol* 140 (2), S. 261–273. DOI: 10.1007/s10658-014-0460-3.
- Nasehi, A.; Kadir, J. B.; Abidin, M. A. Zainal; Wong, M. Y.; Ashtiani, F. Abed (2012): First Report of Gray Leaf Spot on Pepper Caused by *Stemphylium solani* in Malaysia. In: *Plant Disease* 96 (8), S. 1227. DOI: 10.1094/PDIS-03-12-0262-PDN.
- Newman, D. J.; Cragg, G. M. (2016): Natural Products as Sources of New Drugs from 1981 to 2014. In: *Journal of natural products* 79 (3), S. 629–661. DOI: 10.1021/acs.jnatprod.5b01055.
- Newman, D. J.; Cragg, G. M.; Snader, K. M. (2000): The influence of natural products upon drug discovery (Antiquity to late 1999). In: *Nat. Prod. Rep.* 17 (3), S. 215–234. DOI: 10.1039/a902202c.
- Oocolowitz, J. L. (1964): Mass Spectrometry of Naturally Occurring Alkenyl Phenols and Their Derivatives. In: *Anal. Chem.* 36 (11), S. 2177–2181. DOI: 10.1021/ac60217a043.
- Ono, E.; Inoue, J.; Hashidume, T.; Shimizu, M.; Sato, R. (2011): Anti-obesity and anti-hyperglycemic effects of the dietary citrus limonoid nomilin in mice fed a high-fat diet. In: *Biochemical and biophysical research communications* 410 (3), S. 677–681. DOI: 10.1016/j.bbrc.2011.06.055.
- Osaka, I.; Hefty, P. S. (2013): Simple resazurin-based microplate assay for measuring *Chlamydia* infections. In: *Antimicrobial agents and chemotherapy* 57 (6), S. 2838–2840. DOI: 10.1128/AAC.00056-13.
- Pacher, P.; Batkai, S.; Kunos, G. (2006): The endocannabinoid system as an emerging target of pharmacotherapy. In: *Pharmacological reviews* 58 (3), S. 389–462. DOI: 10.1124/pr.58.3.2.
- Pink, R.; Hudson, A.; Mouries, M.; Bendig, M. (2005): Opportunities and challenges in antiparasitic drug discovery. In: *Nature reviews. Drug discovery* 4 (9), S. 727–740. DOI: 10.1038/nrd1824.
- Rabbani, G. H.; Gilman, R. H.; Kabir, I.; Mondel, G. (1985): The treatment of *Fasciolopsis buski* infection in children. A comparison of thiabendazole, mebendazole, levamisole, pyrantel pamoate, hexylresorcinol and tetrachloroethylene. In: *Transactions of the Royal Society of Tropical Medicine and Hygiene* 79 (4), S. 513–515. DOI: 10.1016/0035-9203(85)90081-1.
- Racz, I.; Nadal, X.; Alferink, J.; Banos, J.; Rehnelt, J.; Martin, M. et al. (2008): Crucial role of CB(2) cannabinoid receptor in the regulation of central immune responses during neuropathic pain. In: *The Journal of neuroscience : the official journal of the Society for Neuroscience* 28 (46), S. 12125–12135. DOI: 10.1523/JNEUROSCI.3400-08.2008.
- Räz, B.; Iten, M.; Grether-Bühler, Y.; Kaminsky, R.; Brun, R. (1997): The Alamar Blue® assay to determine drug sensitivity of African trypanosomes (*T.b. rhodesiense* and *T.b. gambiense*) in vitro. In: *Acta Tropica* 68 (2), S. 139–147. DOI: 10.1016/S0001-706X(97)00079-X.
- Santajit, S.; Indrawattana, N. (2016): Mechanisms of Antimicrobial Resistance in ESKAPE Pathogens. In: *BioMed research international* 2016, S. 2475067. DOI: 10.1155/2016/2475067.

- Schöner, T. A.; Kresovic, D.; Bode, H. B. (2015): Biosynthesis and function of bacterial dialkylresorcinol compounds. In: *Applied microbiology and biotechnology* 99 (20), S. 8323–8328. DOI: 10.1007/s00253-015-6905-6.
- Schulz, B.; Sucker, J.; Aust, H. J.; Krohn, K.; Ludewig, K.; Jones, P. G.; Döring, D. (1995): Biologically active secondary metabolites of endophytic *Pezizula* species. In: *Mycological Research* 99 (8), S. 1007–1015. DOI: 10.1016/S0953-7562(09)80766-1.
- Shiono, Y.; Shimanuki, K.; Hiramatsu, F.; Koseki, T.; Tetsuya, M.; Fujisawa, N.; Kimura, K. (2008): Pyrrospirones A and B, apoptosis inducers in HL-60 cells, from an endophytic fungus, *Neonectria ramulariae* Wollenw KS-246. In: *Bioorganic & Medicinal Chemistry Letters* 18 (23), S. 6050–6053. DOI: 10.1016/j.bmcl.2008.10.032.
- Simmons, E. G. (1969): Perfect States of *Stemphylium*. In: *Mycologia* 61 (1), S. 1. DOI: 10.2307/3757341.
- Srivastava, S.; Shankar, P.; Mishra, J.; Singh, S. (2016): Possibilities and challenges for developing a successful vaccine for leishmaniasis. In: *Parasites & vectors* 9 (1), S. 277. DOI: 10.1186/s13071-016-1553-y.
- Stodola, F. H.; Weisleder, D.; Vesonder, R. F. (1973): A new dialkylresorcinol from *Stemphylium majusculum*. In: *Phytochemistry* 12 (7), S. 1797–1798. DOI: 10.1016/0031-9422(73)80406-6.
- Storey, C.; Chopra, I. (2001): Affinities of beta-lactams for penicillin binding proteins of *Chlamydia trachomatis* and their antichlamydial activities. In: *Antimicrobial agents and chemotherapy* 45 (1), S. 303–305. DOI: 10.1128/AAC.45.1.303-305.2001.
- Teiten, M.; Mack, F.; Debbab, A.; Aly, A. H.; Dicato, M.; Proksch, P.; Diederich, M. (2013): Anticancer effect of altersolanol A, a metabolite produced by the endophytic fungus *Stemphylium globuliferum*, mediated by its pro-apoptotic and anti-invasive potential via the inhibition of NF-kappaB activity. In: *Bioorganic & medicinal chemistry* 21 (13), S. 3850–3858. DOI: 10.1016/j.bmc.2013.04.024.
- Ugai, T.; Minami, A.; Fujii, R.; Tanaka, M.; Oguri, H.; Gomi, K.; Oikawa, H. (2015): Heterologous expression of highly reducing polyketide synthase involved in betaenone biosynthesis. In: *Chemical communications (Cambridge, England)* 51 (10), S. 1878–1881. DOI: 10.1039/c4cc09512j.
- Wang, Q.; Qi, Q.; Wang, K.; Li, L.; Bao, L.; Han, J. et al. (2013): Coicenals A-D, four new diterpenoids with new chemical skeletons from the plant pathogenic fungus *Bipolaris coicis*. In: *Organic letters* 15 (15), S. 3982–3985. DOI: 10.1021/ol401736z.
- Wani, M.; Taylor, H.; Wall, M.; Coggon, P.; McPhail, A. (1971): Plant antitumor agents. VI. Isolation and structure of taxol, a novel antileukemic and antitumor agent from *Taxus brevifolia*. In: *J. Am. Chem. Soc.* 93 (9), S. 2325–2327. DOI: 10.1021/ja00738a045.
- WHO (2007): ixabepilone. Online verfügbar unter <https://www.cancer.gov/about-cancer/treatment/drugs/fda-ixabepilone>, zuletzt aktualisiert am 17.01.2011, zuletzt geprüft am 04.04.2017.
- Wijesekara, I.; Zhang, C.; van Ta, Q.; Vo, T.; Li, Y.; Kim, S. (2014): Phycion from marine-derived fungus *Microsporium* sp. induces apoptosis in human cervical carcinoma HeLa cells. In: *Microbiological research* 169 (4), S. 255–261. DOI: 10.1016/j.micres.2013.09.001.
- World Malaria Report 2015 (2015). Geneva, Switzerland: World Health Organization.
- Zapf, S.; Klappach, K.; Pfenning, J.; Ernst, M. (2011): Erarbeitung eines Testverfahrens zur Bestimmung der Protektiv- und Kurativleistung von Fungiziden bei der Bekämpfung des Erregers der

---

Stemphylium-Laubkrankheit *Stemphylium botryosum* in der Spargelkultur (*Asparagus officinalis* L.). In: *Gesunde Pflanzen* 63 (4), S. 167–174. DOI: 10.1007/s10343-011-0261-y.

Zheng, Y.; Qiao, X.; Miao, C.; Liu, K.; Chen, Y.; Xu, L.; Zhao, L. (2016): Diversity, distribution and biotechnological potential of endophytic fungi. In: *Ann Microbiol* 66 (2), S. 529–542. DOI: 10.1007/s13213-015-1153-7.

## 8. Appendix

### 8.1 NMR, UV and IR spectra of the isolated compounds

Figure 51:  $^1\text{H}$ -NMR spectrum of stemphyloxin III (1) in MeOD (600 MHz)

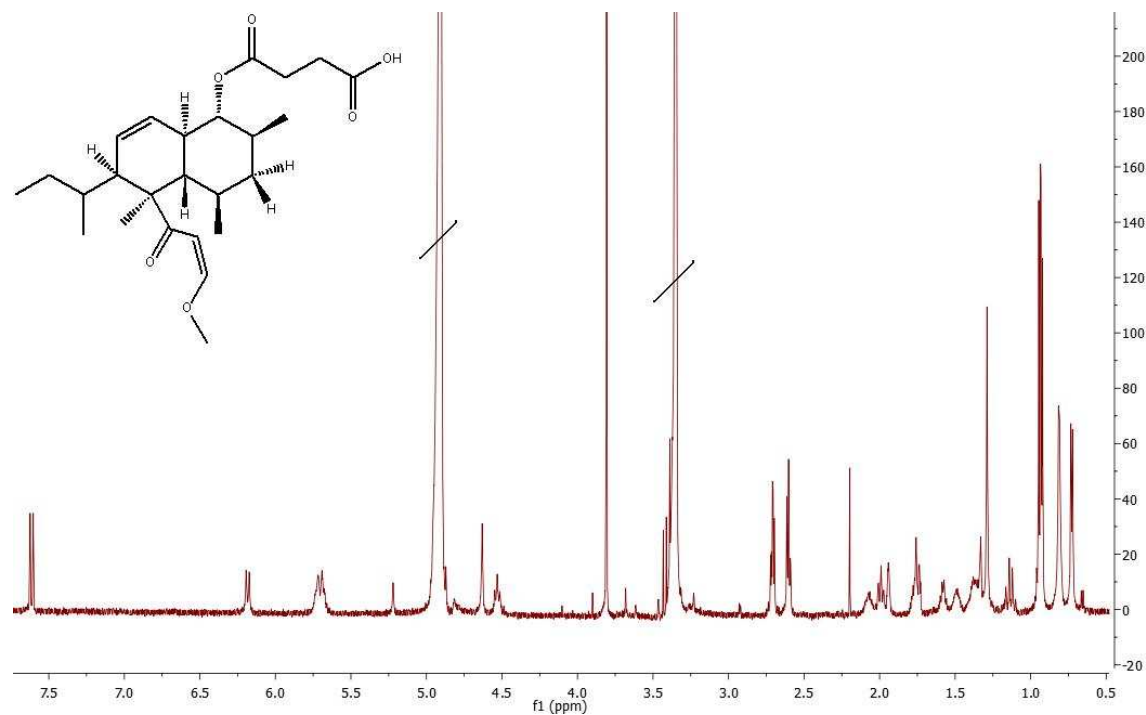
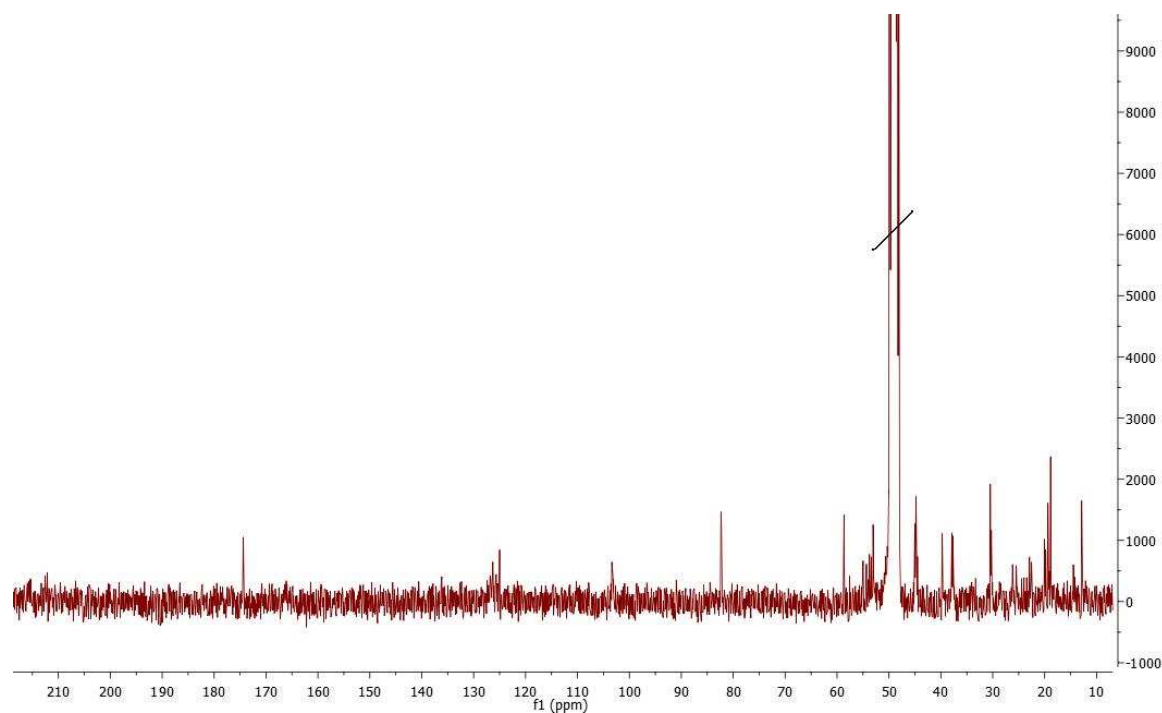
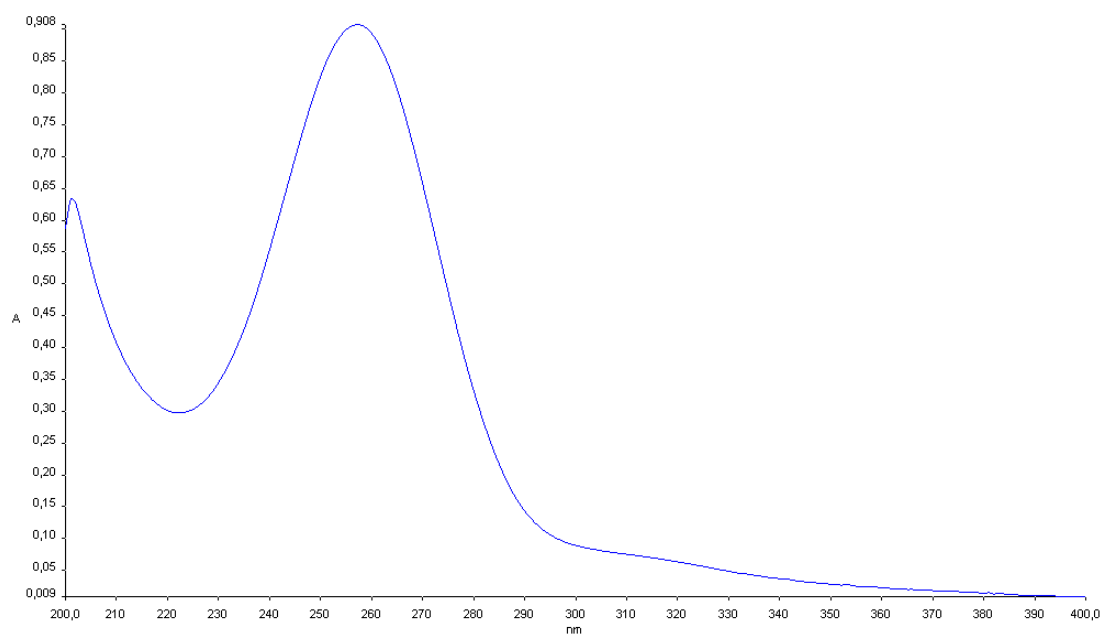
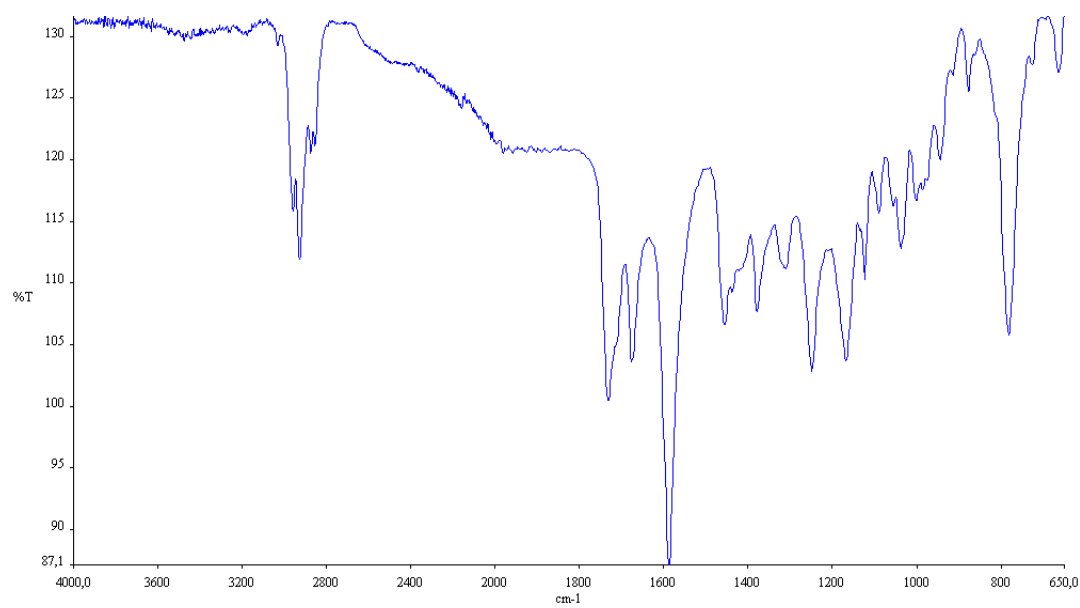
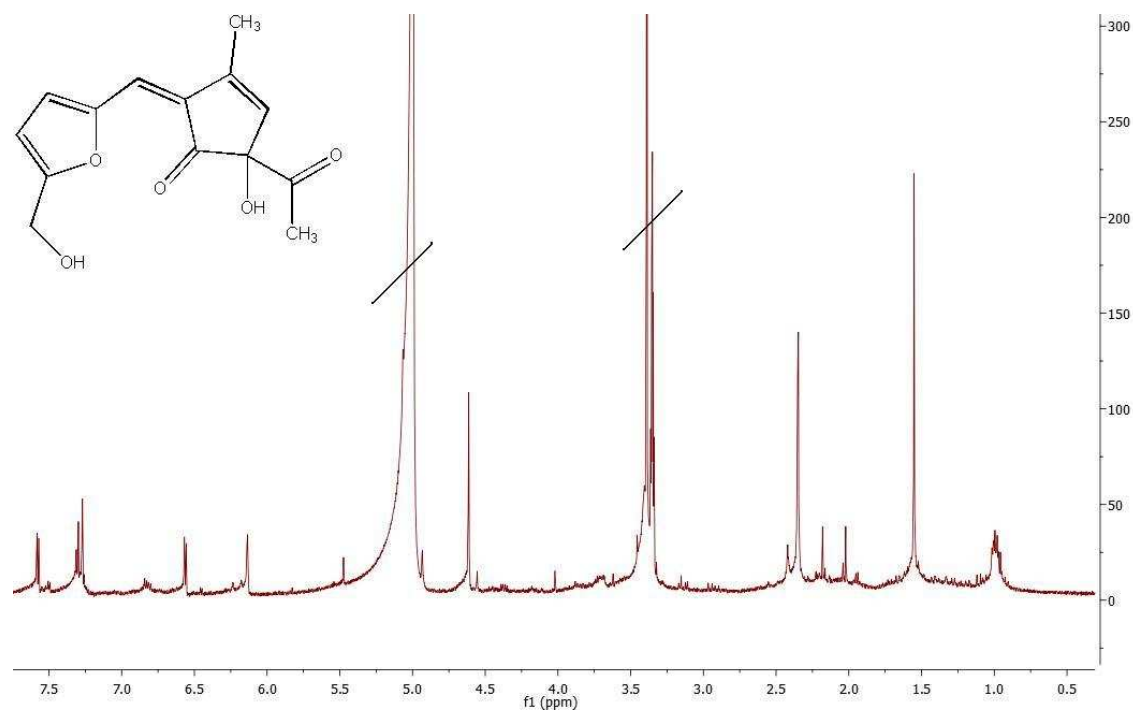
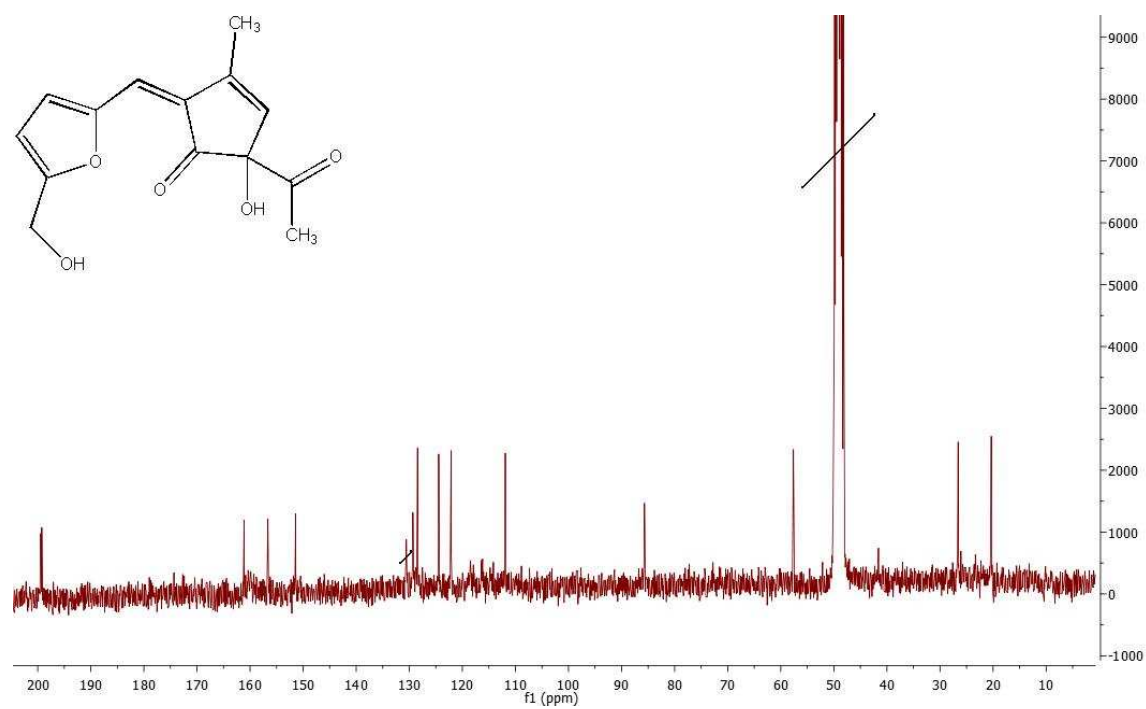
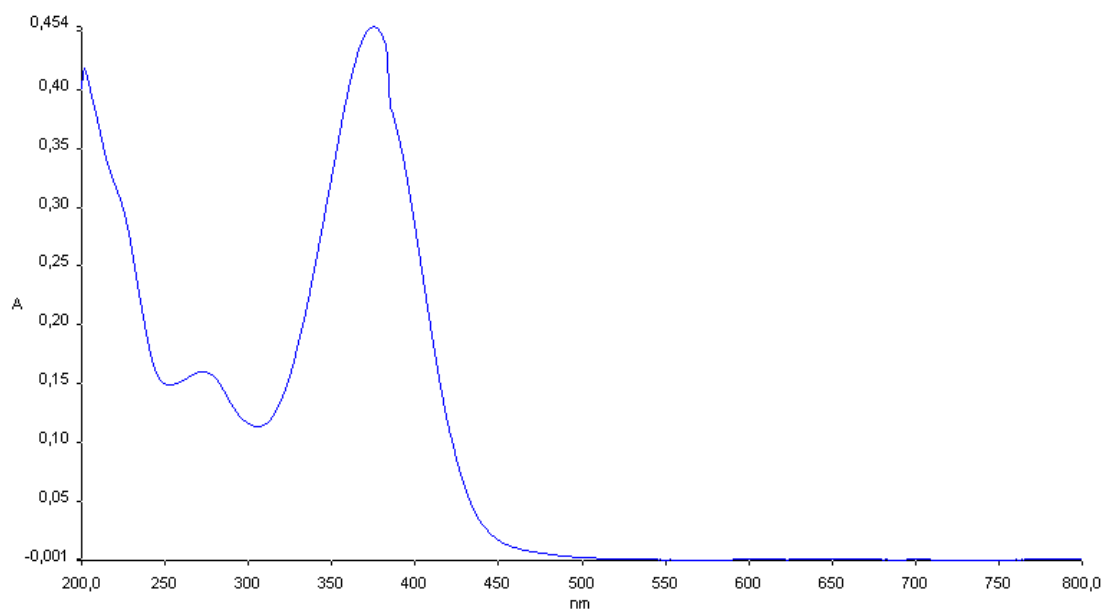
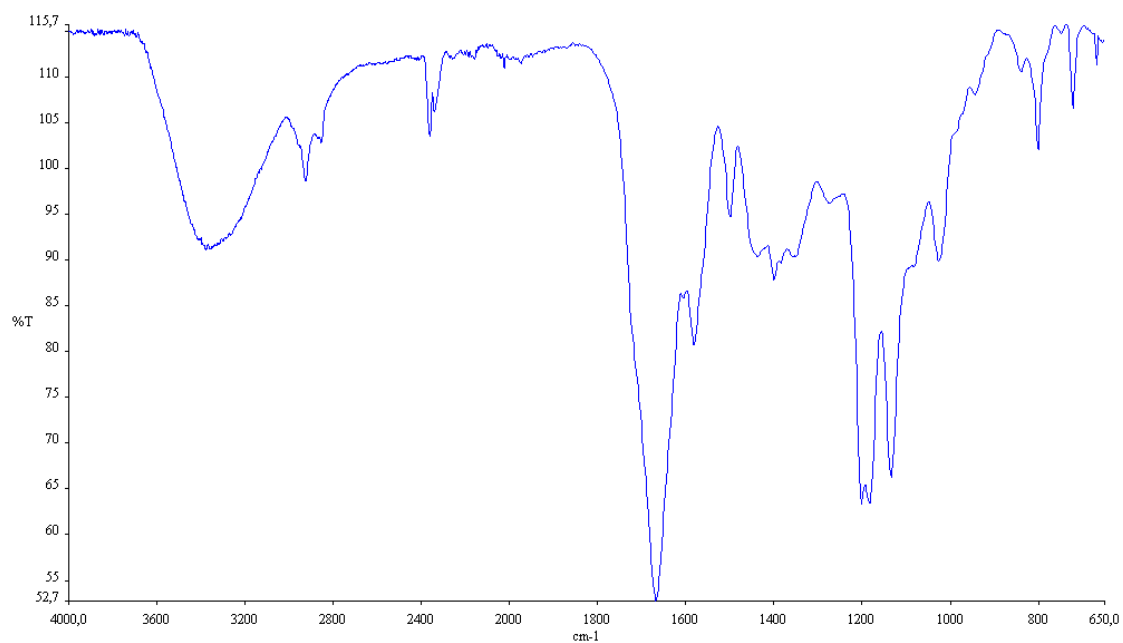


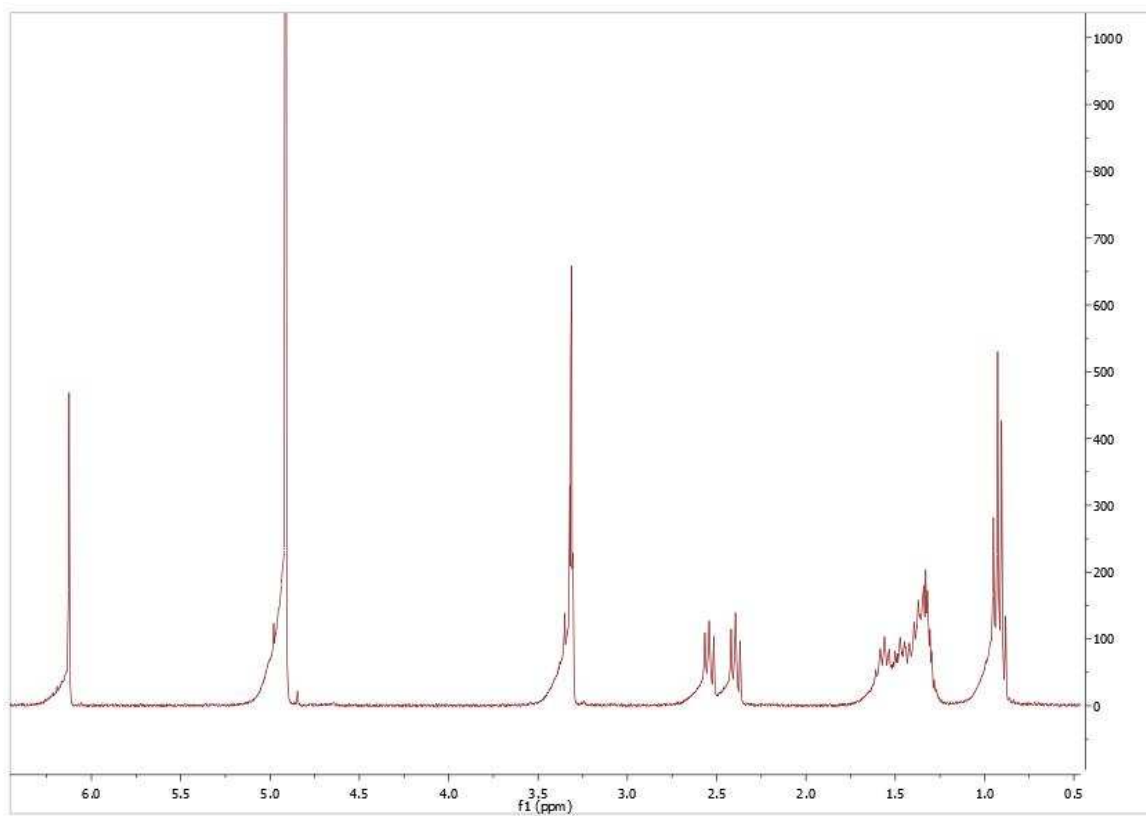
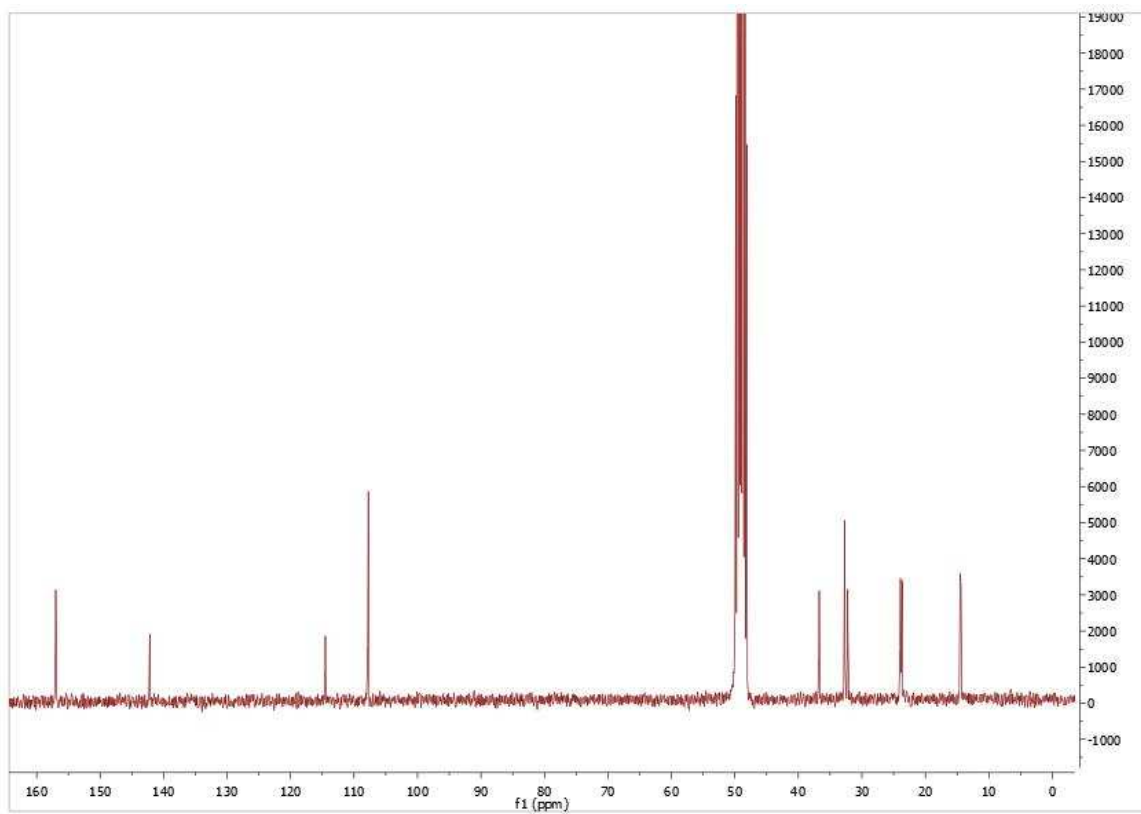
Figure 52:  $^{13}\text{C}$ -NMR spectrum of stemphyloxin III (1) in MeOD (150 MHz)

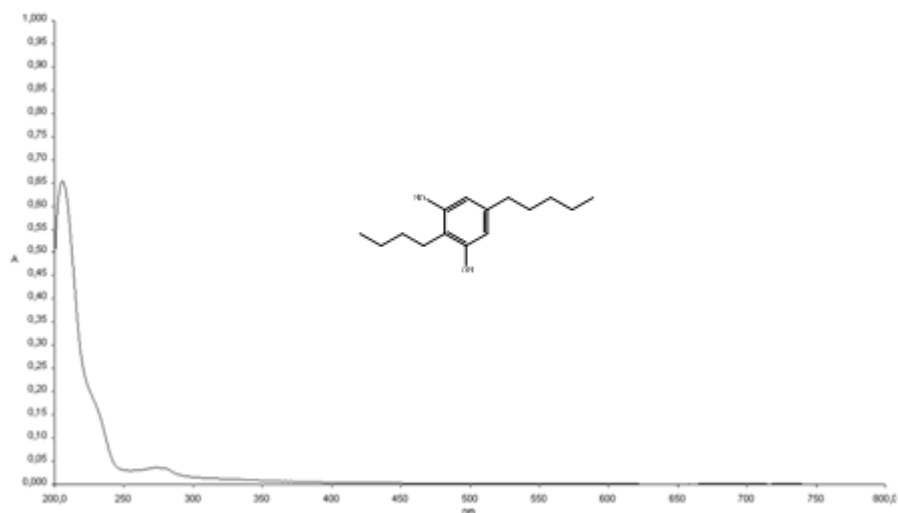
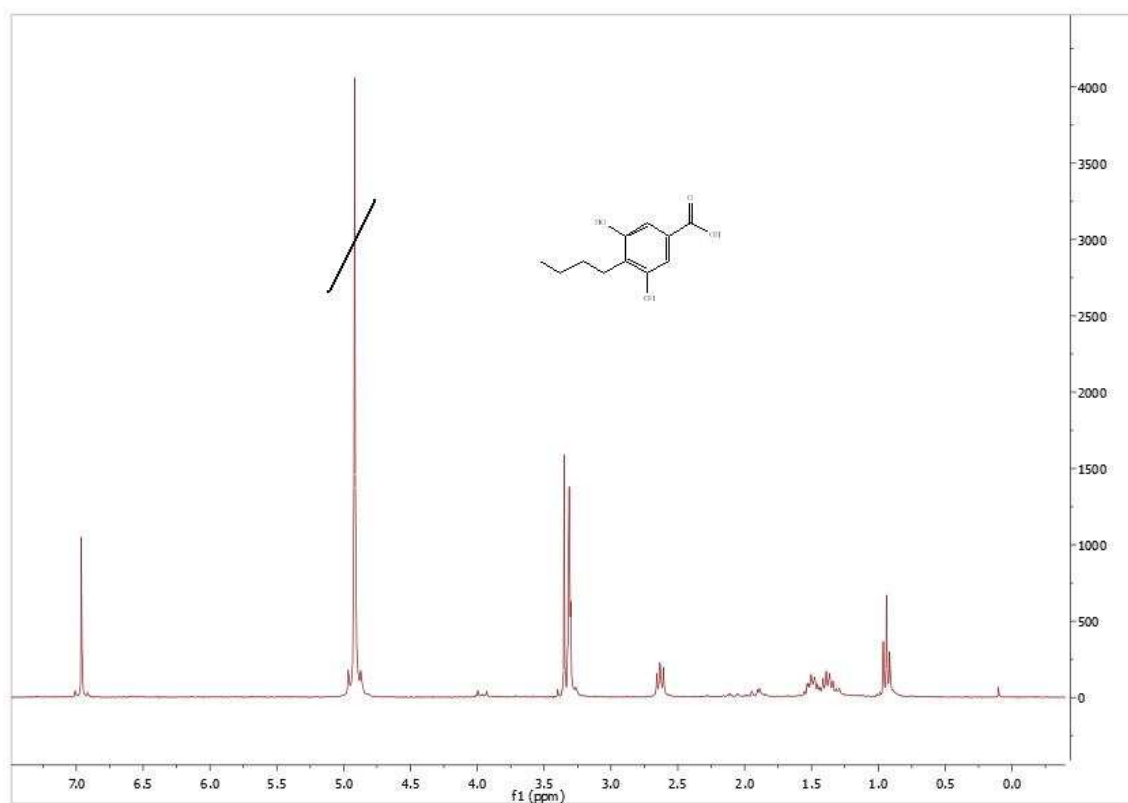


**Figure 53: UV spectrum of stemphyloxin III (1) in MeOH****Figure 54: IR spectrum of stemphyloxin III (1) in Acetone- $d_6$** 

**Figure 55:  $^1\text{H-NMR}$  of stemphylofuran (2) in MeOD (600 MHz)****Figure 56:  $^{13}\text{C-NMR}$  spectrum of stemphylofuran (2) in MeOD (150 MHz)**

**Figure 57: UV spectrum of stemphylofuran (2) in MeOH****Figure 58: IR spectrum of stemphylofuran (2) in Acetone- $d_6$** 

**Figure 59:**  $^1\text{H}$ NMR of stemphol (3) in MeOD (300 MHz)**Figure 60:**  $^{13}\text{C}$ NMR of stemphol (3) in MeOD (75 MHz)

**Figure 61: UV spectrum of stemphol (3) in MeOH****Figure 62:  $^1\text{H}$ -NMR spectrum of 4-butyl-3,5-dihydroxy benzoic acid (4) in MeOD (300 MHz)**

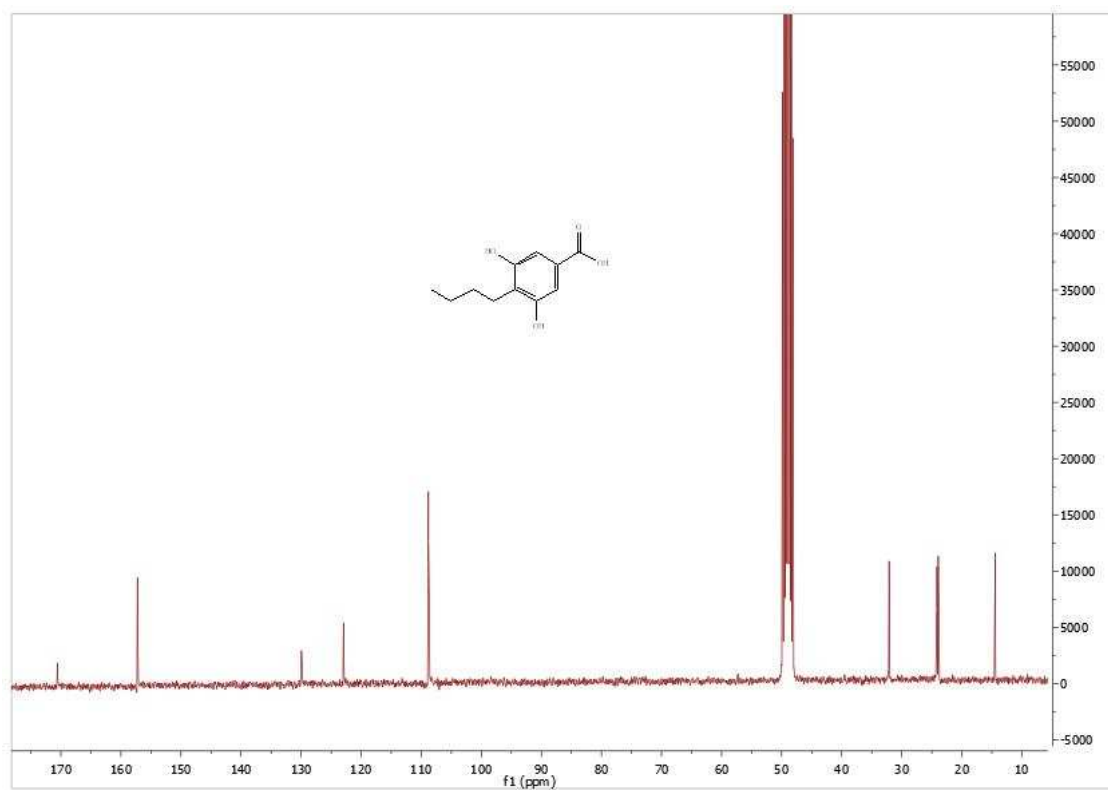
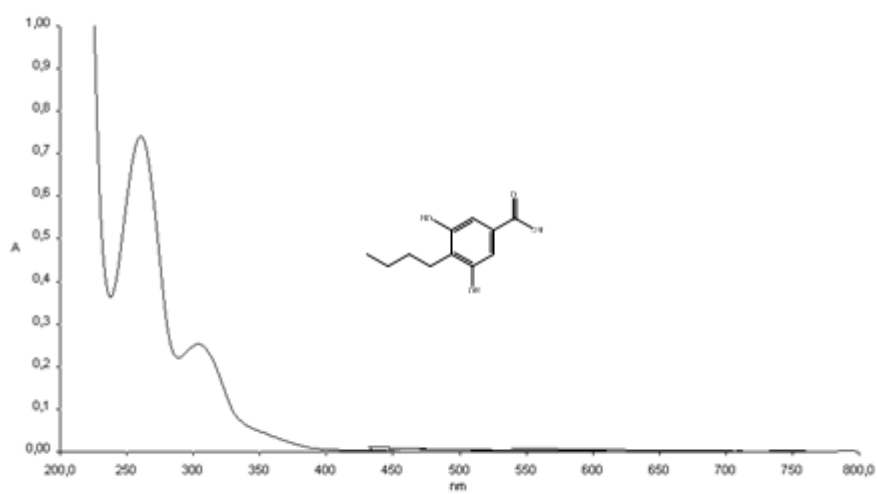
**Figure 63:**  $^{13}\text{C}$ -NMR spectrum of 4-butyl-3,5-dihydroxy benzoic acid (**4**) in MeOD (75 MHz)**Figure 64:** UV spectrum of 4-butyl-3,5-dihydroxy benzoic acid (**4**) in MeOH

Figure 65: IR spectrum of 4-butyl-3,5-dihydroxy benzoic acid (4) in Acetone- $d_6$

